Mandasuchus tanyauchen gen. et sp. nov., a pseudosuchian archosaur from the Manda Beds (?Middle Triassic) of Tanzania

Butler, Richard; Nesbitt, Sterling; Charig, Alan; Gower, D.J.; Barrett, Paul

DOI:
10.1080/02724634.2017.1343728

Document Version
Peer reviewed version

Citation for published version (Harvard):
Butler, R, Nesbitt, S, Charig, A, Gower, DJ & Barrett, P 2018, 'Mandasuchus tanyauchen gen. et sp. nov., a pseudosuchian archosaur from the Manda Beds (?Middle Triassic) of Tanzania', *Journal of Vertebrate Paleontology*, vol. 37, pp. 96-121. https://doi.org/10.1080/02724634.2017.1343728

Mandasuchus tanyauchen gen. et sp. nov., a pseudosuchian archosaur from the Manda Beds (?Middle Triassic) of Tanzania

RICHARD J. BUTLER,*[,1] STERLING J. NESBITT,[2] ALAN J. CHARIG,[3,†] DAVID J. GOWER,[4] and PAUL M. BARRETT[3]

[1]School of Geography, Earth & Environmental Sciences, University of Birmingham, Edgbaston, Birmingham, B15 2TT, United Kingdom, r.butler.1@bham.ac.uk;

[2]Department of Geosciences, Virginia Polytechnic Institute and State University, Blacksburg, Virginia, 24061, USA, sjn2104@vt.edu;

[3]Department of Earth Sciences, The Natural History Museum, Cromwell Road, London SW7 5BD, United Kingdom, p.barrett@nhm.ac.uk;

[4]Department of Life Sciences, The Natural History Museum, Cromwell Road, London SW7 5BD, United Kingdom, d.gower@nhm.ac.uk

*Corresponding author: r.butler.1@bham.ac.uk

[†]Deceased

ABSTRACT—The diverse assemblage of extinct archosaur species known from the Manda Beds of Tanzania has provided key insights into the timing and tempo of the early part of the archosaur radiation during the Middle Triassic. Several archosaur specimens were collected from the Manda Beds in 1933 by F. R. Parrington, and three of these were subsequently described and made the basis of a new genus, '*Mandasuchus*', in a 1956 doctoral dissertation. However, this important fossil material was never formally published and >60 years later '*Mandasuchus*' and '*Mandasuchus tanyauchen*' remain nomina nuda, despite frequent references to them in the literature. Here, we provide a detailed description of this material, provide the first formal diagnosis of *Mandasuchus tanyauchen* gen. et sp. nov., and assess its phylogenetic position. The holotype of *M. tanyauchen* includes a well-preserved partial postcranial skeleton and fragmentary cranial remains. Four referred specimens include two partial skeletons, consisting primary of postcranial remains, a partial maxilla that was previously assigned to the dinosaur clade Saurischia, and a well-preserved astragalus and calcaneum that may belong to the holotype individual. *Mandasuchus tanyauchen* is diagnosed by a unique combination of character states, as well as by two possible autapomorphies (ascending process of maxilla thin and compressed from anterolaterally to posteromedially; femur with distinct pit lateral to the distal-most expression of the posteromedial tuber). Our phylogenetic analysis recovered *M. tanyauchen* within Paracrocodylomorpha, as the sister taxon to all other sampled members of Loricata.

INTRODUCTION

Archosauria—the clade comprising all descendants of the most recent common ancestor of birds and crocodilians (thus including dinosaurs and pterosaurs)—achieved significant taxonomic and morphological diversity during the Triassic, and went on to dominate terrestrial ecosystems globally for the remainder of the Mesozoic. The stratigraphically oldest known fossil representatives of Archosauria are rare occurrences in the latest Early Triassic–earliest Middle Triassic of Germany, Russia, and China (Butler et al., 2011; Nesbitt, 2011; Nesbitt et al., 2011). In Middle Triassic sediments archosaur body fossils are more widespread and common (e.g., Nesbitt, 2003, 2005; Sen, 2005; Butler et al., 2014), with the most extensive sample having been collected from the Manda Beds of the Ruhuhu Basin of southern Tanzania (Haughton, 1932; Huene, 1938a, b, 1939; Charig, 1956; Gebauer, 2004; Thomas, 2004; Butler et al., 2009; Nesbitt et al., 2010, 2013a, b, 2014; Nesbitt and Butler, 2013; Barrett et al., 2015).

The first collections of fossil vertebrate material from the Manda Beds were made by Gordon Murray Stockley of the Tanganyika Geological Survey in 1930 (Stockley, 1932), and were described by Haughton (1932). The Cambridge-based vertebrate paleontologist Francis Rex Parrington made further Manda Beds collections, including a number of important archosaur specimens, during his 1933 expedition to the Ruhuhu Valley, working primarily at or near the sites previously discovered by Stockley (Sidor et al., 2017). Four diapsid specimens from Parrington's collections were sent to Friedrich von Huene in Tübingen for study, and on the basis of two of these Huene described the new genus and species *Parringtonia gracilis* Huene, 1939 (see recent re-descriptions by Nesbitt and Butler [2013] and Nesbitt et al. [2017]), based on a partial skeleton, and a left maxilla that he identified as belonging to an indeterminate saurischian dinosaur (Huene, 1939; see below for redescription

of this specimen). The remainder of the archosaur material collected by Parrington was first studied by AJC (1956) in his unpublished PhD dissertation completed at the University of Cambridge under Parrington's supervision.

Almost all the specimens studied by AJC were subsequently incorporated into the collections of the British Museum (Natural History) (now the Natural History Museum, London), where he worked from 1957 until his death in 1997 (Moody and Naish, 2010). In his PhD dissertation, Charig (1956) described two new archosaur taxa for which he proposed the names '*Mandasuchus longicervix*' and '*Teleocrater tanyura*'. A manuscript supposedly describing '*Mandasuchus*' and '*Teleocrater*' was cited as 'in press' at the journal *Palaeontology* by Charig in Appleby et al. (1967), the "Reptilia" chapter of the Geological Society of London's compendium "The Fossil Record". Although this publication never appeared, the name '*Mandasuchus*' has been used widely in the published literature (e.g., Huene, 1956; Romer, 1966; Charig in Appleby et al., 1967; Charig, 1972; Krebs, 1976; Parrish, 1993), and the pelvis was figured by Charig (1972) and the histology analysed by de Ricqlès et al. (2008). The species name for '*Mandasuchus*' was given as '*M. tanyauchen*' in Appleby et al. (1967), and this is the species name that has generally been used in the literature. '*Mandasuchus*' has even made it into popular literature, with life reconstructions appearing in the Brooke Bond Picture Cards series "Prehistoric Animals" (Charig and Wilson, 1971; Fig. 1) and the popular book "A New Look at the Dinosaurs" (Charig, 1979). Parrish (1993) suggested that the known material of '*Mandasuchus*' was conspecific with *Ticinosuchus ferox* from the Middle Triassic of Switzerland (Krebs, 1965), but did not provide detailed justification for this proposal. Most recently, the material described as '*Mandasuchus*' by Charig (1956) was redescribed by Thomas (2004) in a PhD dissertation that remains unpublished.

Despite its long history in the archosaur literature, '*Mandasuchus*' has never been formally diagnosed or received a published description. As such, the names '*Mandasuchus*', '*Mandasuchus longicervix*', and '*Mandasuchus tanyauchen*' are currently nomina nuda. Our aims in this paper are to describe the known material of '*Mandasuchus*', to formally diagnose the genus and species for the first time, and to assess the phylogenetic position of this taxon.

Institutional Abbreviations—**NHMUK** (formerly BMNH), Natural History Museum, London, UK; **NMT**, National Museum of Tanzania, Dar es Salaam, Tanzania; **PEFO**, Petrified Forest National Park, Arizona, U.S.A.; **TTU**, Museum of Texas Tech University, Paleontology Division, Lubbock, Texas, U.S.A.; **UFRGS**, Universidade Federal do Rio Grande do Sul, Porto Alegre, Brazil; **UMZC**, University Museum of Zoology, University of Cambridge, UK; **USNM**, United States National Museum of Natural History, Washington D.C., U.S.A.

MATERIALS AND METHODS

Most of Parrington's specimens were collected on or near the surface and were contained within a matrix of marl or reddish-brown feldspathic sandstone (Charig, 1956). AJC prepared the specimens during the course of his PhD studies using the following method. Fossils were soaked in water and gently scrubbed to remove mud and loose matrix. Broken surfaces were then matched and glued together. Friable bones were painted with a solution of 'Durofix' in amyl acetate diluted with acetone in order to harden them. Mechanical preparation was then carried out using an automatic mallet, dental burrs, and hand needles. Chemical preparation with acetic acid was applied to some specimens, although AJC did not favor this approach because it tended to damage bone surfaces. Further matching and gluing of broken surfaces was conducted following preparation. Cracks and

joints in the bones were filled with a mixture of modeling clay and gum acacia, and heavier limb bones were reinforced internally using metal pins.

Measurements of many of the bones were provided by AJC in his PhD thesis (Charig, 1956). We present some of these measurements here, but also add a number of additional measurements. Measurements for the holotype are presented in Tables 1–5, and measurements for the referred specimens NHMUK PV R6793 and NHMUK PV R6794 are in Tables S1–S4.

SYSTEMATIC PALEONTOLOGY

ARCHOSAURIA Cope, 1869–1870

PSEUDOSUCHIA Zittel, 1877–1890

SUCHIA Krebs, 1974

LORICATA Merrem, 1820

MANDASUCHUS TANYAUCHEN gen. et sp. nov.

(Figs. 3–26)

Ein Saurischier-Rest Huene, 1939:65.

'*Mandasuchus longicervix*' Charig, 1956:25, plates 1–32.

'*Mandasuchus*' Huene, 1956:453.

'*Mandasuchus*' Charig et al., 1956:215

'*Mandasuchus*' Romer, 1966:368.

'*Mandasuchus tanyauchen*' Charig in Appleby et al., 1967:709.

'*Mandasuchus tanyauchen*' Charig, 1972:131, pl. 3.

'*Mandasuchus*' Sill, 1974:320.

‘*Mandasuchus*’ Krebs, 1976:75.

‘*Mandasuchus tanyauchen*’ Krebs, 1976:75.

‘*Mandasuchus tanyauchen*’ Cruickshank, 1979:170.

‘*Mandasuchus*’ Parrish, 1993:297.

‘*Mandasuchus*’ Juul, 1994:6.

‘*Mandasuchus*’ Gower, 2000:450.

‘*Mandasuchus tanyauchen*’ Gower 2000:465.

‘*Mandasuchus tanyauchen*’ Gower, 2001:121, fig. 1.

‘*Mandasuchus tanyauchen*’ Thomas, 2004:17, figs. 2.4–2.13, 2.15–2.16, pls. 2.1–2.9.

‘*Mandasuchus*’ Sen, 2005:188, figure 9F.

‘*Mandasuchus*’ de Ricqlès et al., 2008:65, table 1, pl. 2.2.

‘*Mandasuchus*’ Lautenschlager and Desojo, 2011:376.

‘*Mandasuchus*’ Nesbitt, 2011:9.

‘*Mandasuchus tanyauchen*’ Nesbitt et al., 2013:252, table 1, fig. 3.

‘*Mandasuchus longicervix*’ Nesbitt et al., 2014:1358, 1369.

Holotype—NHMUK PV R6792 (Figs. 3A, 4, 6, 7, 10–15, 17, 18, 20, 21, 23), partial skeleton representing a single individual, including partial left and right maxillae, right dentary fragment, 33 vertebrae (including cervicals, dorsals, one sacral, and caudals), fragments of dorsal and caudal neural spines, a partial dorsal rib, both scapulae and part of the left coracoid, incomplete right humerus, both pelves, both femora, both tibiae, partial right fibula, a fragmentary metapodial, three osteoderms in situ on neural spine of cervical 6, and several osteoderm fragments. Part of this specimen (fragments including dorsal and caudal neural spines, partial dorsal centrum, fragmentary metapodial) was previously catalogued as UMZC T1117.

Charig (1956) tentatively identified fragments of limb bones as the proximal ends of the radius and ulna of this individual; however, these fragments are now interpreted as representing proximal and distal ends of left and right tibiae of a much smaller archosauromorph individual, may pertain to the smaller archosauromorph specimen (NHMUK PV R16405) collected from the same locality, and likely representing a different taxon to *Mandasuchus*. A small long bone fragment was identified by Charig (1956) as a possible metatarsal fragment; however, we have been unable to identify the element to which this fragment belongs. Consequently, these fragments are excluded from the type specimen. de Ricqlès et al. (2008:table 1) sampled rib fragments from NHMUK PV R6792 histologically, but used the formatted accession number "BM R. 6792-11". Unfortunately, this histological section is currently lost (A. de Ricqlès, pers. comm., August 2016).

Type Locality—West of Irundi, Ruhuhu Valley, southwestern Tanzania (Fig. 2); field collection 11b of Parrington, locality B5 of Stockley (1932). Also excavated by Parrington from the same locality were a fragmentary, smaller archosauromorph (field collection 11a of Parrington: NHMUK PV R16405) and material of the dicynodont *Tetragonias njalilus* (Cruickshank, 1967; field collection 11c of Parrington). Rhynchosaurs (e.g., Parrington specimen 2, *Stenaulorhynchus*) were also collected in the immediate vicinity.

Stratigraphic Occurrence—The holotype and referred specimens were all collected from the Lifua Member of the Manda Beds (?Middle Triassic).

Referred Specimens—NHMUK PV R6793 (Fig. 3B, 8, 16), a partial skeleton apparently representing a single individual, including a fragment of right maxilla with a partially erupted tooth crown, cervical (Ce) vertebrae Ce2–8, dorsal (D) vertebrae D1–5, two additional dorsal centra, one caudal centrum, neural arch and spine fragments, left and right scapulae, partial right coracoid, left and right humeri, left ulna, proximal and distal fragments

of a radius, five complete osteoderms, and several osteoderm fragments. This specimen was listed as BMNH R16401 by Thomas (2004).

NHMUK PV R6794 (Figs. 3C, 9, 19, 22, 24), a partial skeleton apparently representing a single individual, including the odontoid, axial intercentrum, axis, Ce3–8, parts of eight dorsal vertebrae (identified as D1 and D4–D10 by Charig [1956]), 12 caudal vertebrae (six anterior caudals and six distal caudals), rib fragments, left pelvis, partial right femur, left tibia, proximal right fibula, left calcaneum (now lost), and several fragments of osteoderms. The femur was sampled histologically by de Ricqlès et al. (2008), who used the incorrect register number "BM R 6791- 63 R" to refer to this specimen. Unfortunately, this histological section is currently lost (A. de Ricqlès, pers. comm., August 2016). This specimen was listed as BMNH R16402 by Thomas (2004).

NHMUK PV R36950 (Figs. 24, 25), casts of a left astragalus and calcaneum, possibly representing those originally belonging to the holotype individual (see below). The whereabouts of the original specimens from which the casts were made is currently unknown.

NHMUK PV R36889 (Fig. 5), a left maxilla, referred to "Saurischia gen. et sp. indet." by Huene (1939:fig. 1), and tentatively referred to *Mandasuchus* herein (see below).

Localities for Referred Specimens—All referred specimens come from the Ruhuhu Basin, southern Tanzania (Fig. 2). NHMUK PV R6793 comes from Irundi, locality B5 of Stockley (1932), the same locality as the holotype, and is field collection 11 of Parrington. NHMUK PV R6794 comes from Mkongoleko/Njalila, locality B15/2 of Stockley (1932), and is field collection 63 of Parrington. The locality information for NHMUK PV R36950 is undocumented, although it may represent part of the holotype specimen (see below). NHMUK PV R36889 comes from between Matamondo and Linyanya, locality B17 of Stockley (1932), and is field collection 77a of Parrington. This last specimen may have come from much lower in the Lifua Member than the other specimens as it was discovered just

above the Kingori Member of the Manda Beds. Furthermore, it was discovered near a *Kannemeyeria* skull (Cruickshank, 1965; Hancox et al., 2013), which also suggests this locality is stratigraphically older than those yielding the holotype and other referred specimens of *Mandasuchus*.

Diagnosis—The diagnosis is based solely on character states present in the holotype specimen. *Mandasuchus tanyauchen* is distinguished from all other early suchians on the basis of the following combination of features (*indicates possible autapomorphy): *ascending process of maxilla thin and compressed from anterolaterally to posteromedially; weakly incised antorbital fossa of the maxilla; lateral expansions of the neural arches (= spine tables) present in cervical and dorsal vertebrae; unraised muscle scar present on scapula dorsal to glenoid; *femur with distinct pit lateral to the distal-most expression of the posteromedial tuber; osteoderms with spike-like anterior process.

Mandasuchus tanyauchen can be differentiated from *Ticinosuchus ferox* by the less strongly incised antorbital fossa of the maxilla, a much smaller dorsal process of the maxilla, a more strongly expanded distal end of the scapula, and the presence of a small expansion at the distal end of the pubis. The ratio between the length of the cervical centra versus their height is greater in *Mandasuchus tanyauchen* than those of the proportionally shorter cervical vertebrae from the contemporaneous *Stagonosuchus nyassicus* (Huene, 1938) and *Nundasuchus songeaensis* (Nesbitt et al., 2014), although we note that this character state appears to be under ontogenetic control (see below).

Etymology—Genus name is derived from ‘Manda’, for the Manda Beds, combined with ‘suchus’, the Greek term for the Egyptian crocodile-headed god Sobek. The species name is derived from the Greek ‘tany-’, meaning long, and ‘auchen’, meaning neck. The genus and species names were created by AJC, with the species name intended to reference the elongate neck vertebrae.

Comments—Huene (1939) briefly described the incomplete maxilla (NHMUK PV R36889) that we refer tentatively to *Mandasuchus tanyauchen*. Huene regarded it as referable to Saurischia, and identified it as either a member of Coelurosauria or Carnosauria (i.e., as a theropod). Although it would potentially be the oldest known dinosaur record, with the possible exception of *Nyasasaurus* whose exact provenance within the Manda Beds is unknown (Nesbitt et al., 2013a), this specimen has received little attention. Huene's (1939) only justification for the referral to Saurischia was that the alveoli are small and closely packed, but this is not a feature restricted to dinosaurs and we observe no character states that would support referral of NHMUK PV R36889 to Dinosauria or to any dinosaurian subclade. Charig (1956) did not discuss this maxilla, but Thomas (2004) referred it to *M. tanyauchen*. Although neither NHMUK PV R36889 nor the maxilla of the holotype of *M. tanyauchen* (NHMUK PV R6792) is complete, the two are closely similar in size and in morphology. The strongly compressed and thin dorsal process of NHMUK PV R6792 is potentially autapomorphic for *M. tanyauchen*. The dorsal process of NHMUK PV R36889 is also compressed, but the orientation of the compression in dorsal view is slightly different from that of NHMUK PV R6792, being compressed nearly mediolaterally rather than anterolaterally to posteromedially. However, this may result from taphonomic distortion of NHMUK PV R36889. Given the strong morphological similarities present, we tentatively follow Thomas (2004) in referring NHMUK PV R36889 to *M. tanyauchen.*

ANATOMICAL DESCRIPTION

Maxilla

The left and right maxillae are both partially preserved in the holotype (Fig. 4A–F), NHMUK PV R6792. A referred specimen, NHMUK PV R36889 (Fig. 5), provides additional anatomical information, and a small, uninformative maxillary fragment is present in NHMUK PV R6793. In the holotype, the left maxilla is the more complete of the two (Fig. 4A–D), but is broken at its anterior (immediately anterior to the base of the dorsal or ascending process) and posterior extremities, damaged along the alveolar margin and beneath the antorbital fenestra, and the dorsal process has broken away and is lost. The element was originally preserved as five separate fragments, now glued back together, and is 92.5 mm long as preserved. In lateral or medial view the preserved ventral margin of the bone is convex (Fig. 4A, C), being upturned at its anterior end toward the contact with the premaxilla, reaching a maximum convexity immediately posterior to the base of the dorsal process. In ventral view (Fig. 4B), the bone is bowed inwards, such that the medial surface of the bone is anteroposteriorly convex and the lateral surface is anteroposteriorly concave. This bowing may have been exaggerated by post-mortem compression and the way in which individual fragments of the element were glued back together: the bone may have been somewhat straighter in life.

A row of poorly preserved, small, ventrally opening nutrient foramina is present on the lateral surface of the bone, a few (4–5) millimetres dorsal to and parallel to the alveolar margin. The base of the dorsal process of the maxilla is set back from the anterior extremity of the bone, being positioned dorsal to the second and third preserved alveoli, and behind a distinct, but incompletely preserved, anterior process of the maxilla (Fig. 4A). The dorsal process is emarginated along the posterior half of its lateral surface by a distinct, but restricted, antorbital fossa, the anterior border of which is clearly demarcated on the dorsal process by a sharp ridge. Although poorly preserved, the fossa appears to continue posteriorly along most of the length of the posterior process of the maxilla. The broken cross-section of

the dorsal process shows that it was a thin sheet of bone, the long axis of which extends from anterolaterally to posteromedially. The extent of the antorbital fossa and the dimensions of the dorsal process are much smaller in *Mandasuchus tanyauchen* than those of *Ticinosuchus ferox* (Krebs, 1965), *Decuriasuchus quartacolonia* (França et al., 2013), a specimen referred to *Prestosuchus chiniquensis* (UFRGS-PV-0156-T), and *Saurosuchus galilei* (Alcober, 2000).

Most of the maxillary medial surface is smooth and gently convex (Fig. 4C). The palatal process is not preserved. There is a distinct anteroposteriorly extending ledge on the medial surface, positioned approximately 8 mm dorsal to the alveolar margin at the anterior end but extending closer to the alveolar margin posteriorly. Ventral to this ledge, small, triangular interdental plates that are clearly separated are present between adjacent alveoli as in *Decuriasuchus quartacolonia* (França et al., 2013). This is in contrast to the fused interdental plates of some loricatans such as *Postosuchus kirkpatricki* and *Polonosuchus silesiacus* (Nesbitt, 2011).

The left maxilla of NHMUK PV R6792 has 12 alveoli, although the anterior- and posterior-most alveoli are incompletely preserved (Fig. 4B). Based on comparisons to the referred maxilla, NHMUK PV R36889 (Fig. 5), an additional alveolus was probably present at the anterior end, suggesting a complete tooth count of at least 13, which is similar to other paracrocodylomorphs. Alveoli 2–5 of NHMUK PV R6792 are approximately equal in size (anteroposterior length of ca. 9 mm; transverse width of ca. 7 mm), but they decrease slightly in size more posteriorly, with the tenth alveolus being ca. 6.5 mm long and 6 mm wide. The alveoli are transversely compressed, with an oval outline. Fragments of tooth crowns are present in alveoli 2, 3, 4, 6, and 10. Little information is available on the morphology of the crowns, but the replacement crown in alveolus 6 is transversely compressed and recurved,

with fine serrations on its mesial and distal margins. These serrations are chisel-like, with approximately 4 serrations per mm.

Two fragments of the right maxilla of NHMUK PV R6792 are preserved (Fig. 4E, F), and probably represent a continuous section of the tooth row, although there is no clear articulation between the two pieces. The first fragment (Fig. 4E) is 28 mm long anteroposteriorly, and includes the base of the dorsal process of the bone (including the anteroventral corner of the antorbital fossa), the anterior process (broken anteriorly, but slightly more complete than in the left maxilla), and the base of the posterior process. Four alveoli are present, although the anterior- and posterior-most alveoli are incomplete, and the tip of a tooth crown (with a serrated distal margin) is partially exposed in the second alveolus. The morphology and size of the fragment are consistent with that of the left maxilla. On the lateral surface of the anterior process, close to its dorsal margin, a short, curved canal is faintly indicated, and at its posterior end is continuous with a foramen in the maxilla.

The second fragment of right maxilla of the holotype (Fig. 4F) is part of the posterior process of the bone, and is 35 mm long as preserved. Laterally, it is bevelled at its dorsal margin where it forms an antorbital fossa along the ventral margin of the antorbital fenestra. Medially, the ledge that separates the alveoli from the medial surface of the bone is well demarcated. Poorly preserved interdental plates are present. Four alveoli are present, with a fragmentary tooth located in the third of these.

The more complete referred left maxilla, NHMUK PV R36889 (Fig. 5), is nearly complete anteroposteriorly, but lacks most of the dorsal process. It is generally consistent in morphology with the holotype maxilla, although slightly smaller in size. Anterior to the dorsal process there is a well-developed anterior process, the dorsal margin of which is formed by a transversely compressed ridge that extends anteriorly from the base of the dorsal process as in *Ticinosuchus ferox* (Krebs, 1965), which is not preserved in the holotype,

NHMUK PV R6792. This ridge is continuous anteriorly with the lateral margin of the palatal process. A large anteriorly opening foramen sits just ventral to the ridge at the anterior end of the maxilla, adjacent to the contact for the premaxilla. A similar foramen is present in some rauisuchids (Lessner et al., 2016), *Decuriasuchus quartacolonia* (França et al., 2013), and in the erpetosuchid *Parringtonia gracilis* (Nesbitt and Butler, 2013; Nesbitt et al., 2017). The anterior process tapers in dorsoventral height towards its anterior termination. Medial to the anterior process, the palatal process is preserved, and is slightly anteroventrally directed (Fig. 5B, C), similar to early diverging poposauroids such as *Xilousuchus sapingensis* (Wu, 1981; Nesbitt et al., 2011). The medial surface of the palatal process has anteroposteriorly directed grooves and ridges, suggesting that it articulated with its opposing element at the midline, as in Archosauria (Nesbitt, 2011). The medial surface of the maxilla is more strongly convex and inflated than in NHMUK PV R6792, but this is likely the result of matrix expansion, and the medial surface is strongly cracked. There is no clearly preserved articular facet for the palatine.

The dorsal process of the left maxilla of NHMUK PV R36889 is similar to that of NHMUK PV R6792 in being comparatively thin and compressed anteromedially to posterolaterally, although the exact orientation of this process differs slightly between the two. There is a well-defined antorbital fossa, which continues nearly to the end of the posterior process. The dorsoventral depth of this fossa is approximately equal to the dorsoventral height of the lateral surface of the maxilla below the fossa. The fossa tapers in dorsoventral height posteriorly. The ventral margin of the fossa is demarcated by a distinct ridge, which is raised above the lateral surface and is most pronounced in the centre of the bone. The posterior process of the maxilla tapers gently posteriorly, as in *Xilousuchus sapingensis* (Wu, 1981; Nesbitt et al., 2011), and is not rectangular as in *Decuriasuchus quartacolonia* (França et al., 2013) and in most loricatans (e.g., *Prestosuchus chiniquensis*,

Saurosuchus galilei, *Postosuchus kirkpatrickorum*). The dorsal margin of the posterior half of the posterior process forms a transversely compressed ridge. The ventral margin of the maxilla is sigmoidal in lateral view. Twelve alveoli are preserved.

Dentary

A single dentary fragment is present in the holotype, NHMUK PV R6792 (Fig. 4G–I), and is 43 mm long anteroposteriorly, with a maximum dorsoventral height of 17 mm. Its anterior and posterior ends are broken, in each case through an alveolus, and it is slightly damaged along the alveolar margin. The symphysis is not preserved. Charig (1956) identified this as a right dentary on the basis of a slight inclination of the alveoli in what was presumed to be a posterior direction, which seems plausible. The lateral surface of the bone is dorsoventrally convex (Fig. 4G) and a series of small nutrient foramina is present a short distance (4–5 mm) below the alveolar margin. The anterior foramina are more circular, whereas those placed more posteriorly are more elongated anteroposteriorly. On the medial surface (Fig. 4I), the lateral walls of the alveoli are damaged; ventral to this there is a dorsoventrally narrow (3 mm deep) Meckelian groove that extends along the entire preserved length of the element. Small triangular interdental plates are present between several of the alveoli on the medial surface and, as in the maxilla, they do not appear to be fused. Seven similarly sized alveoli are preserved, although the anterior- and posterior-most are incomplete. No tooth fragments are preserved. The depth of the preserved portions suggests that the dentary of *Mandasuchus* was more slender than those of other loricatans and of *Ticinosuchus ferox*.

Vertebrae

As preserved, the vertebral column of the holotype, NHMUK PV R6792, consists of seven cervicals (including the axis), 15 dorsals, one sacral, and nine caudals (Fig. 6). Based on the relative sizes of the vertebrae, Charig (1956) reconstructed the column as including eight cervicals (including the atlas/axis), 17 dorsals (with D2–3 missing), two sacrals (with S1 missing), and a minimum of 11 caudals (as Ca4 and Ca9 are missing from the sequence). This sequence seems reasonable in terms of expected vertebral counts among early archosaurs and given the relative sizes of individual vertebrae.

Axis—The axis is almost complete (Fig. 7A–F), but lacks the odontoid process and the left postzygapophysis. The anteroventral corner of the centrum and the neural arch pedicles are reconstructed in plaster. The centrum is approximately 1.5 times longer than tall in lateral view. Its anterior articular surface is broken and restored with plaster, but the dorsal part of this surface is gently concave. In lateral view, the posterior margin of the centrum is vertical, whereas its ventral margin is concave. The lateral surfaces of the centrum are strongly concave anteroposteriorly and weakly convex dorsoventrally. No vascular or pneumatic foramina are apparent. The two lateral surfaces converge ventrally to form a sharp ventral keel, so that in ventral view the centrum has an hourglass-shaped outline. A thin line of matrix on the left side of the axis might represent the neurocentral junction, but a corresponding feature cannot be traced on the right. The posterior articular surface has a subcircular outline in posterior view and is shallowly concave. The parapophysis is a prominent rounded boss positioned on, or just ventral to, the neurocentral junction. It lies slightly posterior and ventral to the anterodorsolateral corner of the centrum. In lateral view, the axial neural spine is broad and fan-shaped. Its anterior margin slightly overhangs the preserved portion of the centrum, but posteriorly it expands considerably and would have overlapped the third cervical for approximately one-quarter to one-third of its length. The anterior margin of the neural spine is dorsoventrally convex, its dorsal margin is almost

straight and increases in depth posteriorly, and (although broken at its tip) its posterior margin appears to taper to a narrow rounded process as in *Ticinosuchus ferox* (Krebs, 1965). The dorsal edges of the axial neural spine of *Prestosuchus chiniquensis* (UFRGS-PV-0156-T) and *Saurosuchus galilei* (Trotteyn et al., 2011) have much steeper angles in lateral view. In anterior view, the neural spine is thickest at its base, thinning dorsally to form a mediolaterally compressed plate. However, the posterior part of the spine is slightly expanded mediolaterally with respect to its anterior portion in dorsal view, though this does not form a distinct, dorsally flattened, transverse expansion of the dorsal margin ('spine table'). The posterior margin of the spine is excavated by a shallow postspinal fossa. In lateral view, the postzygapophyses extend slightly posterior to the centrum and their articular facets are inclined at an angle of approximately 10º from the horizontal. The articular facets are approximately twice as long as wide, have a subrectangular outline in ventral view with a rounded posterior margin, and possess gently concave surfaces. In posterior view, a thin spinopostzygopophyseal lamina connects the dorsal margin of the postzygapophysis with the posterior margin of the neural spine. There is no indication of an epipophysis.

Only a small part of the axis is preserved in NHMUK PV R6793 (Fig. 8). The axis of NHMUK PV R6794 (Fig. 9A, B) includes the odontoid, axial intercentrum, axial centrum, and the detached neural spine, but lacks other parts of the neural arch. The axial centrum, intercentrum, and odontoid are unfused and the sutures between them are clear. The intercentrum is small, wedge-shaped, and contacts the centrum posteriorly and the odontoid dorsally. In anterior view it has a crescentic outline and a flat articular surface, while in lateral view it is triangular in outline, tapering dorsally with a concave ventral margin. The odontoid contacts the centrum posteriorly and its posteroventral margin overlaps the dorsal part of the axial intercentrum. The dorsal part of the odontoid's anterior surface extends further anteriorly than its ventral part in lateral view, forming the articular surface for the

atlas. In anterior view, this articular surface is transversely and dorsoventrally convex and has a crescentic outline. The articular surface is mediolaterally expanded to overhang the lateral surface of the odontoid. In lateral view, the odontoid has a trapezoidal outline and its lateral surface is strongly concave anteroposteriorly and convex dorsoventrally ('saddle-shaped'). The dorsal surface of the odontoid is shallowly excavated along its midline. A small, elliptical parapophyseal facet is situated on a short pedicle on the anterior margin of the axial centrum at a point level with the dorsal margin of the intercentrum. The axis is identical to that of NHMUK PV R6792 in all other respects. NHMUK PV R6793 also possesses an axial centrum that is identical to that of both NHMUK PV R6792 and R6794.

Post-Axial Cervicals—Six post-axial cervical vertebrae (Ce) are present in the holotype, NHMUK PV R6792 (Figs. 6, 7G–R). Ce3–5 are in articulation with each other. Ce3 includes a poorly preserved partial centrum and neural arch, but is anatomically uninformative; Ce4 consists of a complete neural arch; and Ce5 is an almost complete neural arch. Ce6–7 are almost complete (Fig. 7G–R) and Ce6 has two osteoderms attached to its neural spine. Ce8 consists of an almost complete centrum, lacking the neural arch. No cervical ribs are preserved.

The cervical centra (Ce6–8) are amphicoelous. Ce6 has an elongate centrum that is approximately 1.8 times as long as it is high. This length is similar to that of the highly compressed vertebrae of *Ticinosuchus ferox* (Krebs, 1965), shorter than the homologous vertebrae of poposauroids (e.g., *Qianosuchus mixtus* [Li et al., 2006]; *Arizonasaurus babbitti* [Nesbitt, 2005]), but longer than those of *Stagonosuchus nyassicus* (Gebauer, 2004), *Prestosuchus chiniquensis* (UFRGS-PV-0156-T), *Batrachotomus kupferzellensis* (Gower and Schoch, 2009), and *Saurosuchus galilei* (Trotteyn et al., 2011). Centrum elongation is less in Ce7 and Ce8, each of which has an elongation index of approximately 1.4. The anterior and posterior margins of the centra are vertically oriented, while the ventral margin is concave in

lateral view. The anterior and posterior articular surfaces are subequal in height and width and possess subcircular outlines. The lateral surfaces of the centra are longitudinally concave and lack foramina or fossae. They are separated from the ventral surface of the centrum by gentle breaks in slope, rather than well-defined ventrolateral ridges. The ventral surfaces of the centra are gently convex and a short, low midline keel extends along most of its length, but is less prominent posteriorly. Large parapophyses are present on the anteroventral corners of the centra. The parapophyseal facets are positioned at the end of short, robust pedicles and have concave articular surfaces with subelliptical outlines, whose long axes are directed anteroposteriorly. No distinct centrodiapophyseal laminae are present, but a short, low ridge-like swelling extends between the posterior margin of the diapophysis and the centrum. The neurocentral sutures are not generally visible in this specimen, but appear to be obliterated in Ce7.

In anterior view, the neural canal of Ce6 has a subelliptical outline, with its long axis oriented mediolaterally (Fig. 7G). However, all of the posterior neural canal openings and the anterior opening of Ce7 have subcircular outlines (Fig. 7H, M, N). In lateral view, the neural arch pedicles are robust and extend for almost the full length of the centrum. Anteriorly, the margin of the neural arch is flush with the centrum and posteriorly it terminates a short distance anterior to the centrum's posterior margin (Ce4, Ce6–7). The diapophysis is positioned on the neural arch, at the level of the neurocentral junction and close to the anterior margin of the neural arch. It is a short, flange-like structure with a narrow, subelliptical cross-section whose long axis extends anteroposteriorly. The region dorsal to the diapophyses and ventral to the zygapophyses is smoothly convex anteroposteriorly and lacks laminae or fossae. The prezygapophyses are oriented anterodorsally at approximately 20º from the horizontal and extend for a short distance anterior to the centrum. They have stout, subtriangular cross-sections and terminate in bluntly rounded apices. Their articular facets are

flat to very gently concave and have a subquadate outline in dorsal view. In anterior view, the prezygapophyses diverge from each other at an angle of approximately 140º. A deep, but small, prespinal fossa with a subcircular outline is present at the base of the neural spine, between the prezygapophyses. A spinoprezygapophyseal lamina connects the dorsal margin of the prezygapophysis with the anteroventral corner of the neural spine. The postzygapophyses are positioned higher on the neural arch than the prezygapophyses and extend beyond the posterior margin of the centrum for a short distance. The postzygopophyses have stout, subtriangular cross-sections and diverge from each other at angle of approximately 80º in posterior view. Their articular facets face ventrolaterally and are flat to slightly concave, with subquadrate outlines. In posterior view, the postzygapophyses are separated by a deep postspinal fossa, which has a dorsoventrally elongate, elliptical outline. The lateral margin of the postzygapophysis forms a prominent ridge, which extends anteroventrally and then anteriorly to merge with the lateral margin of the prezygapophysis, forming a lamina in an approximately equivalent position to the epipophyseal-prezygapophyseal lamina of some other archosaurs (Wilson, 2012), although an epipophysis is not present. A stout ridge linking the dorsal margin of the postzygapophysis with the posterolateral surface of the neural spine is positionally equivalent to the spinopostzygopophyseal lamina of some other archosaurs. Epipophyses are absent from all post-axial cervicals whereas epipophyses do appear in some paracrocodylomorphs (e.g., *Batrachotomus kupferzellensis* [Gower and Schoch, 2009]; *Xilousuchus sapingensis* [Nesbitt et al., 2011]).

In Ce4–6, the neural spine is anteroposteriorly elongate (Fig. 7I, J): that of Ce7 is shorter (Fig. 7O, P), reflecting the less elongate form of this vertebra in comparison with those preceding it. In lateral view, the spine is narrowest at its base and flares anteroposteriorly towards its apex, with the summit of the spine representing its maximum

length, giving the spine an inverted trapezoidal outline. The spine bases are mediolaterally compressed, but the spine summit expands laterally to form a distinct flat surface ('spine table'), whose lateral margins overhang the remainder of the neural spine, as in most suchians. In dorsal view, the transverse expansion is flat and those of Ce4 and Ce5 have subrectangular outlines. In Ce6 and Ce7, the transverse expansion is subtriangular or teardrop-shaped in outline, tapering posteriorly (Fig. 7L, R). This is associated with a greater mediolateral expansion of the anterior margin of the neural spine relative to the posterior part of the spine, and the expanded anterior margin of the spine bears a low midline ridge in a position equivalent to the prespinal lamina. Hyposphenes and hypantra are absent.

Cervical ribs are not preserved in either NHMUK PV R6792 or NHMUK PV R6793. However, several partial cervical ribs are articulated with their respective centra in NHMUK PV R6794 (Fig. 9A, B), the best preserved of which is the left rib of Ce5. The cervical ribs are double-headed and, in anterior view, the tuberculum and capitulum diverge from each other at an angle of approximately 30º, forming a short 'V'-shaped cleft between them. The tuberculum is slightly longer than the capitulum, and ventrally the two processes merge with the rib shaft. In lateral view, the tuberculum extends dorsally to form an angle of approximately 90º with the rib shaft, and is parallel-sided for most of its length. The capitulum is largely obscured by the tuberculum in lateral view, but a small portion of it is visible as it extends slightly anterodorsally, rather than strictly dorsally. The dorsal-most part of both the tuberculum and capitulum is expanded anteroposteriorly and mediolaterally with respect to the rest of the process, forming a broad, subelliptical articular facet that contacts the diapophysis or parapophysis, respectively. The rib shaft is divided into anterior and posterior processes. The anterior process is shorter than the posterior process and tapers to form a stout, sub-triangular, rounded apex, which is much more robust than that of *Ticinosuchus ferox* (Krebs, 1965). It has a subtriangular transverse cross-section that is

widest ventrally. By contrast, the posterior process is more slender and elongate. Its dorsal surface is excavated by a longitudinal groove that originates from the point where the tuberculum and capitulum merge with the shaft and it deepens posteriorly and extends for the full length of the posterior process. The groove is asymmetrically developed, with the parapet defining the groove laterally being much lower in height than the medial parapet, giving the posterior process a 'J'-shaped cross-section in posterior view. This deep groove receives the anterior process of the next cervical rib in the series, as in most other pseudosuchians with cervical ribs preserved; by contrast, poposauroids have much longer cervical ribs that do not appear to contact each other (e.g., *Qianosuchus mixtus*: Li et al., 2006).

The cervical vertebrae of NHMUK PV R6793 and NHMUK PV R6794 (Figs. 8, 9) closely resemble those of the holotype and provide some additional information on their morphology. In both of the referred specimens, Ce3 possesses a prominent ridge or keel on the midline of the ventral surface, but this is reduced to a faint ridge in the other cervicals, matching the morphology of the posterior cervicals in NHMUK PV R6792. The cervical centra of NHMUK PV R6793 have similarly elongate proportions to those of the holotype, but those of NHMUK PV R6794 (which is the largest of the three specimens) are moderately less elongate than those of the holotype: Ce5 and Ce6 have length/height ratios of ~1.5. Thus, the proportions of the cervical centra appear to change during ontogeny, becoming proportionately shorter in the largest individuals. In both NHMUK PV R6793 and NHMUK PV R6794, the parapophyses are stout elliptical facets set on short pedicles that arise from the anteroventral corners of the centrum. In Ce3–4 the diapophyses are on the anterodorsal corner of the centrum, immediately posterior to its anterior margin, but these migrate dorsally to lie on the neural arch at the level of the neurocentral junction in more posterior cervicals. In both referred specimens, the diapophyses are robust, subelliptical facets, whose long axes are oriented anteroposteriorly. The neurocentral junctions of NHMUK PV R6793 (the

smallest of the three specimens) are all visible, but those of NHMUK PV R6794 are fused and obliterated. A small, distinct fossa is present on the lateral surfaces of the neural spines in Ce6–8 of NHMUK PV R6793, which are less well developed in the other two specimens. This fossa is defined by a raised rim of bone and is positioned immediately dorsal to the ridge arising from the lateral surface of the postzygapophysis. It has a subelliptical outline in lateral view. Finally, Ce7–8 of NHMUK PV R6793 bear distinct spine tables, but they are not expanded to the same extent as those of the holotype. Many of these minor differences likely represent ontogenetic or individual variation: NHMUK PV R6793 is considerably smaller than the holotype, whereas NHMUK PV R6794 is considerably larger.

Dorsal Vertebrae—Fifteen dorsal vertebrae (D) are present in the holotype (Figs. 6, 10, 11). Charig (1956) suggested that D2–3 are missing from the specimen to give a total vertebral count of 17 dorsals. For convenience, we follow his numbering convention herein, but we reverse the order of Charig's D14 and D13 (as marked on the specimens in ink) because we consider 'D14' to lie anterior to 'D13' due to the wider separation between its para- and diapophyses. All dorsal centra are complete. D1, D5, and D15 are represented solely by centra; partial neural arches are present on D4, D6, and D15; and complete or near-complete neural arches are present for D7–14 and D17. D10 and D11 are preserved in articulation. One fragmentary dorsal rib is preserved.

The dorsal centra are longer than tall with length/height ratios of approximately 1.4 along the entire series, similar to the condition in *Ticinosuchus ferox* (Krebs, 1965). They are amphicoelous, with circular articular surfaces. In lateral view, the anterior and posterior margins are vertically oriented, and the ventral margin is gently concave. The lateral surfaces of the centra are shallowly concave longitudinally and dorsoventrally convex. Nutrient foramina and pneumatic fossae are absent, but a shallow excavation is present in the dorsal part of the lateral surface of the centrum, immediately ventral to the neurocentral junction, as

in most other archosauriforms. Parapophyses are present on the anteroventrolateral corner of the centrum in D1 but migrate dorsally on the following vertebrae, reaching the level of the neurocentral junction in D5 and moving on to the neural arch in D6. The parapophyses on D1–6 of the holotype are poorly preserved and have indistinct outlines. In the anterior dorsal vertebrae (D1–10) the lateral surfaces are separated from the ventral surfaces by a distinct break in slope (Fig. 10C, D), but ridges dividing these surfaces are either absent or only very weakly expressed. Centra in the posterior dorsal vertebrae (D11–17) have a more spool-like morphology (e.g., Fig. 10K), with the lateral and ventral surfaces merging smoothly into each other. The ventral surfaces of all dorsal vertebrate lack either grooves or keels. In dorsal view, the centra are deeply excavated to form the neural canal, with this excavation reaching its maximum depth at midlength.

In anterior and posterior views, the neural canal openings are almost circular in outline, with the exception of D17 where the opening is subrectangular and taller than wide. All of the neurocentral junctions are obliterated along the entire dorsal series of the holotype. In lateral view, the prezygapophyses project anterodorsally, forming an angle of approximately 30º with the horizontal. In D1–11 they lie in the same horizontal plane as the diapophyses, but from D12–17 they extend further dorsally than the diapophyses. In all dorsal vertebrae, the prezygapophyses project a short distance beyond the anterior margin of the centrum and have a subtriangular transverse cross-section. The articular surface of the prezygapophysis has an ovate outline in dorsal view. These surfaces are flat, face almost strictly dorsally, and are inclined only slightly medially. A deep, narrow, ‘V’-shaped cleft separates the prezygapophyses in dorsal view and extends as far posteriorly as the base of the neural spine. A prominent spinoprezygapophyseal lamina connects the posterior margin of the prezygapophysis with the neural spine, and the left and right laminae frame a deep prespinal fossa that extends dorsally for a short distance along the anterior margin of the

neural spine. In D6–D9, a thin, but prominent, prezygodiapophyseal lamina is also present, which forms the dorsal margin of a dorsoventrally narrow, horizontally inclined prezygapophyseal-paradiapophyseal fossa. In D10–D17 a distinct prezygodiapophyseal lamina is absent; instead, a low rounded ridge extends between the lateral surface of the prezygapophysis and the dorsal margin of the parapophysis.

In D6–D12, the parapophyseal facet is small and elliptical, with its long axis oriented vertically. It has a concave articular surface and is positioned on a short parapophysis that projects laterally from the anteroventral corner of the neural arch. In these vertebrae, the dorsal margin of the parapophysis is connected to the underside of the diapophysis by a well-developed parapodiapophyseal lamina, which forms the ventral margin of the prezygapophyseal-paradiapophyseal fossa and the dorsal margin of a large centrodiapophyseal fossa. In D6 and D7, a low ridge connects the ventral margin of the parapophysis with the centrum, but in these and all other dorsals a distinct anterior centrodiapophyseal lamina is absent. The parapophysis is situated ventral to the diapophysis in D6–11, but in D11–D13 is increasingly dorsal, becoming almost level with the diapophysis. In D13–17, the parapophyses merge with the diapophyses, obliterating the paradiapophyseal laminae from D14 onward and forming a combined articular facet with an ‘8’-shaped cross-section.

In all dorsals, the diapophysis projects laterally in dorsal view and almost horizontally or very slightly ventrally in anterior view. It has a flattened triangular or subelliptical longitudinal cross-section that is dorsoventrally deepest along its posterior margin. The dorsal surface of the process is flat. In D7–11 the posteroventral margin of the diapophysis supports a prominent posterior centrodiapophyseal lamina, which forms the posterior margin of a deep triangular, ventrally opening centrodiapophyseal fossa and the anterior margin of a small, deep, posteriorly opening postzygapophyseal-centrodiapophyseal fossa. In D7, a small

foramen is present within the deepest part of the centrodiapophyseal fossa, which appears to communicate with another foramen positioned on the dorsal surface of the neural arch, just lateral to the base of the neural spine. This second foramen is positioned within a shallow depression. It is not possible to determine if the foramen within the centrodiapophyseal fossa is present in any of the other dorsal vertebrae as a result of either lack of preparation or poor preservation, although it is plausibly present in other vertebrae with similarly deep centrodiapophyseal fossae. The depression and associated foramen does, however, seem to be present in at some of the other middle and posterior dorsals, though it is not clear if the foramina are genuine features or a consequence of over-preparation within these small depressions. In D7–11, the posterior margin of the diapophysis is linked to the ventral margins of the postzygapophyses by a well-developed postzygodiapophyseal lamina, which forms the dorsal boundary of the postzygapophyseal-centrodiapophyseal fossa. However, both the posterior centrodiapophyseal lamina and the postzygodiapophyseal laminae are absent in D12 onwards, with the coincident absence of the postzygapophyseal-centrodiapophyseal fossa.

The postzygapophyses project a short distance beyond the posterior margin of the centrum. In posterior view, they diverge from each other at an angle of approximately 10º to the vertical and are separated by a deep, slit-like postspinal fossa that extends for approximately half of the total neural spine height. The fossa is defined by prominent spinopostzygopophyseal laminae, as also occurs in *Stagonosuchus nyassicus* and *Ticinosuchus ferox* (Lautenschlager and Desojo, 2011). The articular surfaces of the postzygapophyses face ventrolaterally and in ventral view are triangular in outline and shallowly concave. There is no evidence for a distinct hyposphene.

In lateral view, the neural spine forms a large subrectangular or trapezoidal plate that extends dorsally and is inclined slightly posteriorly. It expands asymmetrically so that its

anterior and posterior margins diverge as they extend dorsally, with the result that the posterior margin of the spine overhangs the posterior margin of the vertebra. The anterior, posterior, and dorsal margins of the spine are all straight. In anterior view, the ventral part of the neural spine is mediolaterally compressed, but it expands laterally at its distal part (= 'spine table'), although this feature is not as prominent as in the middle and posterior cervicals. Similar expansions are present in *Nundasuchus songeaensis* (Nesbitt et al., 2014), some earlier diverging suchians (e.g., *Parringtonia gracilis*: Nesbitt and Butler, 2013; Nesbitt et al., 2017), possibly in *Ticinosuchus ferox* (Krebs, 1965), and *Saurosuchus galilei* (Trotteyn et al., 2011), but are absent in rauisuchids (Nesbitt, 2011). The distal surface is excavated by a shallow midline groove that extends for its entire length. In dorsal view the expansion has a narrow elliptical outline that is widest posteriorly. The posterior margins of the spines bear shallow, roughened grooves.

The only available dorsal rib in the holotype, NHMUK PV R6792, is a fragment of rib shaft (Fig. 12C, D). It is anteroposteriorly flattened, with an elliptical transverse cross-section. Both the anterior and posterior surfaces bear a shallow dorsoventral groove that extends along its entire length. This rib was sampled histologically by de Ricqlès et al. (2008).

The anterior dorsal vertebrae of NHMUK PV R6793 (Fig. 8) provide additional information that is absent from the holotype. In general, they are very similar to the middle dorsal vertebrae of the holotype, but differ in several respects. As in the holotype, the parapophyses are positioned on the centrum in D1–3 and slightly dorsal to the neurocentral junction in D4. In D1 the parapophysis is on the ventrolateral corner of the centrum, and is increasingly dorsally positioned in each subsequent vertebra. The parapophyseal facet has an elliptical outline, with the long axis of the ellipse oriented subvertically, and the articular facet is gently concave. D1–5 each possess prominent paradiapophyseal,

prezygodiapophyseal, posterior centrodiaopophyseal, spinoprezygapophyseal, and spinopostzygapophyseal laminae. These laminae frame well developed prezygapophyseal-paradiapophyseal, centrodiapophyseal, postzygapophyseal-centrodiapophyseal, prespinal, and postspinal fossae (Gower, 2001), as in the middle dorsal vertebrae of the holotype. The only difference in neural arch laminae fossae between NHMUK PV R6793 and the middle dorsals of the holotype is in the size and shape of the prezygapophyseal-paradiapophyseal fossa: in D1–4 of NHMUK PV R6793 this fossa is much larger and has a wide, triangular outline, due to the more ventral position of the parapophysis. However, D5 of NHMUK PV R6793 has a more dorsally positioned parapophysis (on the lateral surface of the neural arch), which creates a narrower prezygapophyseal-paradiapophyseal fossa that it is much more similar in extent and outline to that of the holotypic middle dorsal vertebrae. The only other substantive difference between the anterior dorsal vertebrae of NHMUK PV R6793 and the middle dorsal vertebrae of the holotype is in neural spine height: the neural spines of NHMUK PV R6793 are shorter than centrum height, whereas the opposite occurs in the middle dorsal vertebrae of the holotype.

Aside from their larger size, the dorsal vertebrae of NHMUK PV R6794 do not differ in any way from those of either the holotype or NHMUK PV R6793 (Fig. 9C, D). NHMUK PV R6794 includes one partial dorsal rib, consisting of the proximal end only. The capitulum forms an elongate process that extends for a considerable distance dorsal to the tuberculum. It has a subcircular, concave articular facet, and a subcircular cross-section that decreases in diameter ventrally. The articular facet of the tuberculum is elliptical in outline, with the long axis of this ellipse oriented transversely. Shallow concavities separate the capitulum from the tuberculum on both the anterior and posterior surfaces of the proximal end. The proximal-most part of the rib shaft has a subtriangular cross-section.

Sacral Vertebrae—The second sacral vertebra is present in the holotype (Fig. 13), is slightly distorted, and missing its neural spine and the postzygapophyses. The right rib and diapophysis have been heavily reconstructed and some plaster has been used to repair the left rib. The anterior articular surface of the centrum is subcircular in outline, whereas the posterior surface is shield-shaped, but the shapes of both surfaces have been altered by oblique shearing. Both articular surfaces are flat to very shallowly concave in their central regions. The anterior articular surface is both taller and wider than the posterior surface. The centrum is spool-shaped, with longitudinally concave lateral surfaces. The lateral surfaces are strongly convex dorsoventrally and merge ventrally to form a smoothly continuous surface. Ventral midline structures, such as a groove or keel, are absent. There is no indication of any centrodiapophyseal laminae or buttresses. The rib articulates with the centrum, via a facet that occupies the dorsal part of the centrum lateral surface. The rib facet occupies the center of the lateral surface and is approximately equal to half centrum length.

In anterior view, the neural canal opening is wider than tall, but this is reversed posteriorly to become taller than wide. The prezygapophyses are short, triangular processes that barely extend beyond the anterior surface of the centrum and that diverge from each other at an angle of approximately 70º in dorsal view. They lack distinct articular surfaces and are continuous with low, but distinct, spinoprezygopophyseal laminae that frame a shallow, triangular prespinal fossa.

The sacral rib extends laterally and slightly ventrally and posteriorly. A thin, sheet-like flange projects posteriorly from its posterdorsal corner. In lateral view, the articular facet for the ilium has a teardrop-shaped outline and a shallowly concave surface. The size of the sacral rib appears smaller than that of *Stagonosuchus nyassicus* (Gebauer, 2004) and *Nundasuchus songeaensis* (Nesbitt et al., 2014); however, the difference in size may be the result of incomplete preservation in *Mandasuchus tanyauchen*.

Caudal Vertebrae—Nine caudal vertebrae (Ca) are preserved in NHMUK PV R6792 (Figs. 6, 14), which Charig (1956) identified as Ca1–3, Ca5–8, and Ca10–11. These identifications are plausible and consistent with changes in morphology along the series. Although it is possible that some are incorrect by a position or two, these identifications are used for convenience herein. All of the preserved centra are essentially complete, but only Ca1, Ca5, and Ca11 include substantial portions of the neural arch. None of the vertebrae are complete.

The proportions of the centra change along the series. In Ca1 the centrum is slightly longer than it is tall (length/height ratio = 1.08); in Ca2, Ca3, and Ca5 the length/height ratio is ~1.0; and in the more posterior vertebrae the centra become more elongate with length/height ratios of 1.12–1.35. All of the centra are mildly amphicoelous. The anterior and posterior articular surfaces of the centra in Ca1–8 are subcircular and approximately as broad as they are tall, whereas in Ca10–11 they are elliptical and taller than wide. The anterior articular surface of each centrum is usually taller and wider than its posterior articular surface. Distinct anterior chevron facets are absent. Posterior chevron facets are absent in Ca1–3, but are present from Ca5 onwards. The posterior chevron facets are bevelled anteriorly and have ‘W’-shaped outlines in posterior view, with a deep midline notch.

The centra of Ca1–2 are spool-shaped with longitudinally concave and dorsoventrally convex lateral surfaces that merge ventrally around a smooth curve, so that the centrum has a subcircular transverse cross-section at midlength. The ventral midline in Ca1–2 possesses neither a groove nor a keel. The lateral surfaces of Ca3–11 are also longitudinally concave and dorsoventrally convex, but in contrast to the proximal-most caudals the lateral surfaces of the centrum are divided from the ventral surface by a distinct break in slope. This becomes a more prominent and ridge-like feature from Ca5 onward, giving the centra a subquadrate transverse cross-section at midlength. The ventral surface of Ca3 is flat, but those of Ca5

onward bear a midline groove that extends for the full length of the ventral surface, becoming deeper posteriorly. This groove is continuous with the notch dividing the two lobes of the posterior chevron facet.

In Ca1 and Ca5 the neural canal is subelliptical in outline and wider than tall. None of the caudals preserve the prezygapophyses, but prominent prezygodiapophyseal and spinoprezygopophyseal laminae are present in Ca1 and Ca5, and these also appear to be present in *Ticinosuchus ferox* (Krebs, 1965). A shallow depression lies ventral to the prezygodiapophyseal lamina that could be regarded as a prezygapophyseal-centrodiapophyseal fossa, though the ventral margin of this depression is bounded only by a low ridge that occupies the position of the anterior centrodiapophyseal lamina. The spinoprezygopophyseal laminae form the boundaries of a deep, triangular prespinal fossa. The caudal ribs are incompletely preserved, but it can be determined that they projected laterally and slightly posteriorly, and that they had a subtriangular transverse cross-section. There is no evidence for the presence of a posterior centrodiapophyseal lamina. The postzygapophyses are only partially preserved in Ca1 and Ca5, but they were triangular in cross-section and each supported a short but prominent spinopostzygapophyseal lamina. These laminae frame a deep, slit-like postspinal fossa. The neural spines have a subrectangular outline in lateral view and project dorsally and slightly posteriorly. They are anteroposteriorly short, with similar proportions to those of *Ticinosuchus ferox* (Krebs, 1965), and mediolaterally flattened plate-like structures with straight anterior, posterior, and dorsal margins. In anterior view, the neural spine thickens slightly towards its dorsal edge, but it does not form the distinct lateral expansion (‘spine table’) at the distal end that is seen in the cervical and dorsal regions. The phylogenetic distribution of lateral expansions of the distal neural spine in caudal vertebrae is not clear, but expansions do occur in aetosaurs (Parker, 2016), *Parringtonia gracilis* (Nesbitt and Butler, 2013), and possibly in

Ticinosuchus ferox (Krebs, 1965) and *Batrachotomus kupferzellensis* (Gower and Schoch, 2009), but they are absent in *Polonosuchus silesiacus* (Sulej, 2005). None of the caudals are sufficiently preserved to confirm whether or not a distinct anterior prong ('accessory neural spine': see Lautenschlager and Desojo, 2011) was present.

The neural spine of Ca11 is poorly preserved, but differs in morphology from those in Ca1 and Ca5. Caudal ribs, zygapophyses, and pre- and postspinal fossae are still present, although all of these features are reduced in size and prominence. Most obviously the neural spine is shorter, projecting only a short distance dorsal to the postzygapophyses. In addition, the neural spine is a different shape, with a posteriorly sloping anterior margin that meets with the vertically orientated posterior margin to form a rounded triangular apex.

The caudal vertebrae preserved in both NHMUK PV R6793 and NHMUK PV R6794 are identical to those of the holotype in almost every respect (Figs. 8, 9). The only minor difference is that in Ca4–7 of NHMUK PV R6794, the ventral grooves on the centra are slightly less distinct than in the holotype.

Chevrons are not preserved in any of the available specimens, with the exception of a small uninformative fragment attached to one of the distal caudal centra of NHMUK PV R6794.

Scapulacoracoid

Both scapulae are preserved in the holotype, NHMUK PV R6792 (Fig. 15). Both are missing small portions of their dorsal margins, and are damaged along the anterior margin of the blade and proximal end, with the acromion missing. The scapula and coracoid are not fused, and the articular surface for the coracoid is straight. The scapula consists of an expanded ventral plate and a blade that expands in anteroposterior width towards its distal end, and this expansion is greater than that present in *Ticinosuchus ferox* (Krebs, 1965). The

ventral plate is transversely expanded adjacent to the glenoid, but tapers to a thin sheet anteriorly. The scapula is strongly arched along its length in anterior or posterior view, and has a concave posterior margin in lateral view. It forms approximately one-third of the glenoid fossa. The glenoid faces mostly posteriorly and slightly laterally. There is an oval, laterally facing scar on the posterior margin of the lateral surface of the blade, slightly dorsal to the glenoid, but this is not distinctly raised from the surface of the bone, unlike in, for example, *Batrachotomus kupferzellensis* (Gower and Schoch, 2009). Part of the left coracoid is preserved in articulation with the left scapula of the holotype (Fig. 15), although it is incomplete along ventral and anterior margins and provides little anatomical information. The rim of the coracoid foramen is partially preserved: the foramen lies entirely within the coracoid, and is directly anterior to the glenoid fossa. The ventral margin of the posterolateral portion of the preserved portion of the coracoid is thickened relative to the more anterior portion, as in most crown archosaurs (Nesbitt, 2011).

Left and right scapulae and a partial right coracoid are present in NHMUK PV R6793 (Fig. 16A–E), but they do not add any more anatomical information to that provided by the holotype, with which they are consistent in morphology.

Humerus

The proximal and distal ends of the holotypic right humerus, NHMUK PV R6792, are preserved (Fig. 17), and have been attached to each other via a reconstructed midshaft region. This reconstruction (by AJC) was based upon comparisons with the humeri of the referred specimen NHMUK PV R6793, which preserves the midshaft region. The proximal end of the holotype humerus is damaged along most of its margins, limiting information on the proximal articular surface. The head is confluent with the rest of the bone and is not offset. The short but well-developed deltopectoral crest was originally more complete (as figured in

Charig, 1956), but has since been damaged. Its apex is level with a point that is slightly less than 20% of the reconstructed length of the bone. There is a faint muscle scar (= likely for the origin of the M. triceps: Gower and Schoch, 2009) on the posterolateral surface of the proximal end, expressed as a pit with rugosities on the distal margin. Distal to this muscle scar a faint proximodistally extending ridge (supinator ridge) marks the boundary between the main shaft and the deltopectoral crest.

The distal end of the holotype humerus is well preserved. The ectepicondylar groove is well developed with a prominent supinator process anteroventral to it. At its lateral margin, the supinator process curls slightly posterolaterally, but does not enclose the ectepicondylar groove to form a foramen as occurs in some aetosaurs (e.g., *Longosuchus meadei*: Sawin, 1947). Posteriorly, the two condyles are separated by a broad, well-developed fossa; anteriorly the condyles and the distal surface frame a triangular depression on the anterior surface. The lateral condyle is circular in distal view, whereas the medial condyle is broader mediolaterally than anteroposteriorly.

The two humeri of NHMUK PV R6793 are consistent in morphology with the holotype (Fig. 16F–P). The left humerus has a short, but well developed, deltopectoral crest and a complete proximal margin that is strongly convex in anterior or posterior view.

Ulna and Radius

The left ulna is present in NHMUK PV R6793 (Fig. 16Q–V), but is missing its distal end. The bone is straight in lateral and anterior views. The proximal end expands anteriorly relative to the shaft in lateral view, and medially in anterior view. It has a low but distinct olecranon process and a well-developed lateral tuber, as in all archosaurs (Nesbitt, 2011). Shallow, broad grooves extend proximodistally along the middle of the medial and lateral surfaces of the shaft. The ulna of *Mandasuchus tanyauchen* is much more robust than those

of *Ticinosuchus ferox* (Krebs, 1965), *Postosuchus alisonae* (Peyer et al., 2008), and *Batrachotomus kupferzellensis* (Gower and Schoch, 2009). Several fragments in NHMUK PV R6793 may represent parts of the proximal and distal ends of the radius, but they provide little anatomical data.

Ilium

All three pelvic bones are present on each side of the holotype, NHMUK PV R6792, and have been glued into articulation with each other (Fig. 18). The right ilium is mostly complete but the pubic peduncle has been reconstructed. On the left side the distal tip of the postacetabular process is missing, the dorsal margin of the iliac blade is damaged, and the bone is reconstructed at the point where the ischial and pubic peduncles converge. The preacetabular process of the ilium is complete, short, terminates well posterior to the level of the anterior tip of the pubic peduncle, and is broadly rounded in lateral view. In dorsal view the preacetabular process bends gently medially towards its anterior tip but is mostly projected anteriorly. The dorsolateral margin of the process has many well-developed nearly vertical grooves and ridges. This scarred surface terminates immediately dorsal to the anteroposterior midpoint of the acetabulum. The dorsal margin of the ilium is straight in lateral view. The postacetabular process of the ilium is nearly complete on the right side, and is elongate, probably being at least as long anteroposteriorly as the anteroposterior length of the acetabulum. The ventral margin of the ilial postacetabular process is folded inwards to form a near horizontal shelf (medial ridge) that expands in transverse width towards its posterior end. In lateral view the postacetabular process tapers in dorsoventral height towards its posterior end. The dorsolateral margin of the process is slightly rugose. A well-defined supraacetabular rim overhangs the deeply concave acetabulum. Dorsal to this rim, there is no development of a distinct vertical ridge or crest as in *Prestosuchus chiniquensis* (UFRGS-

PV-0629-T: Liparini and Schultz, 2013), *Stagonosuchus nyassicus* (Gebauer, 2004), aetosaurs, and phytosaurs. This contrasts with the presence of a well-defined vertical ridge in some loricatans (e.g., *Batrachotomus kupferzellensis*: Gower and Schoch, 2009) and poposauroids (*Arizonasaurus babbitti*: Nesbitt, 2005). It cannot be confirmed unequivocally from the holotype if the acetabulum was completely closed or not, because parts of it are broken on both sides; however, the acetabulum is completely closed in the referred specimen NHMUK PV R6794. The overall morphology of the ilium is comparable to that of *Ticinosuchus ferox* (Lautenschlager and Desojo, 2011), although detailed comparisons are limited as the ilia of the latter are compressed and preserved only in medial view.

On the medial surface, there are two sacral rib scars medial to the dorsal part of the acetabulum. The scar for the first sacral rib is immediately posterior to the conjunction of the preacetabular process and the pubic peduncle, and extends onto the ventral base of the preacetabular process. The scar for the second sacral rib is anterior to the conjunction of the ischiadic peduncle and the postacetabular process. It tapers onto the postacetabular process, with its dorsal margin formed by the medial ridge. These two sacral rib scars correspond to the plesiomorphic primordial sacral vertebrae in Archosauria (see Nesbitt, 2011).

The complete left ilium of NHMUK PV R6794 (Fig. 19) is consistent with the morphology of the holotype, and does not add much information, with the exception of demonstrating the closure of the acetabulum.

Pubis

The pubes of the holotype, NHMUK PV R6792, are mostly complete (Fig. 18), but in both the thin pubic apron is damaged and incomplete, and both are damaged along their acetabular margins, including the contact with the ischium. The pubis is slightly longer than the ischium, and slightly longer than the anteroposterior length of the ilium as also occurs in

other paracrocodylomorphs (Nesbitt, 2011). The acetabulum extends onto the ventral half of the proximal surface of the pubis, forming a concavity, as in *Stagonosuchus nyassicus* (Gebauer, 2004) and *Prestosuchus chiniquensis* (UFRGS-PV-0629-T: Liparini and Schultz, 2013). This is well preserved on the left side, but the proximal end of the right pubis has suffered damage. The ambiens process is a low anteroventrally-to-posterodorsally elongated ridge along the lateral edge of the proximal end of the bone. Parallel and anterodorsal to this ridge, there is a shallow groove. The obturator fenestrae are incomplete on both sides, but the parts of the rims that are present suggest that they were circular and proportionally smaller than those in *Fasolasuchus tenax* (Bonaparte, 1981) and Crocodylomorpha (Nesbitt, 2011). The pubic apron is broken medially on both elements along most of its length, but is transversely complete at its distal end, where it forms a flattened articular surface for contact with the opposing element. The combined pubic apron does not narrow distally, unlike the condition in some poposauroids (Nesbitt, 2007). The shaft of the pubis is gently rounded laterally, and tapers medially to form the apron. The distal end of the element is slightly expanded anteroposteriorly, forming a very weakly developed 'boot'; this 'boot' is absent in *Ticinosuchus ferox* (Krebs, 1965; Lautenschlager and Desojo, 2011). The distal surface is slightly concave and incompletely ossified.

The left pubis of NHMUK PV R6794 is relatively complete, but as in the holotype the acetabular margin and apron are damaged. It is consistent in morphology with the holotype, but the distal boot is more strongly developed (Fig. 19), and mostly expanded posteriorly, and the distal surface is convex and rugose, suggesting that it is fully ossified. The distal boot is mediolaterally thick and rounded as in *Stagonosuchus nyassicus* (Gebauer, 2004), *Prestosuchus chiniquensis* (UFRGS-PV-0629-T: Liparini and Schultz, 2013), and *Batrachotomus kupferzellensis* (Gower and Schoch, 2009), but in contrast to the mediolaterally thin distal boots of poposauroids (Nesbitt, 2007, 2011).

Ischium

The right ischium of the holotype, NHMUK PV R6792, is well preserved (Fig. 18), and nearly complete, although damaged along its anteroventral margin close to the acetabulum. The left ischium is less well preserved, and is partially reconstructed slightly proximal to midlength, and close to the distal end, as well as also being damaged along its anteroventral margin. The acetabulum extends onto the proximal ischium, with its posteroventral rim being defined by a sharp ridge. A weakly defined muscle scar appears to be present on the dorsal surface of the ischium, as in a variety of archosauriforms (Ezcurra, 2016), at approximately one-fourth of the way along the bone from the proximal surface. The middle third of the shaft is triangular in cross-section, being transversely broader dorsally with a flattened dorsal margin, and tapering ventrally. More distally the shaft has a more oval cross-section, tapering to sharp ridges at the dorsal and ventral surfaces. The distal end expands dorsally, ventrally, and transversely as in *Ticinosuchus ferox* (Krebs, 1965) and paracrocodylomorphs (e.g., *Arizonasaurus babbitti*: Nesbitt, 2005). The ischia have an extensive contact on the midline that extends along at least half of the proximodistal length of the element, as in *Ticinosuchus ferox* (Krebs, 1965) and paracrocodylomorphs (e.g., *Postosuchus kirkpatrickorum* [Weinbaum, 2013]; *Prestosuchus chiniquensis* [UFRGS-PV-0629-T: Liparini and Schultz, 2013]). Although the ischia have extensive contact, they were preserved separately. This is rare in paracrocodylomorphs because most ischia are firmly attached to one another and preserved in articulation; however, separation does occur in some other taxa (*Batrachotomus kupferzellensis*: Gower and Schoch, 2009). In cross-section this articulation would be heart-shaped with a ventrally directed point.

The left ischium of NHMUK PV R6794 (Fig. 19) is badly damaged along the acetabular margin and the ventral margin of the shaft, and post-mortem distortion has

accentuated the curvature of the shaft. The element is consistent in morphology with the ischia of the holotype, and does not add additional anatomical information.

Femur

Both femora are preserved in the holotype, NHMUK PV R6792 (Fig. 20), but are missing parts of their proximal ends and distal surfaces. Proximally, there is a well-defined anterolateral tuber. The posteromedial tuber is well defined, and forms a short, distally extending ridge on the posterior surface of the bone. It is not possible to assess the presence of an anteromedial tuber because the proximal end is incompletely preserved. If both tubera on the medial surface were complete, they appear they would have been about the same size as in other paracrocodylomorphs (Nesbitt, 2011). The preserved proximal surface of the right femur suggests that the proximal surface may have borne a proximal groove as in some pseudosuchians (e.g., poposauroids: Nesbitt, 2007) and other archosaurs (e.g., silesaurids: Nesbitt et al., 2010), although its extent and orientation cannot be confirmed. There is a slight bulbous expansion on the posterolateral surface of the proximal part of the bone, in a position equivalent to the dorsolateral trochanter in dinosauriforms (Langer and Benton, 2006). There is small but distinct and unusual pit on the posterior surface, lateral to the distal-most expression of the posteromedial tuber, and proximal and slightly lateral to the fourth trochanter. This pit has an ovoid outline, and is present on both femora of the holotype as well as in a fragment of the proximal shaft of right femur in NHMUK PV R6794. This pit is not present, as far as we are aware, in other early pseudosuchians, and is identified here as an autapomorphy of *Mandasuchus tanyauchen*. On the anterolateral surface of the femur there is a short, raised ‘trochanteric shelf’ (which may represent the attachment site of the M. iliofemoralis based on the interpretation of a similar feature in *Erythrosuchus africanus*: Gower, 2003; Nesbitt, 2011) that reaches the lateral margin of the femur. The fourth

trochanter is robust and mound-like, with an oval scar on its anteromedial surface as typical for most pseudosuchians. The posterolateral edge of the midshaft is formed by a sharp proximodistally extending ridge. The femoral shaft expands distally to form two condyles (poorly preserved on both elements of the holotype) that are weakly separated on the posterior surface, with a shallow concavity present on the anterior surface. Two fragments of the right femur of NHMUK PV R6794 (Fig. 24) are consistent in morphology with the holotype.

Tibia

Both tibiae are preserved in the holotype, NHMUK PV R6792 (Fig. 21). The left is complete, whereas the right is broken into three pieces and is less well preserved with badly weathered external surfaces in several parts. The tibia is straight and expanded at its proximal and distal ends. The tibia is approximately 80% of the length of the femur. The proximal surface of the left tibia is damaged, but is well preserved on the right side, and the lateral condyle of the tibia is clearly distinctly depressed, as in pseudosuchians (Nesbitt, 2011). A short cnemial crest is present, forming a slight ridge, but this differs in extent from the well developed feature present in dinosauromorphs (Sereno and Arcucci, 1994). This is continuous more distally with a sharper proximodistal ridge that terminates approximately 25 mm short of the distal surface. At about 30% along the length of the tibia there is a small posteriorly placed pit on the medial surface that represents the likely attachment site of the M. puboischiotibialis (following Gower, 2003). The distal end of the bone is approximately ‘kidney bean’-shaped in distal view. As with other suchians, the distal surface is saddle shaped rather than flat, matching the flexed articular surface on the astragalus (see below). The anterolateral part of the distal end of the tibia is upturned and gently concave, and articulated with a convexity on the proximal surface of the astragalus close to the latter’s

fibular articular surface. The posterior half of the distal end of the tibia is convex, and articulated with a medially placed concavity on the proximal surface of the astragalus.

A complete left tibia is preserved in NHMUK PV R6794 (Fig. 22), and is considerably larger and more robust than that of the holotype, but otherwise matches it very closely in morphology.

Fibula

The proximal 40% of the right fibula is preserved in the holotype, NHMUK PV R6792 (Fig. 23). The proximal end is transversely compressed with an ellipsoid outline in proximal view. The posteromedial surface has a ridge demarcating a muscle scar. The M. iliofibularis scar is located on the anterolateral surface of the bone, at approximately one-third of the way down the bone, close to the distal end of the preserved fragment, as in most non-aetosaur early suchians (Nesbitt, 2011). This scar has the form of a distinctly raised oval rugosity located at the proximal end of a proximodistal crest.

A short section of the proximal right fibula is also present in NHMUK PV R6794 (Fig. 24), but is broken prior to the M. iliofibularis scar. It is generally similar to the holotype fibula in morphology, although the ridge on the posteromedial surface is more strongly developed, and the proximal surface is not as flat as in the holotype, but is higher posteriorly than anteriorly.

Proximal Tarsals

Charig (1956) described a left calcaneum as part of NHMUK PV R6794. Thomas (2004) reported that the whereabouts of this specimen was unknown, and we have also been unable to locate it. Charig (1956) did not describe any other ankle material of *Mandasuchus*, but Cruickshank (1979) mentioned (but did not describe) a cast of a complete left astragalus

and calcaneum of *Mandasuchus* that he had been sent by AJC. Thomas (2004:34) described these elements on the basis of casts loaned to her by Cruickshank, and considered it "most likely" that they belonged to the holotype, NHMUK PV R6792, but did not explain this interpretation. The whereabouts of both the original fossil material from which these casts were made and the casts studied by Thomas (2004) are currently unknown. The casts described here were molded and cast with plaster by an unknown person and presented to Paul Sereno by AJC (P. Sereno, pers. comm.). The plaster casts were subsequently remolded by one of us (SJN), and cast in urethane plastic (Smooth-on 300). Although it is plausible that they represent the same individual as the holotype based on size (the astragalus and the left tibia of NHMUK PV R6792 articulate well together), in the absence of locality data the tarsals have been assigned a separate accession number, NHMUK PV R36950. The morphology of the calcaneum is completely consistent with that shown in Charig's (1956:pl. 32A–F) figures of the missing calcaneum of NHMUK PV R6794 and also consistent with the tarsal morphology of other early suchian archosaurs, supporting the referral of NHMUK PV R36950 to *Mandasuchus tanyauchen*.

The left astragalus (Fig. 25) is complete. The proximal surface bears two large articular facets. The more lateral facet for the fibula is concave, faces proximolaterally, and is subtriangular in lateral view. The fibular and tibial facets meet anteriorly whereas there is a clear gap between the articular surfaces posteriorly. Although imperfectly preserved, the tibial facet is clearly slightly 'flexed' (sensu Sereno, 1991) where the anterior portion of the facet slightly faces proximally and anteriorly and the posterior portion of the facet is more strongly concave and faces proximally and posteriorly. This flexure is matched by the distal end of the tibia (see above); similar flexure of the tibial facet of the astragalus is present in all suchians and some avemetatarsalians (Nesbitt, 2011). The tibial facet is surrounded by a low,

poorly delimited ridge, in contrast with the much more distinct bounding ridges seen in other suchians (e.g., shuvosaurids: Nesbitt, 2007).

Anteriorly, the astragular 'roller' is well developed medially and lies medial to a subrectangular and deeply concave anterior hollow. The distal edge in anterior view is distinctly convex and transitions into a distinct astragular peg laterally. The peg is distinctly separated from the rest of the body of the astragalus by the posterior groove proximally and posteriorly. The well-developed peg is similar to those of other Triassic suchians (e.g., *Revueltosaurus callenderi* [PEFO 34561]; *Postosuchus kirkpatricki* [TTU P9002]) and is much better developed than those of phytosaurs (e.g., *Smilosuchus gregorii* [USNM 18313]) and the contemporaneous *Nundasuchus songeaensis* (NMT RB48). The peg fits into a concave surface of the calcaneum, creating the characteristic 'crocodile-normal' (sensu Chatterjee, 1978) ankle of pseudosuchians. Posteriorly, the convex distal surface of the peg continues medially and transitions into a broadly convex posterior surface.

The left calcaneum (Fig. 26) is complete. In proximal view, the calcaneum bears a hemicylindrical articulation surface for the fibula laterally and a concave surface for articulation with the peg of the astragalus medially. The articulation surface for the fibula is at a low angle to the posterior portion of the calcaneal tuber and it arcs anteriorly to meet the articulation surface for distal tarsal 4. Medial to the articulation surface for the fibula, there is a distinct but shallow pit that receives the lateral termination of the peg of the astragalus when the proximal tarsals are in articulation. This pit is not as deep laterally and is smaller than that of the loricatan *Batrachotomus kupferzellensis* (Gower and Schoch, 2009) and the poposauroids *Poposaurus gracilis* (Schachner et al., 2011) and *Effigia okeeffeae* (Nesbitt, 2007), but is similar is shape to that of aetosaurian sister taxon *Revueltosaurus callenderi* (PEFO 34561). The articulation surface for the peg of the astragalus is concave and has a similar angle to the rest of the body of the element as in the calcaneum of *B. kupferzellensis*

(Gower and Schoch, 2009). Distally, the anterior surface bears a nearly flat and broadly triangular surface for articulation with distal tarsal 4. This surface is separated from the posterior surface of calcaneal tuber by a shallow but distinct fossa as in loricatans (Nesbitt, 2011).

When held in articulation with the astragalus, the calcaneal tuber projects posteriorly and nearly perpendicular (~90º) to the mediolateral plane of the proximal tarsals, as in other suchian archosaurs (Parrish, 1986; Sullivan, 2015). The calcaneal tuber is wide in proximal view, about twice as wide as tall, as in *Revueltosaurus callenderi* (PEFO 34561), and the loricatans *Prestosuchus chiniquensis* (Huene, 1942) and *Batrachotomus kupferzellensis* (Gower and Schoch, 2009). The posterior surface of the tuber is simply convex without any grooves. In lateral view, there is a slight expansion of the tuber as in *Nundasuchus songeaensis* (NMT RB48: Nesbitt et al., 2014). The calcaneal tuber of *Mandasuchus tanyauchen* expands slightly ventrally and significantly dorsally as in other suchians (Nesbitt, 2011).

Osteoderms

Several incomplete osteoderms are present in the holotype, NHMUK PV R6792 (Figs. 7G–J, L, 12A, B), including three partial osteoderms preserved in articulation with the right side of Ce6 (Fig. 7G–J, L). Several articulated osteoderms are present in NHMUK PV R6793, and have been embedded in a transparent resin block. Osteoderm fragments are also present in NHMUK PV R6794. The osteoderms are generally subquadrate in outline, approximately as long as they are wide, and have a rounded lateral edge. The best-preserved examples bear an anteriorly projecting spike that fits with a slight depression on the ventral surface of the preceding osteoderm, as in *Ticinosuchus ferox* (Krebs, 1965). The osteoderms were paired in paramedian rows and it seems that they were staggered, as in other early

loricatans and *Ticinosuchus ferox* (see Nesbitt, 2011). The osteoderms are relatively short compared to the adjacent vertebrae. The number per vertebra is not clear, but it was likely five osteoderms per two vertebrae as in *Nundasuchus songeaensis* (Nesbitt et al., 2014), *Prestosuchus chiniquensis* (UFRGS-PV-0156-T: Nesbitt, 2011), and *Saurosuchus galilei* (Trotteyn et al., 2011).

Life reconstruction

A new life reconstruction, prepared by Mark Witton, is presented here (Fig. 27). The reconstruction is based on the proportions of the largest known specimen (NHMUK PV R6794), and missing body parts (primarily the skull) were based largely on the closely related taxon *Prestosuchus* (see below).

PHYLOGENETIC ANALYSIS

We incorporated the holotype and referred specimens of *Mandasuchus tanyauchen* into the dataset of Nesbitt (2011), including the modifications made by Butler et al. (2014) and with the addition of data for *Nundasuchus songeaensis* from Nesbitt et al. (2014). The holotype of *M. tanyauchen* (NHMUK PV R6792), the proximal tarsals that probably belong to the holotype (NHMUK PV R36950), and the two referred specimens represented by partial skeletons (NHMUK PV R6793, NHMUK PV R6794) were scored as a single terminal taxon (*M. tanyauchen*). Almost all of the scores for this terminal taxon derive from the holotype (NHMUK PV R6792) and NHMUK PV R36950, and the scores from the referred specimens (NHMUK PV R6793, NHMUK PV R6794) are consistent with those of the holotype but do not allow any more missing data for the holotype to be scored. A second terminal taxon (= '*Mandasuchus* total') includes scores also for the referred maxilla (NHMUK PV R36889),

allowing an additional two characters to be scored. Of the terminal taxa included by Nesbitt (2011), we used the combined *Prestosuchus* terminal taxon and the combined *Lewisuchus*/*Pseudolagosuchus* terminal taxon, and we a priori excluded *Archosaurus rossicus*, *Parringtonia gracilis*, and *Erpetosuchus granti* following Nesbitt and Butler (2013) and Butler et al. (2014). *Mandasuchus tanyauchen* and '*Mandasuchus* total' were included as separate terminal taxa in different iterations of the analysis. Our two analyses therefore included 80 operational taxonomic units and 413 characters. The scores for the ilium of *Rauisuchus tiradentes* analysed by Nesbitt (2011) were removed and character 52 was scored as '?' for this taxon following Lautenschlager and Rauhut (2015). The rhynchosaur *Mesosuchus browni* was used as the outgroup to root the most parsimonious trees (MPTs). The dataset was analyzed in PAUP* 4.0b10 (Swofford, 2002) using a heuristic search subjected to 1000 random addition replicates with tree bisection and reconnection branch swapping. Characters 32, 52, 121, 137, 139, 156, 168, 188, 223, 247, 258, 269, 271, 291, 297, 328, 356, 399, and 413 were ordered following Nesbitt (2011) with the additions made by Butler et al. (2014). Zero length branches were collapsed if they lacked support under any of the most parsimonious reconstructions.

We recovered 180 most parsimonious trees (consistency index = 0.363; retention index = 0.768) with tree length 1333 using the '*Mandasuchus* total' terminal taxon. The relationships of the included archosauriforms in the strict consensus tree (Fig. 28) were nearly identical with those recovered from analysis of the most recent iterations of the dataset (Butler et al., 2014; Nesbitt et al., 2014). *Mandasuchus tanyauchen* was recovered as the sister taxon of all other loricatans within Paracrocodylomorpha. The same result was recovered when '*Mandasuchus* total' was analysed. In the strict consensus, *Nundasuchus songeaensis* and Gracilisuchidae form a polytomy with the clade comprising *Ticinosuchus ferox* + Paracrocodylomorpha.

The immediate phylogenetic position of *Mandasuchus tanyauchen* is not well supported, with minimal Bremer support for both Loricata and non-*M. tanyauchen* loricatans. *Mandasuchus tanyauchen* is supported as a paracrocodylomorph (Bremer support = 1) by the presence of an expanded distal end of the pubis (character 283, state 1). *Mandasuchus tanyauchen* is supported as a member of Loricata by a knob-shaped and robust attachment site for the M. iliofibularis on the fibula (339-1), and a ventrally located fossa on the calcaneum that separates the articulation surface for distal tarsal 4 and the distal end of the tuber (371-2). The monophyly of other loricatans to the exclusion of *M. tanyauchen* is supported by cranial and postcranial character states. *Mandasuchus tanyauchen* has a posteriorly tapering maxilla, whereas the posterior part of the maxilla of the other Triassic loricatans expands dorsally (27-1). The anterior margin of the antorbital fenestra in *M. tanyauchen* is broadly rounded in lateral view whereas the angle of the anterior margin is much smaller in *Prestosuchus chiniquensis*, *Saurosuchus galilei*, and most other Triassic loricatans. In comparison with *M. tanyauchen*, other loricatans have proportionally longer pubes (278-1, 282-1), the proximal portion of the fibula is more rounded in proximal view, and the M. iliofibularis scar on the fibula is located near the midshaft (340-1).

DISCUSSION

Phylogenetic Position

Mandasuchus tanyauchen has not previously been included in any formal, published phylogenetic analysis. Charig (1956) identified *M. tanyauchen* as a pseudosuchian most similar to the Brazilian taxon *Prestosuchus chiniquensis*, and used the family name Prestosuchidae (which was, however, a nomen nudum, and is now attributed to Romer [1966]) for these two species, as well as *Spondylosoma absconditum* and *Stagonosuchus*

nyassicus. He considered prestosuchids to be ancestral to sauropodomorph dinosaurs such as *Plateosaurus* (see also Charig et al., 1965; Charig in Appleby et al., 1967). Huene (1956) listed *Mandasuchus* as part of the family Ornithosuchidae, together with a disparate group of taxa that included species now recognised as ornithosuchids, erpetosuchids, and crocodylomorphs. Romer (1966) followed Charig (1956) in referring *Mandasuchus* to Prestosuchidae, whereas Krebs (1976) referred *M. tanyauchen* to Rauisuchidae.

Parrish (1993) did not include *M. tanyauchen* in his data matrix, though, in suggesting that *M. tanyauchen* was conspecific with *Ticinosuchus ferox,* he considered it a suchian more closely related to *Prestosuchus chiniquensis* and *Saurosuchus galilei* than to any other sampled archosaur. Juul (1994) and Sen (2005) also considered *M. tanyauchen* to be closely related to *P. chiniquensis* and *T. ferox*. However, recent phylogenetic analyses (e.g., Nesbitt, 2011) have failed to find compelling support for a clade approximating the Prestosuchidae of Parrish (1993) and subsequent authors. Instead, prestosuchids seem to form a polyphyletic assemblage of early suchians (*T. ferox*) and early loricatans (*P. chiniquensis*, *S. galilei*), sharing a similar body plan that is likely plesiomorphic for Suchia as a whole (Nesbitt, 2011). Gower (2001) depicted *Mandasuchus* as a suchian lying outside a clade comprising other loricatans, but provided no justification for this position, and described *Mandasuchus* as a 'rauisuchian' (sensu Gower, 2000).

Incomplete knowledge (and some degree of homoplasy) means that it is currently not possible to compellingly resolve the precise relationships of many Triassic suchians. However, we are confident that *Mandasuchus tanyauchen* is a suchian that does not belong to the distinctive clades Aetosauria, Gracilisuchidae, Poposauroidea, Rauisuchidae, or Crocodylomorpha. Furthermore, although showing affinities to loricatans, the limited cranial material means that there is no compelling evidence that it is especially closely related to any single known loricatan genus. Parrish (1993:297) considered that "homologous bones of

"*Mandasuchus*" and *Ticinosuchus ferox* are extremely similar" and he recognised "no taxonomic distinction" between the two. *Ticinosuchus ferox* is known from the Middle Triassic of Switzerland and Italy, from a completely, but heavily laterally flattened holotype, as well as some referred material. We recognised a number of differences between *M. tanyauchen* and *T. ferox* (see Diagnosis), and our phylogenetic analysis did not recover a sister-group relationship between *M. tanyauchen* and any other single suchian species. These results support the hypotheses that *M. tanyauchen* is not conspecific with *T. ferox* and not obviously congeneric with any known taxon.

Historical Significance of *Mandasuchus*

When Charig (1956) studied the known material, knowledge of Triassic suchians was quite different and more scanty than today. The available material of *Mandasuchus* was among the best preserved and most complete for any 'rauisuchian'. By the turn of the century, knowledge of Triassic suchians remained poorly established, as exemplified by the review of 'rauisuchians' by Gower (2000), of which *Mandasuchus* was considered an example. Had the known material of *Mandasuchus* been formally published and described following AJC's PhD work (see Moody and Naish [2010] for a discussion of why AJC did not publish), it would have played a crucial role in the history of 'rauisuchian' paleobiology and, speculatively, might have sped up the onset of the revolution in that field that occurred between the reviews of Gower (2000) and Nesbitt et al. (2013). Since Charig's unpublished thesis, many new taxa and fossil specimens have been discovered and documented in detail, and there has been a recent surge of interest in Triassic archosaur diversity and diversification due to both the discovery of new taxa and the detailed study of historically collected material (Nesbitt et al., 2013). Some of the newly described taxa and specimens are known from good cranial as well as postcranial material (e.g., *Batrachotomus kupferzellensis*, *Effigia okeeffeae*,

and *Decuriasuchus quartacolonia*) and these have played a pivotal role in the new understanding of suchian diversity and phylogeny. The known material of *Mandasuchus* is no longer exceptional, is less spectacular by comparison, and fits into an established framework rather than overturning hypotheses of suchian phylogeny. Nevertheless, our description of *Mandasuchus* finally documents and unveils a taxon that has been frequently mentioned, rather elusively, in the literature over the last 60 years, and adds an important element to our understanding of Manda Beds faunal communities. Moreover, it provides additional insights into the plesiomorphic body plan of suchian archosaurs, and demonstrates that this body plan persisted well into the Middle Triassic, significantly later than the Early Triassic origin of the clade (Butler et al., 2011).

ACKNOWLEDGMENTS

We thank S. Chapman and L. Steel for access to the Manda archosaur collection (NHMUK), M. Lowe and J. Head for access to UMZC collections, and A. Milner, A. de Ricqlès, and P. Sereno for discussion. Specimen photography was by H. Taylor (NHM Image Resources). SJN was supported by National Science Foundation grant DBI-0306158. This work was supported by a Marie Curie Career Integration Grant to RJB (PCIG14-GA-2013-630123). We thank M. Lacerda and J. Desojo for constructive and helpful reviews and R. Irmis for editorial work. M. Witton is thanked for creating the skeletal reconstructions in Figure 3 and the life restoration in Figure 27.

LITERATURE CITED

Alcober, O. 2000. Redescription of the skull of *Saurosuchus galilei* (Archosauria: Rauisuchidae). Journal of Vertebrate Paleontology 20:302–316.

Appleby, R. M., A. J. Charig, C. B. Cox, K. A. Kermack, and L. B. H. Tarlo. 1967. Reptilia; pp. 695–731 in W. B. Harland, C. H. Holland, M. R. House, N. F. Hughes, A. B. Reynolds, M. J. S. Rudwick, G. E. Satterthwaite, L. B. H. Tarlo, and E. C. Willey (eds.), The Fossil Record. The Geological Society of London, London.

Barrett, P. M., S. J. Nesbitt, and B. R. Peecook. 2015. A large-bodied silesaurid from the Lifua Member of the Manda beds (Middle Triassic) of Tanzania and its implications for body-size evolution in Dinosauromorpha. Gondwana Research 27:925–931.

Bonaparte, J. F. 1981. Descripcion de *Fasolasuchus tenax* y su significado en la sistematica y evolucion de los Thecodontia. Revista del Museo Argentino de Ciencias Naturales 'Bernardino Rivadavia' 3:55–101.

Butler, R. J., P. M. Barrett, R. L. Abel, and D. J. Gower. 2009. A possible ctenosauriscid archosaur from the Middle Triassic Manda Beds of Tanzania. Journal of Vertebrate Paleontology 29:1022–1031.

Butler, R. J., S. L. Brusatte, M. Reich, S. J. Nesbitt, R. R. Schoch, and J. J. Hornung. 2011. The sail-backed reptile *Ctenosauriscus* from the latest Early Triassic of Germany and the timing and biogeography of the early archosaur radiation. PLoS ONE 6:e25693.

Butler, R. J., C. Sullivan, M. D. Ezcurra, J. Liu, A. Lecuona, and R. B. Sookias. 2014. New clade of enigmatic early archosaurs yields insights into early pseudosuchian phylogeny and the biogeography of the archosaur radiation. BMC Evolutionary Biology 14:128.

Charig, A. J. 1956. New Triassic archosaurs from Tanganyika including *Mandasuchus* and *Teleocrater*. Unpublished PhD dissertation, University of Cambridge, Cambridge (United Kingdom), 503 pp., 53 pls.

Charig, A. J. 1972. The evolution of the archosaur pelvis and hind-limb: an explanation in functional terms; pp. 121–155 in K. A. Joysey, and T. S. Kemp (eds.), Studies in Vertebrate Evolution. Oliver & Boyd, Edinburgh.

Charig, A. J. 1979. A New Look at the Dinosaurs. Heinemann, London, 160 pp.

Charig, A. J., and M. Wilson. 1971. Brooke Bond Picture Cards: Prehistoric Animals. Brooke Bond Oxo Ltd, Croydon, 26 pp.

Charig, A. J., J. Attridge, and A. W. Crompton. 1965. On the origin of the sauropods and the classification of the Saurischia. Proceedings of the Linnean Society of London 176:197–221.

Chatterjee, S. 1978. A primitive parasuchid (Phytosaur) reptile from the Upper Triassic Maleri Formation of India. Palaentology 21:83–127.

Cruickshank, A. R. I. 1965. On a specimen of the anomodont reptile *Kannemeyeria latifrons* (Broom) from the Manda Formation of Tanganyika, Tanzania. Proceedings of the Linnean Society of London 176:149–157.

Cruickshank, A. R. I. 1967. A new dicynodont genus from the Manda Formation of Tanzania (Tanganyika). Journal of Zoology 153:163–208.

Cruickshank, A. R. I. 1979. The ankle joint in some early archosaurs. South African Journal of Science 75:168–178.

França, M. A. G., M. C. Langer, and J. Ferigolo. 2013. The skull anatomy of *Decuriasuchus quartacolonia* (Pseudosuchia: Suchia: Loricata) from the middle Triassic of Brazil; pp. 469–501 in S. J. Nesbitt, J. B. Desojo, and R. B. Irmis (eds.), Anatomy, Phylogeny and Palaeobiology of Early Archosaurs and their Kin. Geological Society of London, Special Publications, 379.

Gebauer, E. V. I. 2004. Neubeschreibung von *Stagonosuchus nyassicus* v. Huene, 1938 (Thecodontia, Rauisuchia) from the Manda Formation (Middle Triassic) of southwest Tanzania. Neues Jahrbuch für Geologie und Paläontologie, Abhandlungen 231:1–35.

Gower, D. J. 2000. Rauisuchian archosaurs (Reptilia, Diapsida): An overview. Neues Jahrbuch für Geologie und Paläontologie, Abhandlungen 218:447–488.

Gower, D. J. 2001. Possible postcranial pneumaticity in the last common ancestor of birds and crocodilians: evidence from *Erythrosuchus* and other Mesozoic archosaurs. Naturwissenschaften 88:119–122.

Gower, D. J. 2003. Osteology of the early archosaurian reptile *Erythrosuchus africanus* Broom. Annals of the South African Museum 110:1–84.

Gower, D. J., and R. S. Schoch. 2009. Postcranial anatomy of the rauisuchian archosaur *Batrachotomus kupferzellensis*. Journal of Vertebrate Paleontology 29:103–122.

Hancox, P. J., K. D. Angielczyk, and B. S. Rubidge. 2013. *Angonisaurus* and *Shansiodon*, dicynodonts (Therapsida, Anomodontia) from subzone C of the *Cynognathus* Assemblage Zone (Middle Triassic) of South Africa. Journal of Vertebrate Paleontology 33:655–676.

Haughton, S. H. 1932. On a collection of Karroo vertebrates from Tanganyika Territory. Quarterly Journal of the Geological Society of London 88:634–671.

Huene, F. von. 1938a. Ein grosser Stagonolepide aus der jüngeren Trias Ostafrikas. Neues Jahrbuch für Mineralogie, Geologie und Paläontologie, Beilage-Band Abteilung B 80:264–278.

Huene, F. von. 1938b. *Stenaulorhynchus*, ein Rhynchosauride der ostafrikanischen Obertrias. Nova Acta Leopoldina, Neue Folge 6:83–121.

Huene, F. von. 1939. Ein kleiner Pseudosuchier und ein Saurischier aus den ostafrikanischen Mandaschichten. Neues Jahrbuch für Mineralogie, Geologie und Paläontologie, Beilage-Band Abt. B 81:61–69.

Huene, F. von. 1942. Die fossilien Reptilien des südamerikanishen Gondwanalandes. Ergebnisse der Sauriergrabungen in Südbrasilien, 1928/1929. C. H. Beck, München, 332 pp.

Huene, F. von. 1956. Paläontologie un Phylogenie der niederen Tetrapoden. VEB Gustav Fisher Verlag, Jena, 716 pp.

Juul, L. 1994. The phylogeny of basal archosaurs. Palaeontologia africana 31:1–38.

Krebs, B. 1965. *Ticinosuchus ferox* n. g. n. sp. Ein neuer Pseudosuchier aus der Trias des Monte San Giorgio. Schweizerische Paläontologische Abhandlungen 81:1–140.

Krebs, B. 1976. Pseudosuchia; pp. 40–98 in A. J. Charig, B. Krebs, H.-D. Sues, and F. Westphal (eds.), Thecodontia, Handbuch der Paläoherpetologie 13. Gustav Fisher Verlag, Stuttgart.

Langer, M. C., and M. J. Benton. 2006. Early dinosaurs: A phylogenetic study. Journal of Systematic Palaeontology 4:309–358.

Lautenschlager, S., and J. B. Desojo. 2011. Reassessment of the Middle Triassic rauisuchian archosaurs *Ticinosuchus ferox* and *Stagonosuchus nyassicus*. Paläontologische Zeitschrift 85:357–381.

Lautenschlager, S., and O. W. M. Rauhut. 2015. Osteology of *Rauisuchus tiradentes* from the Late Triassic (Carnian) Santa Maria Formation of Brazil, and its implications for rauisuchid anatomy and phylogeny. Zoological Journal of the Linnean Society 173:55–91.

Lessner, E. J., M. R. Stocker, N. D. Smith, A. H. Turner, R. B. Irmis, and S. J. Nesbitt. In press. A new taxon of rauisuchid (Archosauria, Pseudosuchia) from the Upper

Triassic of New Mexico increases the diversity and temporal range of the clade. PeerJ.

Li, C., X.-C. Wu, Y.-N. Cheng, T. Sato, and L. Wang. 2006. An unusual archosaurian from the marine Triassic of China. Naturwissenschaften 93:200–206.

Liparini, A., and C. L. Schultz. 2013. A reconstruction of the thigh musculature of the extinct pseudosuchian *Prestosuchus chiniquensis* from the *Dinodontosaurus* Assemblage Zone (Middle Triassic Epoch), Santa Maria 1 Sequence, southern Brazil; pp. 441–468 in S. J. Nesbitt, J. B. Desojo, and R. B. Irmis (eds.), Anatomy, Phylogeny and Palaeobiology of Early Archosaurs and their Kin. Geological Society of London, Special Publications, 379.

Moody, R. T. J., and D. Naish. 2010. Alan Jack Charig (1927–1997): an overview of his academic accomplishments and role in the world of fossil reptile research; pp. 89–109 in R. T. J. Moody, E. Buffetaut, D. Naish, and D. M. Martill (eds.), Dinosaurs and Other Extinct Saurians: A Historical Perspective. Geological Society of London, Special Publications, 343.

Nesbitt, S. J. 2003. *Arizonasaurus* and its implications for archosaur divergence. Proceedings of the Royal Society, Series B, Biological Sciences 270(Supplement: Biology Letters):S234–S237.

Nesbitt, S. J. 2005. The osteology of the pseudosuchian *Arizonasaurus babbitti*. Historical Biology 17:19–47.

Nesbitt, S. J. 2007. The anatomy of *Effigia okeeffeae* (Archosauria, Suchia), theropod-like convergence, and the distribution of related taxa. Bulletin of the American Museum of Natural History 302:1–84.

Nesbitt, S. J. 2011. The early evolution of archosaurs: relationships and the origin of major clades. Bulletin of the American Museum of Natural History 352:1–292.

Nesbitt, S. J., and R. J. Butler. 2013. Redescription of the archosaur *Parringtonia gracilis* from the Middle Triassic Manda Beds of Tanzania, and the antiquity of Erpetosuchidae. Geological Magazine 150:225–238.

Nesbitt, S. J., R. J. Butler, and D. J. Gower. 2013b. A new archosauriform (Reptilia: Diapsida) from the Manda Beds (Middle Triassic) of southwestern Tanzania. PLoS ONE 8:e72753.

Nesbitt, S. J., J. Liu, and C. Li. 2011. A sail-backed suchian from the Heshanggou Formation (Early Triassic: Olenekian) of China. Earth and Environmental Science Transactions of the Royal Society of Edinburgh 101:271–284.

Nesbitt, S. J., P. M. Barrett, S. Werning, C. A. Sidor, and A. J. Charig. 2013a. The oldest dinosaur? A Middle Triassic dinosauriform from Tanzania. Biology Letters 9:20120949.

Nesbitt, S. J., C. A. Sidor, K. D. Angielczyk, R. M. H. Smith, and L. A. Tsuji. 2014. A new archosaur from the Manda beds (Anisian, Middle Triassic) of southern Tanzania and its implications for character state optimizations at Archosauria and Pseudosuchia. Journal of Vertebrate Paleontology 34:1357–1382.

Nesbitt, S. J., C. A. Sidor, R. B. Irmis, K. D. Angielczyk, R. M. H. Smith, and L. A. Tsuji. 2010. Ecologically distinct dinosaurian sister-group shows early diversification of Ornithodira. Nature 464:95–98.

Nesbitt, S. J., S. L. Brusatte, J. B. Desojo, A. Liparini, M. A. G. França, J. C. Weinbaum, and D. J. Gower. 2013. Rauisuchia; pp. 241–274 in S. J. Nesbitt, J. B. Desojo, and R. B. Irmis (eds.), Anatomy, Phylogeny and Palaeobiology of Early Archosaurs and their Kin. Geological Society of London, Special Publications, 379.

Nesbitt, S. J., M. R. Stocker, W. G. Parker, T. A. Wood, C. A. Sidor, and K. D. Angielczyk. 2017. The braincase and endocast of *Parringtonia gracilis*, a Middle Triassic suchian

(Archosauria: Pseudosuchia); pp. xxx–xxx in C. A. Sidor and S. J. Nesbitt (eds.), Vertebrate and climatic evolution in the Triassic rift basins of Tanzania and Zambia. Society of Vertebrate Paleontology Memoir 17. Journal of Vertebrate Paleontology 37 (6, supplement).

Parker, W. G. 2016. Revised phylogenetic analysis of the Aetosauria (Archosauria: Pseudosuchia); assessing the effects of incongruent morphological character sets. PeerJ 4:e1583.

Parrish, J. M. 1986. Locomotor adaptations in the hindlimb and pelvis of the Thecodontia. Hunteria 1:1–35.

Parrish, J. M. 1993. Phylogeny of the Crocodylotarsi, with reference to archosaurian and crurotarsan monophyly. Journal of Vertebrate Paleontology 13:287–308.

Peyer, K., J. G. Carter, H.-D. Sues, S. E. Novak, and P. E. Olsen. 2008. A new suchian archosaur from the Upper Triassic of North Carolina. Journal of Vertebrate Paleontology 28:363–381.

Ricqlès, A. de, K. Padian, F. Knoll, and J. R. Horner. 2008. On the origin of high growth rates in archosaurs and their ancient relatives: Complementary histological studies on Triassic archosauriforms and the problem of a "phylogenetic signal" in bone histology. Annales de Paléontologie 94:57–76.

Romer, A. S. 1966. Vertebrate Paleontology. Third Edition. The University of Chicago Press, Chicago, 468 pp.

Sawin, H. J. 1947. The pseudosuchian reptile *Typothorax meadei*. Journal of Paleontology 21:201–238.

Schachner, E. R., P. L. Manning, and P. Dodson. 2011. Pelvic and hindlimb myology of the basal archosaur *Poposaurus gracilis* (Archosauria: Poposauroidea). Journal of Morphology 272: 1464–1491.

Sen, K. 2005. A new rauisuchian archosaur from the Middle Triassic of India. Palaeontology 48:185–196.

Sereno, P. C. 1991. Basal archosaurs: phylogenetic relationships and functional implications. Society of Vertebrate Paleontology Memoir 2:1–53.

Sereno, P. C., and A. B. Arcucci. 1994. Dinosaurian precursors from the Middle Triassic of Argentina: *Lagerpeton chanarensis*. Journal of Vertebrate Paleontology 13:385–399.

Sidor et al. 2017. Introduction to the memoir chapter……TBC

Sill, W. D. 1974. The anatomy of *Saurosuchus galilei* and the relationships of the rauisuchid thecodonts. Bulletin of the Museum of Comparative Zoology 146:317–362.

Stockley, G. M. 1932. The geology of the Ruhuhu coalfields, Tanganyika Territory. Quarterly Journal of the Geological Society of London 88:610–622.

Sulej, T. 2005. A new rauisuchian reptile (Diapsida: Archosauria) from the Late Triassic of Poland. Journal of Vertebrate Paleontology 25:78–86.

Sullivan, C. 2015. Evolution of hind limb posture in Triassic archosauriforms; pp. 107–124 in K. P. Dial, N. Shubin, and E. L. Brainerd (eds.), Great Transformations in Vertebrate Evolution. University of Chicago Press, Chicago.

Thomas, K. M. 2004. Rauisuchian relationships and the evolution of the archosaur hindlimb. Unpublished PhD thesis, University of Cambridge, Cambridge (United Kingdom).

Trotteyn, M. J., J. B. Desojo, and O. Alcober. 2011. Nuevo material postcraneano de *Saurosuchus galilei* Reig (Archosauria: Crurotarsi) del Triasico Superior del centro-oeste de Argentina. Ameghiniana 48:605–620.

Wu, X.-C. 1981. The discovery of a new thecodont from north east Shanxi. Vertebrata PalAsiatica 19:122–132.

Submitted 03 September 2016; accepted XX XX XXXX.

FIGURE CAPTIONS

FIGURE 1. Reconstruction of *Mandasuchus* and accompanying caption commissioned for the Brooke Bond Picture Card album on "Prehistoric Animals" (Charig and Wilson, 1971). [planned for column width]

FIGURE 2. Geographic positions of the localities for the type (NHMUK PV R6792: locality B5) and referred specimens (NHMUK PV R6793: locality B5; NHMUK PV R6794: locality B15; NHMUK PV R36889: locality B17) of *Mandasuchus tanyauchen* gen. et sp. nov. (modified from Nesbitt et al., 2014). Locality numbers based on Stockley (1932). Dashed lines indicate Ruhuhu Basin fault boundaries. Dotted filled area shows the outcrop of the Kingori Sandstone, dashed filled area shows the outcrop of the Manda Beds. [planned for column width]

FIGURE 3. Skeletal reconstructions showing the majority of the elements preserved in, and relative sizes of, each of the three partial skeletons referred to *Mandasuchus tanyauchen* gen. et sp. nov. **A**, NHMUK PV R6792. **B**, NHMUK PV R6793. **C**, NHMUK PV R6794. Reconstructions created by Mark Witton.

FIGURE 4. Cranial remains of the holotype of *Mandasuchus tanyauchen* gen. et sp. nov. (NHMUK PV R6792). Left maxilla in **A**, lateral view; **B**, ventral (occlusal) view; **C**, medial view; **D**, dorsal view. Two fragments of the right maxilla in **E**, lateral view; **F**, medial view. Partial right dentary in **G**, lateral view; **H**, dorsal (occlusal) view; **I**, medial view. Scale bar equals 10 mm. Arrows indicate anterior direction. Numbers in **B** and **H** refer to alveoli.

Abbreviations: *****, autapomorphically narrow dorsal process; **anfo**, antorbital fossa; **Mg**, Meckelian groove; **nf**, nutrient foramina; **t**, tooth. [planned for column width]

FIGURE 5. Referred left maxilla of *Mandasuchus tanyauchen* gen. et sp. nov. (NHMUK PV R36889) in **A**, lateral view; **B**, ventral view; **C**, medial view; **D**, dorsal view; **E**, anterior view; **F**, posterior view. Scale bar equals 10 mm. Numbers in **B** refer to alveoli. **Abbreviations**: *****, autapomorphically narrow dorsal process; **anfe**, antorbital fenestra; **anfo**, antorbital fossa; **f**, foramen; **nf**, nutrient foramina; **pp**, palatal process; **t**, tooth. [planned for column width]

FIGURE 6. The cervical, dorsal, and caudal vertebral column of the holotype of *Mandasuchus tanyauchen* gen. et sp. nov. (NHMUK PV R6792) in suggested articulation, mostly following Charig (1956). Numbers below vertebrae are those used by AJC, and are written in pen on the specimens themselves. As described in the text, we mostly agree with this inferred sequence, but reverse the order of 'D14' and 'D13'. **A**, cervical vertebrae in lateral view and in dorsal view (top); **B**, transitional and anterior dorsal vertebrae in lateral view; **C**, posterior dorsal vertebrae in lateral view; **D**, caudal vertebrae in lateral view. Anterior is to the left. Scale bars equal 10 mm. **Abbreviations**: **Ca**, caudal vertebra**; Ce**, cervical vertebra; **D**, dorsal vertebra. [planned for column width]

FIGURE 7. Selected cervical vertebrae of the holotype of *Mandasuchus tanyauchen* gen. et sp. nov. (NHMUK PV R6792). Axis in **A**, anterior view; **B**, posterior view; **C**, right lateral view; **D**, left lateral view; **E**, ventral view; **F**, dorsal view. Middle cervical vertebra (cervical 6 of AJC) in **G**, anterior view; **H**, posterior view; **I**, right lateral view; **J**, left lateral view; **K**, ventral view; **L**, dorsal view. Posterior cervical vertebra (cervical 7 of AJC) in **M**, anterior

view; **N**, posterior view; **O**, right lateral view; **P**, left lateral view; **Q**, ventral view; **R**, dorsal view. Scale bars equal 10 mm. **Abbreviations**: **de**, distal expansion; **dia**, diapophysis; **nc**, neural canal; **ns**, neural spine; **os**, osteoderm; **par**, parapophysis; **pl**, plaster; **poz**, postzygapophysis; **prz**, prezygapophysis; **rf**, rib facet; **spol**, spinopostzygapophyseal lamina. [planned for column width]

FIGURE 8. Vertebral column of *Mandasuchus tanyauchen* gen. et sp. nov. (NHMUK PV R6793). Cervical vertebrae and anterior dorsal vertebrae, 2–12. Numbers below vertebrae are those used by AJC, and are written in pen on the specimens themselves. **A**, left lateral view; **B**, right lateral view. Scale bar equals 10 mm. Arrows indicate anterior direction. **Abbreviations**: **ax,** axis; **Ca**, caudal vertebra**; Ce**, cervical vertebra; **D**, dorsal vertebra. [planned for page width]

FIGURE 9. Vertebral column of *Mandasuchus tanyauchen* gen. et sp. nov. (NHMUK PV R6794). Numbers below vertebrae are those used by AJC, and are written in pen on the specimens themselves. Cervical vertebrae 1–8 in **A**, left lateral view; **B**, right lateral view. Dorsal vertebrae (~D4–D10, fragment of 'D1' not shown) in **C**, left lateral view; **D**, right lateral view. Anterior caudal vertebrae in **E**, left lateral view; **F**, right lateral view. Middle to posterior caudal vertebrae in **G**, left lateral view; **H**, right lateral view. Scale bar equals 50 mm. Arrows indicate anterior direction. **Abbreviations**: **at,** atlas; **ax,** axis; **Ca**, caudal vertebra; **cer,** cervical rib; **Ce**, cervical vertebra; **D**, dorsal vertebra; **PC**, posterior caudal vertebra. [planned for column width]

FIGURE 10. Selected dorsal vertebrae of the holotype of *Mandasuchus tanyauchen* gen. et sp. nov. (NHMUK PV R6792). Anterior to mid dorsal vertebra ('D7') in **A**, anterior view; **B**,

posterior view; **C**, right lateral view; **D**, left lateral view; **E**, ventral view; **F**, dorsal view. Articulated middle dorsal vertebrae (‘D10’ and ‘D11’) in **G**, anterior view; **H**, posterior view; **I**, right lateral view; **J**, left lateral view; **K**, ventral view; **L**, dorsal view. Scale bar equals 10 mm. **Abbreviations**: **de**, distal expansion; **dia**, diapophysis; **nc**, neural canal; **ns**, neural spine; **par**, parapophysis; **poz**, postzygapophysis; **prz**, prezygapophysis. [planned for column width]

FIGURE 11. Selected dorsal vertebrae of the holotype of *Mandasuchus tanyauchen* gen. et sp. nov. (NHMUK PV R6792). Middle to posterior dorsal vertebra (‘D14’) in **A**, anterior view; **B**, posterior view; **C**, right lateral view; **D**, left lateral view; **E**, ventral view; **F**, dorsal view. Middle to posterior dorsal vertebra (‘D13’) in **G**, anterior view; **H**, posterior view; **I**, right lateral view; **J**, left lateral view; **K**, ventral view; **L**, dorsal view. Posterior dorsal vertebra (‘D17’) in **M**, anterior view; **N**, posterior view; **O**, right lateral view; **P**, left lateral view; **Q**, ventral view; **R**, dorsal view. Scale bars equal 10 mm. **Abbreviations**: **de**, distal expansion; **dia**, diapophysis; **nc**, neural canal; **ns**, neural spine; **p-d**, parapophysis and diapophysis; **par**, parapophysis; **poz**, postzygapophysis; **prz**, prezygapophysis. [planned for column width]

FIGURE 12. Osteoderms and rib of the holotype of *Mandasuchus tanyauchen* gen. et sp. nov. (NHMUK PV R6792). Two articulated osteoderms in **A**, dorsal view; **B**, ventral view. Rib fragment in **C**, two views. Scale bars equal 10 mm. **Abbreviations**: **ap**, anterior process. [planned for column width]

FIGURE 13. Second sacral vertebra of the holotype of *Mandasuchus tanyauchen* gen. et sp. nov. (NHMUK PV R6792) in **A**, anterior view; **B**, posterior view; **C**, left lateral view; **D**,

right lateral view; **E**, ventral view; **F**, dorsal view. Scale bar equals 10 mm. **Abbreviations**: **nc**, neural canal; **ns**, neural spine; **pl**, plaster; **poz**, postzygapophysis; **prz**, prezygapophysis; **sr**, sacral rib. [planned for page width]

FIGURE 14. Selected caudal vertebrae of the holotype of *Mandasuchus tanyauchen* gen. et sp. nov. (NHMUK PV R6792). Anterior caudal vertebra ('Ca1') in **A**, anterior view; **B**, posterior view; **C**, right lateral view; **D**, left lateral view; **E**, ventral view; **F**, dorsal view. Anterior caudal vertebra ('Ca5') in **G**, anterior view; **H**, posterior view; **I**, right lateral view; **J**, left lateral view; **K**, ventral view; **L**, dorsal view. Anterior caudal vertebral centrum ('Ca7') in **M**, anterior view; **N**, posterior view; **O**, right lateral view; **P**, left lateral view; **Q**, ventral view; **R**, dorsal view. Middle caudal vertebra ('Ca11') in **S**, anterior view; **T**, posterior view; **U**, right lateral view; **V**, left lateral view; **W**, ventral view; **X**, dorsal view. Scale bars equal 10 mm. **Abbreviations**: **cr,** caudal rib; **nc**, neural canal; **ns**, neural spine; **poz**, postzygapophysis; **prz**, prezygapophysis. [planned for column width]

FIGURE 15. Pectoral girdle of the holotype of *Mandasuchus tanyauchen* gen. et sp. nov. (NHMUK PV R6792). Left scapulocoracoid in **A**, lateral view; **B**, posterior view; **C**, medial view; **D**, anterior view. Right scapula in **E**, lateral view; **F**, posterior view; **G**, medial view; **H**, anterior view; **I**, proximal view. Scale bar equals 50 mm. **Abbreviations**: **cf**, coracoid foramen; **co**, coracoid; **gl**, glenoid; **sc**, scapula. [planned for column width]

FIGURE 16. Pectoral and forelimb elements of *Mandasuchus tanyauchen* gen. et sp. nov. (NHMUK PV R6793). Left scapula in **A**, lateral view; **B**, posterior view; **C**, medial view; **D**, anterior view; **E**, proximal view. Right humerus in **F**, proximal view; **G**, distal view; **H**, posterior view; **I**, lateral view; **J**, anterior view; **K**, medial view. Left humerus in **L**, proximal

view; **M**, posterior view; **N**, lateral view; **O**, anterior view; **P**, medial view. Left ulna in **Q**, proximal view; **R**, distal view; **S**, posteromedial view; **T**, posterolateral view; **U**, anterolateral view; **V**, anteromedial view. Scale bars equal 10 mm. **Abbreviations**: **a.**, articulates with; **co**, coracoid; **dp**, deltopectoral crest; **gl**, glenoid; **gr**, groove; **hh**, humeral head; **lr**, lateral ridge; **ol**, olecranon process; **re**, reconstructed area. [planned for column width]

FIGURE 17. Right humerus of the holotype of *Mandasuchus tanyauchen* gen. et sp. nov. (NHMUK PV R6792) in **A**, proximal view; **B**, distal view; **C**, anterolateral view; **D**, anteromedial view; **E**, posterolateral view; **F**, posteromedial view. Scale bar equals 50 mm. **Abbreviations**: **dp**, deltopectoral crest; **g**, groove; **hh**, humeral head; **pl**, plaster. [planned for column width]

FIGURE 18. Ilium, pubis, and ischium of the holotype of *Mandasuchus tanyauchen* gen. et sp. nov. (NHMUK PV R6792). Left ilium, pubis, and ischium in **A**, dorsal view; **B**, anterior view; **C**, lateral view; **D**, medial view; **E**, posterior view; **F**, ventral view. Right ilium, pubis, and ischium in G, posterior view; H, medial view; I, ventral view; K, dorsal view; J, lateral view; L, anterior view. Scale equals 50 mm. **Abbreviations**: **ac**, acetabulum; **ap**, anterior iliac process; **is**, ischium; **of**, obturator foramen; **pu**, pubis; **sac**, supra-acetabular crest. [planned for page width]

FIGURE 19. Left ilium, pubis, and ischium of *Mandasuchus tanyauchen* gen. et sp. nov. (NHMUK PV R6794). **A**, lateral view; **B**, medial view. Scale bar equals 50 mm. **Abbreviations**: **ace**, acetabulum; **ap**, anterior process; **ib**, ischial ‘boot’; **is**, ischium; **pb**, pubic ‘boot’; **pu**, pubis; peduncle; **sac**, supra-acetabular crest. [planned for page width]

FIGURE 20. Femora of the holotype of *Mandasuchus tanyauchen* gen. et sp. nov. (NHMUK PV R6792). Right femur in **A**, proximal view; **B**, posteromedial view; **C**, posterolateral view; **D**, anterolateral view; **E**, anteromedial view; **F**, distal view. Left femur in **G**, proximal view; **H**, posteromedial view; **I**, posterolateral view; **J**, anterolateral view; **K**, anteromedial view; **L**, distal view. Scale bars equal 50 mm. **Abbreviations**: *****, autapomorphic pit on femur; **alt**, anterolateral tuber; **amt**, anteromedial tuber; **ctf**, crista tibiofibularis; **ft**, fourth trochanter; **g**, groove; **ifs**, iliofemoralis scar; **pmt**, posteromedial tuber. [planned for page width]

FIGURE 21. Tibiae of the holotype of *Mandasuchus tanyauchen* gen. et sp. nov. (NHMUK PV R6792). Proximal portion of the right tibia in: **A**, proximal view; **B**, lateral view; **C**, anterior view; **D**, medial view; **E**, posterior view. Distal portion of the right tibia in: **F**, lateral view; **G**, anterior view; **H**, medial view; **I**, posterior view; **J**, distal view. Left tibia in: **K**, proximal view; **L**, distal view; **M**, lateral view; **N**, anterior view; **O**, medial view; **P**, posterior view. Scale bar equals 50 mm. **Abbreviations**: **cn**, cnemial crest; **d**, depression. [planned for column width]

FIGURE 22. Left tibia of *Mandasuchus tanyauchen* gen. et sp. nov. (NHMUK PV R6794) in **A**, proximal view; **B**, distal view; **C**, lateral view; **D**, anterior view; **E**, medial view; **F**, posterior view; Scale bar equals 50 mm. Arrows indicate anterior direction. **Abbreviation**: **cn**, cnemial crest; **d**, depression. [planned for column width]

FIGURE 23. Right fibula of the holotype of *Mandasuchus tanyauchen* gen. et sp. nov. (NHMUK PV R6792) in **A**, proximal view; **B**, lateral view; **C**, posterior view; **D**, medial view; **E**, anterior view. Scale bar equals 10 mm. **Abbreviation**: **if**, scar for M. iliofibularis. [planned for column width]

FIGURE 24. Fragmentary remains of *Mandasuchus tanyauchen* gen. et sp. nov. (NHMUK PV R6794). Proximal portion of the right fibula in **A**, medial view; **B**, lateral view. Partial rib head in **C**, ?anterior view; **D**, ?posterior view. Incomplete proximal portion of the right femur in **E**, anterolateral view; **F**, anteromedial view; **G**, posteromedial view; **H**, posterolateral view. Incomplete distal portion of the right femur in **I**, anterior view; **J**, lateral view; **K**, posterior view; **L**, medial view. Scale bars equal 10 mm. **Abbreviations**: *****, autapomorphic pit on femur; **4th**, fourth trochanter; **hs**, histology section location. [planned for column width]

FIGURE 25. Cast of left astragalus of *Mandasuchus tanyauchen* gen. et sp. nov. (NHMUK PV R36950) in **A**, anterior view; **B**, proximal view; **C**, medial view; **D**, distal view; **E**, lateral view; **F**, posterior view. Scale bar equal 1 cm. **Abbreviations**: **a.**, articulates with; **ah**, anterior hollow; **ca**, calcaneum tuber **fi**, fibula; **peg**, peg of the astragalus that fits into the calcaneum; **pg**, posterior groove; **ti**, tibia. Scale bar equals 10 mm. [planned for column width]

FIGURE 26. Cast of left calcaneum of *Mandasuchus tanyauchen* gen. et sp. nov. (NHMUK PV R36950) in **A**, anterior view; **B**, proximal view; **C**, medial view; **D**, distal view; **E**, lateral view; **F**, posterior view. Scale bar equals 10 mm. Arrows indicate anterior direction. **Abbreviations**: **a.**, articulates with; **as**, astragalus; **fi**, fibula; **fo**, fossa; **t4**, 4th tarsal; **tu**, tuber. [planned for column width]

FIGURE 27. Life reconstruction of *Mandasuchus tanyauchen* gen. et sp. nov., created by Mark Witton. Copyright Mark Witton/Natural History Museum, London. [planned for page width]

FIGURE 28. Phylogenetic relationships of *Mandasuchus tanyauchen* gen. et sp. nov. among Archosauria. Relationships have been collapsed within the clades Avemetatarsalia, Ornithosuchidae, Aetosauria, Gracilisuchidae, Poposauroidea, Rauisuchidae, and Crocodylomorpha. [planned for page width]

TABLE 1. Measurements of the cervical, dorsal, and caudal vertebrae of *Mandasuchus tanyauchen* (NHMUK PV R6792: holotype) (emended from Charig, 1956). The proposed order of vertebrae within the column follows that proposed by Charig (1956) and reflects some uncertainly in the exact positions of the vertebrae. Measurements for 'D13' and 'D14' reflect the positions identified by Charig (1956), and numbered as such on the specimens in ink; however, as discussed in the text we consider 'D14' to lie anterior to 'D13' in the vertebral column. Abbreviations: Cd, caudal vertebra; CHA, height of anterior centrum articular surface; CHP, height of posterior centrum articular surface; CL, centrum length; CMW, centrum minimum transverse width; Cv, cervical vertebra; CWA, width of anterior centrum articular surface; CWP, width of posterior centrum articular surface; D, dorsal vertebra; NAH, neural arch height (from dorsal margin of centrum to dorsal margin of neural spine); S, sacral vertebra. All measurements are provided in mm. Measurements that are too distorted/incomplete to include are denoted by a hyphen.

Vertebra	CL	CHA	CWA	CHP	CWP	CMW	NAH
Cv2	27	-	-	18	19	7	37
Cv3	-	16	19	-	-	-	-
Cv4	-	-	-	-	-	-	32
Cv5	-	-	-	-	-	-	33
Cv6	40	22	23	22	24	13	32
Cv7	35	22	25	25	23	11	33
Cv8	35	23	23	24	25	12	-

D1	29	23	28	22	24	-	-
D4	29	22	25	22	21	12	-
D5	30	24	23	22	24	12	-
D6	29	20	22	20	22	11	-
D7	28	23	23	21	23	11	35
D8	29	23	25	24	24	12	36
D9	30	23	24	23	23	11	38
D10	28	23	25	25	25	12	38
D11	30	25	26	26	26	13	40
D12	31	26	25	26	27	14	42
D13	29	24	24	25	27	14	42
D14	30	24	24	24	26	12	41
D15	-	-	-	24	28	17	43
D16	31	25	28	27	29	18	-
D17	31	26	27	26	29	15	44
S2	33	29	32	-	-	17	-
Cd1	27	26	28	26	27	15	46
Cd2	27	26	27	27	25	15	-
Cd3	26	27	26	26	25	14	-
Cd5	24	24	25	24	24	15	49
Cd6	30	24	24	24	21	14	-
Cd7	27	24	22	22	19	11	-
Cd8	28	24	21	19	19	12	-

Cd10	25	18	14	20	16	9	-
Cd11	25	19	18	16	14	10	-

TABLE 2. Measurements of the forelimb and pectoral girdle elements of *Mandasuchus tanyauchen* (NHMUK PV R6792: holotype). Some standard measurements are unavailable due to incompleteness. All measurements are provided in mm. Measurements indicated with '*' are minima, due to breakage or abrasion.

Element/measurement	
Right humerus	
Maximum width of proximal end	50*
Maximum width of distal end	39
Distance between proximal margin and base of deltopectoral crest	44*
Midshaft circumference	42
Right scapula	
Dorsoventral length	128
Left scapula	126
Dorsoventral length	

TABLE 3. Measurements of the pelvic girdle elements of *Mandasuchus tanyauchen* (NHMUK PV R6792: holotype). All measurements are provided in mm. Measurements indicated with '*' are minima, due to breakage or abrasion.

Element/measurement	
Right ilium	
Length	110*
Length of anterior iliac process	11
Length of posterior iliac process	52*
Height of iliac blade dorsal to acetabulum	29
Anteroposterior diameter of acetabulum	49
Left ilium	
Length	89*
Length of anterior iliac process	9*
Length of posterior iliac process	32*
Height of iliac blade dorsal to acetabulum	27*
Anteroposterior diameter of acetabulum	55
Right pubis	
Length	136
Maximum anteroposterior length of proximal end	36*

Maximum mediolateral width of proximal end	21
Mediolateral width of pubis at midshaft	27*
Mediolateral width of distal end	26*
Left pubis	
Length	135
Maximum anteroposterior length of proximal end	32*
Maximum mediolateral width proximal end	18*
Mediolateral width of pubis at midshaft	27*
Mediolateral width of distal end	29
Right ischium	
Length	128
Maximum anteroposterior length of proximal end	39*
Maximum mediolateral width of proximal end	23
Anteroposterior width of shaft at midlength	16
Anteroposterior width of distal end	21*
Left ischium	
Length	117*
Maximum anteroposterior length of proximal end	44*
Maximum mediolateral width of proximal end	22
Anteroposterior width of shaft at midlength	19*

TABLE 4. Measurements of the hind limb elements of *Mandasuchus tanyauchen* (NHMUK PV R6792: holotype). Some standard measurements are unavailable due to incompleteness. All measurements are provided in mm. Measurements indicated with '*' are minima, due to breakage or abrasion.

Element/measurement	
Right femur	
Length	212*
Width of proximal end (posteromedial to posterolateral)	49
Width of distal end (posteromedial to posterolateral)	44*
Shaft diameter at midlength in anterolateral view	23
Shaft circumference	63
Distance from proximal margin to proximal margin of fourth trochanter	51
Left femur	
Length	221
Width of proximal end (posteromedial to posterolateral)	49
Width of distal end (posteromedial to posterolateral)	47*
Shaft diameter at midlength in anterolateral view	23
Shaft circumference	65
Distance from proximal margin to proximal margin of fourth	49

trochanter	
Right tibia	
Anteroposterior length of proximal end	43*
Mediolateral width of proximal end	33*
Anteroposterior length of distal end	31
Mediolateral width of distal end	22
Left tibia	
Length	173*
Anteroposterior length of proximal end	44*
Mediolateral width of proximal end	34*
Midshaft diameter in lateral view	17
Anteroposterior length of distal end	31
Mediolateral width of distal end	21
Right fibula	
Anteroposterior diameter of proximal end	24
Mediolateral diameter of proximal end	13

TABLE 5. Measurements of casts of the proximal tarsals of *Mandasuchus tanyauchen* (NHMUK PV R36950, which potentially represent part of the holotype). All measurements are provided in mm.

Element/measurement	
Left astragalus	
Maximum mediolateral width	37
Maximum anteroposterior length	26
Maximum dorsoventral height (lateral margin)	29
Left calcaneum	
Maximum mediolateral width	27
Maximum anteroposterior length	34
Maximum dorsoventral height (lateral margin)	29

Mandasuchus tanyauchen gen. et sp. nov., a pseudosuchian archosaur from the Manda Beds of Tanzania

RICHARD J. BUTLER,*[,1] STERLING J. NESBITT,[2] ALAN J. CHARIG,[3,†] DAVID J. GOWER,[4] and PAUL M. BARRETT[3]

[1]School of Geography, Earth & Environmental Sciences, University of Birmingham, Edgbaston, Birmingham, B15 2TT, United Kingdom;

[2]Department of Geosciences, Virginia Polytechnic Institute and State University, Blacksburg, Virginia, 24061, USA;

[3]Department of Earth Sciences, The Natural History Museum, Cromwell Road, London SW7 5BD, United Kingdom;

[4]Department of Life Sciences, The Natural History Museum, Cromwell Road, London SW7 5BD, United Kingdom

*Corresponding author: r.butler.1@bham.ac.uk

[†]Deceased

TABLE S1. Measurements of the cervical, dorsal, and caudal vertebrae of *Mandasuchus tanyauchen* (NHMUK PV R6793) (emended from Charig, 1956). The proposed order of vertebrae within the column follows that proposed by Charig (1956) and reflects some uncertainly in the exact positions of the vertebrae. Vertebrae 'X' and 'Y' are mid–posterior dorsal centra, 'Z' is a probable caudal centrum. Abbreviations: CHA, height of anterior centrum articular surface; CHP, height of posterior centrum articular surface; CL, centrum length; CMW, centrum minimum transverse width; Cv, cervical vertebra; CWA, width of anterior centrum articular surface; CWP, width of posterior centrum articular surface; D, dorsal vertebra; NAH, neural arch height (from dorsal margin of centrum to dorsal margin of neural spine). All measurements are provided in mm. Measurements that are too distorted/incomplete to include are denoted by a hyphen.

Vertebra	CL	CHA	CWA	CHP	CWP	CMW	NAH
Cv2	21	14	12	-	13	4	-
Cv3	25	14	15	15	14	6	-
Cv4	28	14	16	14	15	7	27
Cv5	29	14	16	15	16	8	-
Cv6	28	15	17	16	16	7	-
Cv7	26	16	17	16	17	8	27
Cv8	24	17	19	17	19	8	26
D1	20	16	20	16	19	8	-
D2	19	16	21	17	19	9	26
D3	19	15	20	16	18	8	26
D4	19	15	19	15	17	-	-
D5	-	15	18	-	-	8	27
"X"	23	20	18	17	17	8	-
"Y"	22	-	17	20	17	9	-
"Z"	21	14	-	-	-	5	-

TABLE S2. Measurements of the forelimb and pectoral girdle elements of *Mandasuchus tanyauchen* (NHMUK PV R6793). Some standard measurements are unavailable due to incompleteness. All measurements are provided in mm. Measurements indicated with '*' are minima, due to breakage or abrasion.

Element/measurement	
Left scapula	
Length	83*
Anteroposterior length of ventral expansion	36*
Right humerus	
Length	102
Maximum width of distal end	27
Midshaft circumference	27
Left humerus	
Maximum width of proximal end	36
Distance between proximal margin and base of deltopectoral crest	29
Midshaft circumference	26
Left ulna	
Anteroposterior length of proximal end	16
Mediolateral width of proximal end	21

TABLE S3. Measurements of the cervical, dorsal, and caudal vertebrae of *Mandasuchus tanyauchen* (NHMUK PV R6794) (emended from Charig, 1956). The proposed order of vertebrae within the column follows that proposed by Charig (1956) and reflects some uncertainly in the exact positions of the vertebrae. D1 is preserved, but is too incomplete to provide measurements and no complete neural arches are present in any of the preserved vertebrae. Abbreviations: Cd, caudal vertebra; CHA, height of anterior centrum articular surface; CHP, height of posterior centrum articular surface; CL, centrum length (or maximum length in the case of the odontoid process); CMW, centrum minimum transverse width; Cv, cervical vertebra; CWA, width of anterior centrum articular surface; CWP, width of posterior centrum articular surface; D, dorsal vertebra; PCd, posterior caudal (exact position in the tail unknown). All measurements are provided in mm. Measurements that are too distorted/incomplete to include are denoted by a hyphen.

Vertebra	CL	CHA	CWA	CHP	CWP	CMW
Odontoid	14	9	24	20	24	-
Cv2	37	29	25	31	27	10
Cv3	43	29	28	32	31	13
Cv4	49	30	29	33	33	15
Cv5	50	30	32	35	36	16
Cv6	49	33	-	37	39	16
Cv7	45	35	38	36	41	15
Cv8	-	37	40	-	-	17
D4	37	37	39	35	37	17
D5	36	37	38	37	37	16
D6	-	37	37	-	-	15
D7	38	36	37	35	38	16
D8	38	36	37	37	37	15
D9	38	36	37	36	38	15
D10	-	38	38	-	-	-
Cd1	38	43	43	41	-	22
Cd2	36	41	-	42	40	20
Cd4	36	40	39	39	35	18
Cd5	33	40	-	36	-	19
Cd6	35	39	-	36	32	18
Cd7	33	-	29	31	28	16
PCd1	-	18	17	-	-	9
PCd2	27	17	16	17	16	8
PCd3	27	17	16	16	15	8
PCd4	26	16	15	16	15	7
PCd5	28	16	15	16	14	7
PCd6	26	15	14	15	14	7

TABLE S4. Measurements of the pelvic girdle and hind limb elements of *Mandasuchus tanyauchen* (NHMUK PV R6794). Some standard measurements are unavailable due to incompleteness. All measurements are provided in mm. Measurements indicated with '*' are minima, due to breakage or abrasion.

Element/measurement	
Left tibia	
Length	221
Anteroposterior length of proximal end	61
Mediolateral width of proximal end	50
Midshaft diameter in lateral view	24
Anteroposterior length of distal end	42
Mediolateral width of distal end	33
Right fibula	
Anteroposterior diameter of proximal end	33
Mediolateral diameter of proximal end	21
Left ilium	
Length	172*
Length of anterior iliac process	16*
Length of posterior iliac process	87*
Height of iliac blade dorsal to acetabulum	33
Anteroposterior diameter of acetabulum	77
Dorsoventral diameter of acetabulum	73
Length of pubic articular surface	64
Length of ischiac articular surface	65
Left pubis	
Length	157
Maximum mediolateral width of proximal end	30
Left ischium	
Length	183
Maximum anteroposterior length of proximal end	63
Maximum mediolateral width of proximal end	39

LITERATURE CITED

Charig, A. J. 1956. New Triassic archosaurs from Tanganyika including *Mandasuchus* and *Teleocrater*. Unpublished PhD dissertation, University of Cambridge, Cambridge, 503 pp., 53 pls.

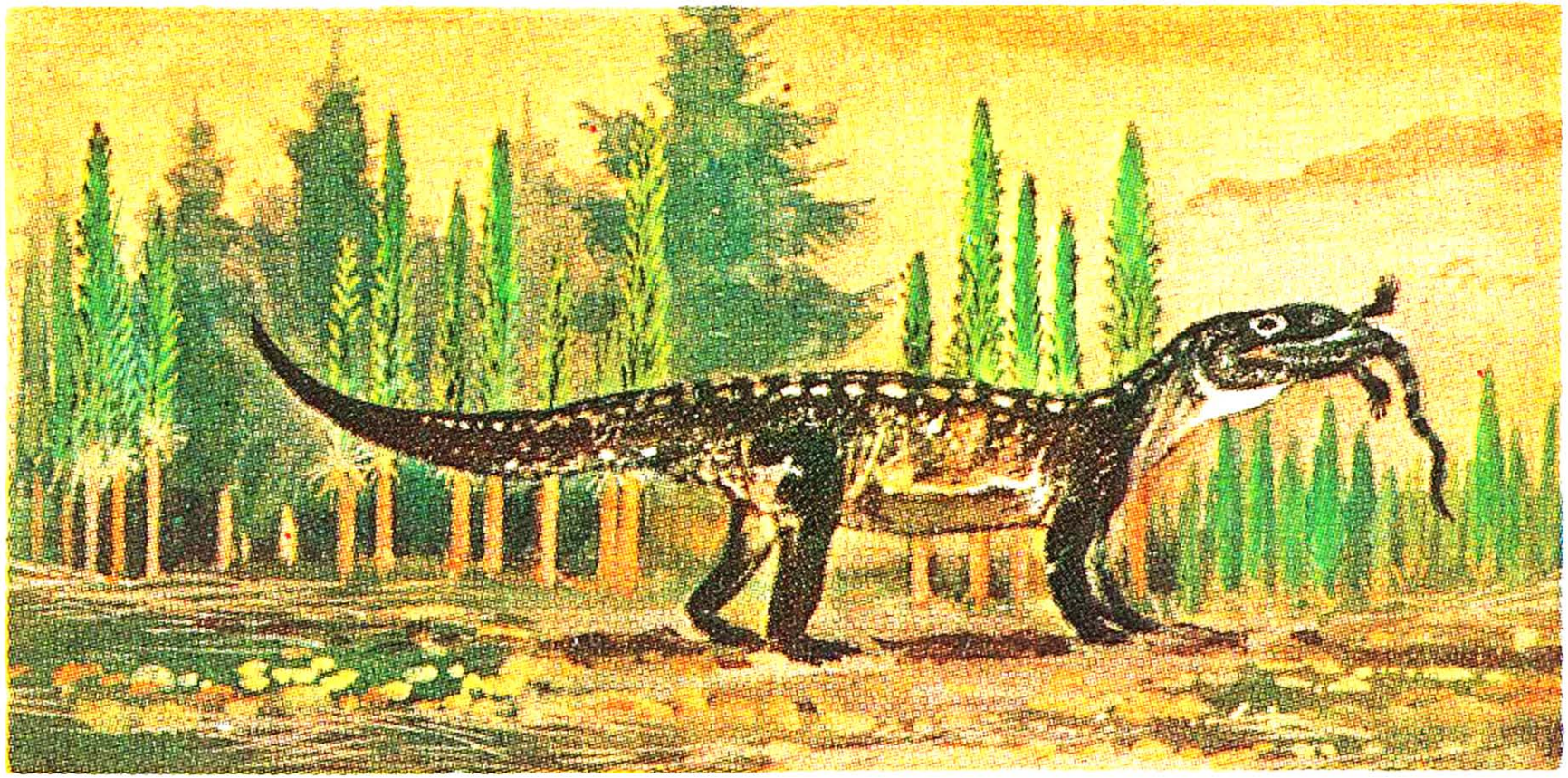

9. MANDASUCHUS (*from Manda in Tanzania and Greek 'crocodile'*)
This reptile was a typical pseudosuchian, belonging to the group from which dinosaurs, pterosaurs, crocodiles and birds all evolved. Contrary to what is stated in many books, however, most of the pseudosuchians showed no tendency towards walking or running on their hind legs alone. *Mandasuchus* lived in Tanzania in Middle Triassic times, 210 million years ago. It was of crocodile-like size and build, with large teeth of the carnivorous type, a double row of armour-plates down the middle of the back and hind legs rather longer than the front ones. Its habits too were probably like those of modern crocodiles, though it may have been less fond of the water.

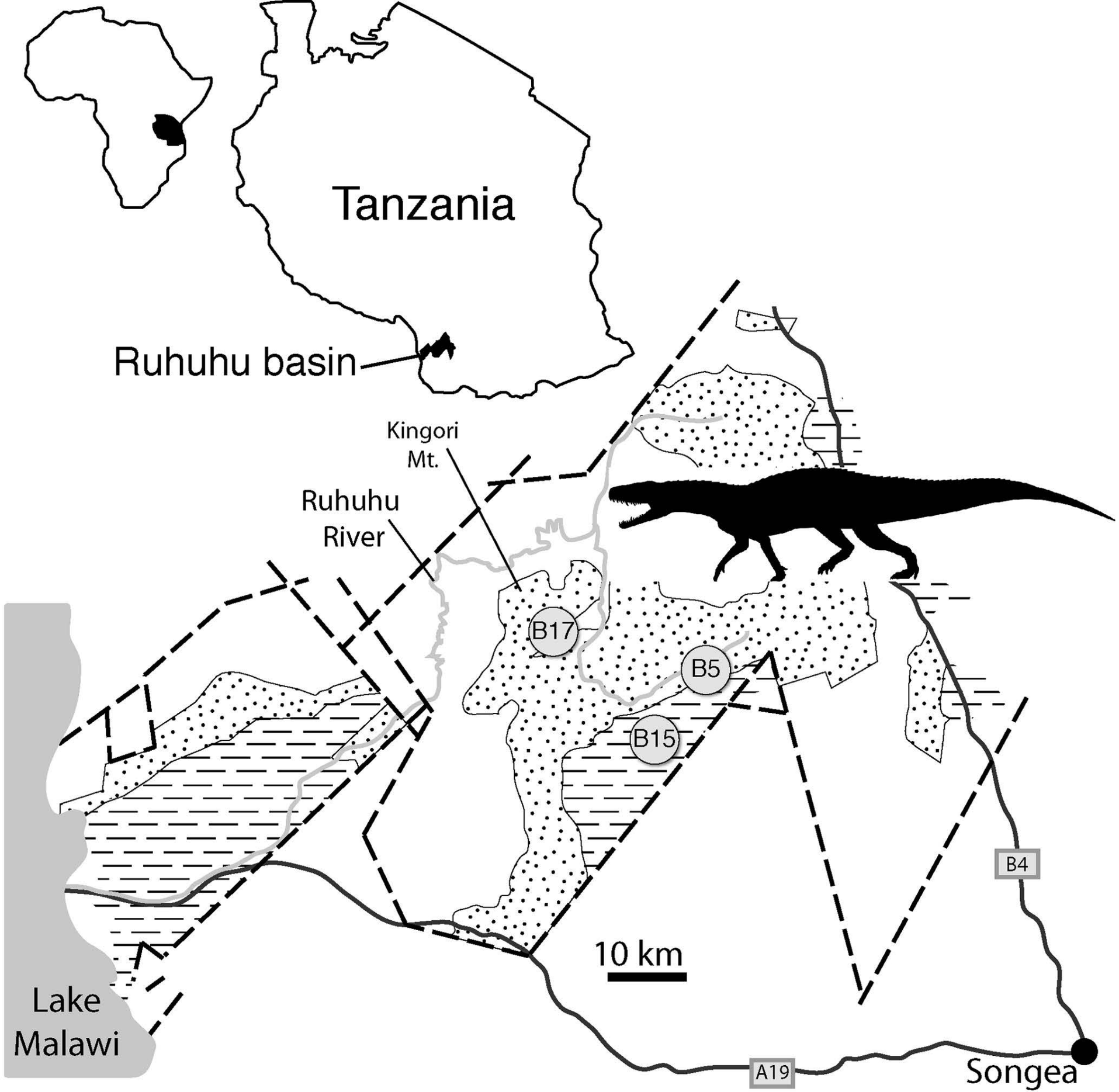
Tanzania
Ruhuhu basin
Kingori
Mt.
Ruhuhu
River
B17
B5
B15
B4
10 km
Lake
Malawi
A19
Songea

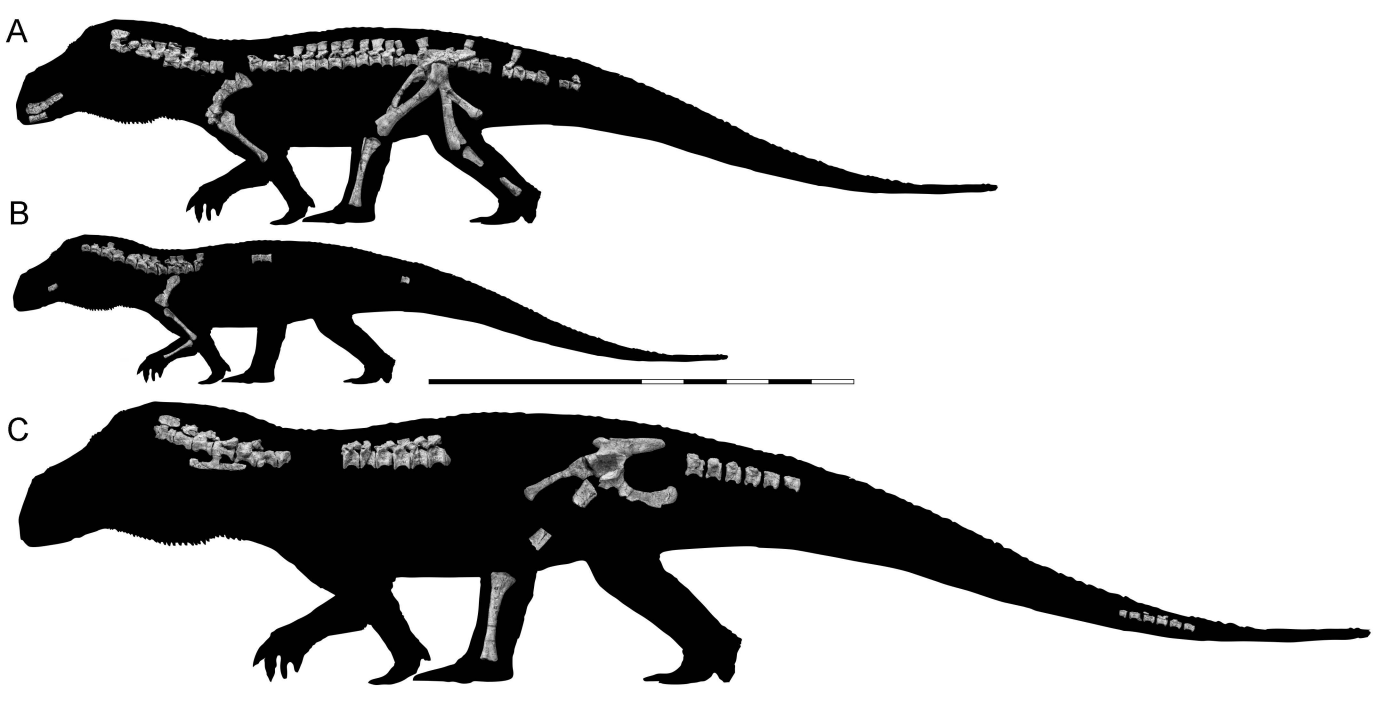
A
B
C

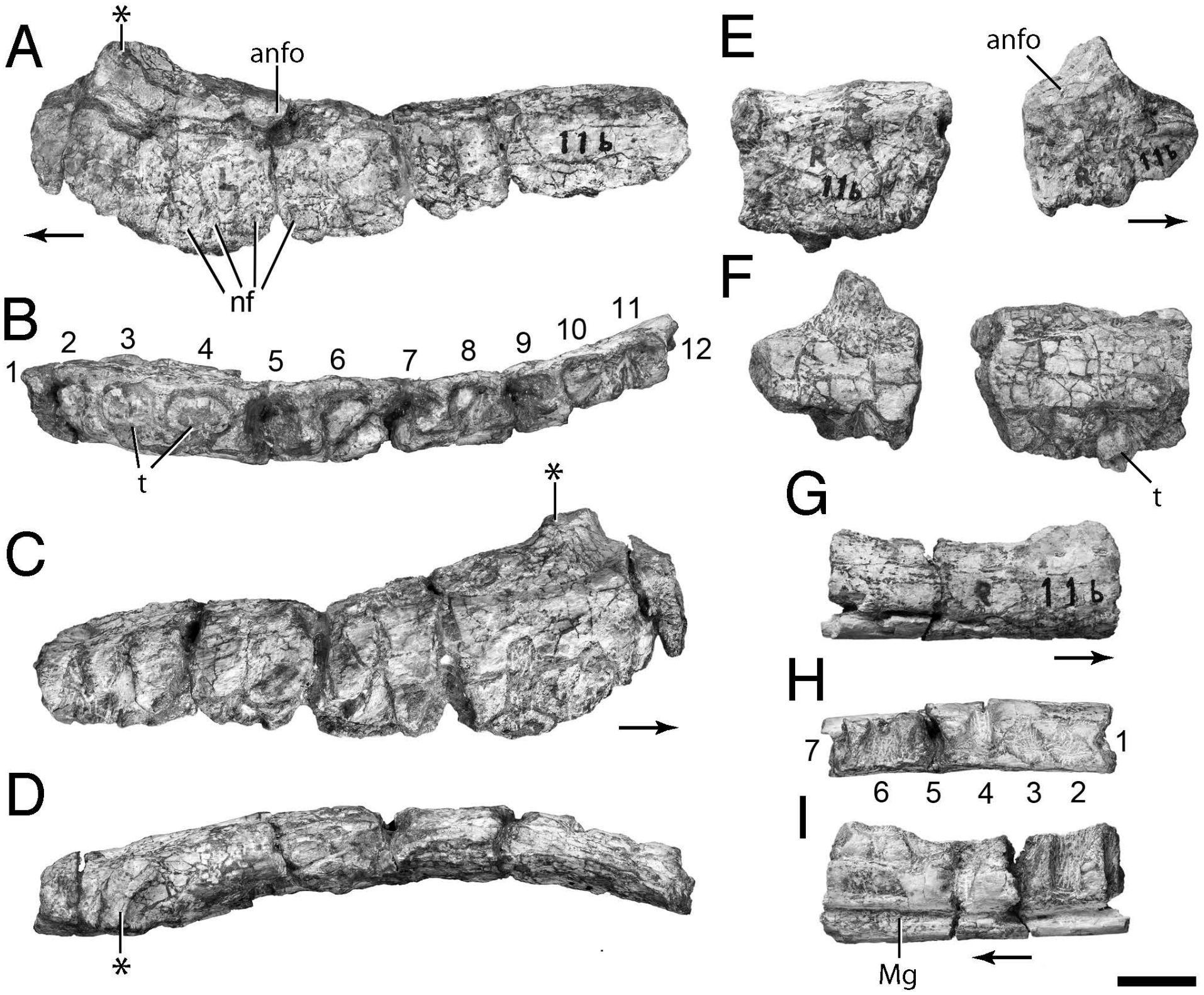
A
anfo
nf
11b
B
1
2
3
4
5
6
7
8
9
10
11
12
t
C
D
E
anfo
R
11b
F
t
G
R
11b
H
7
1
6
5
4
3
2
I
Mg

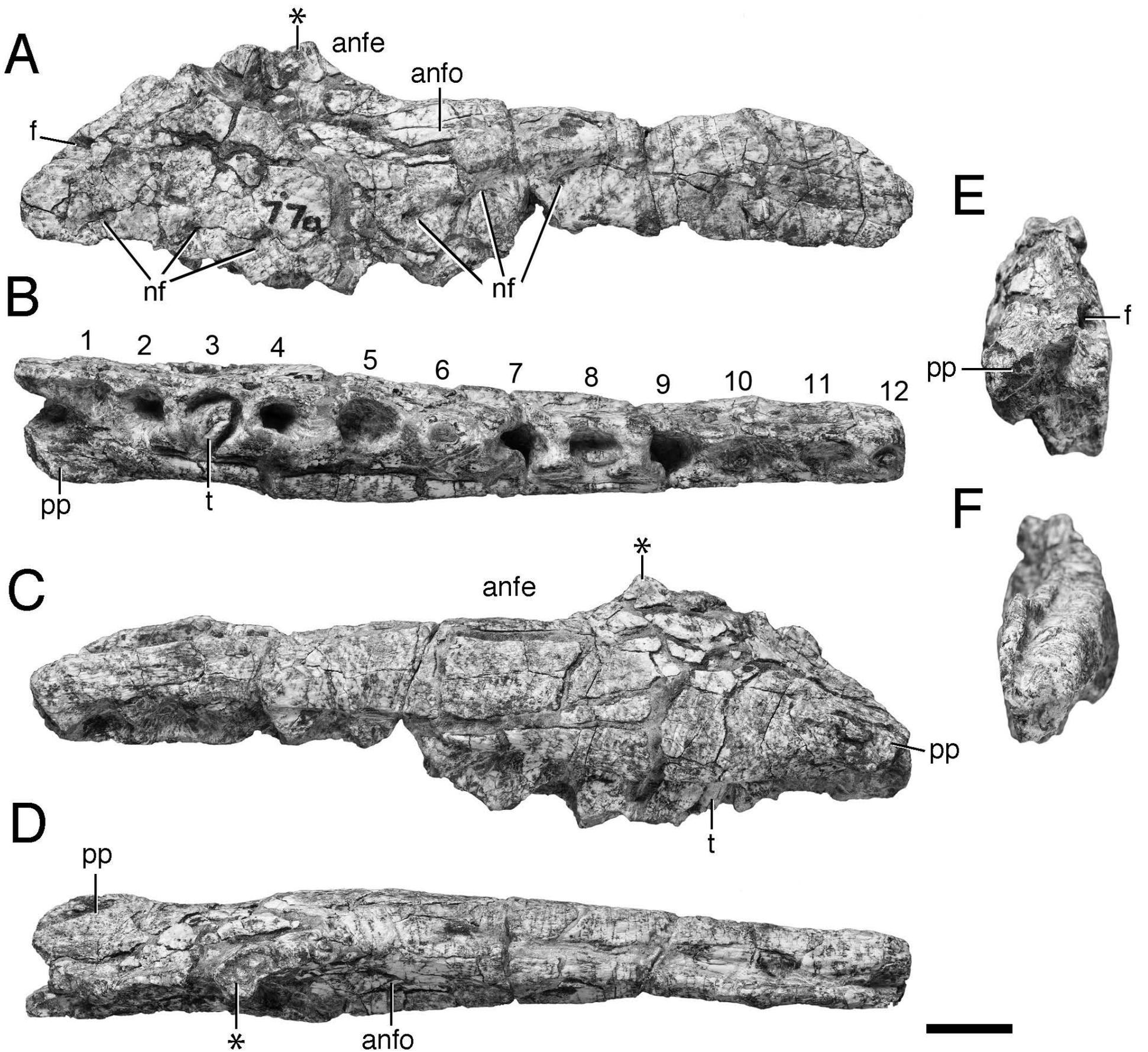
A
*
anfe
anfo
f
nf
nf
B
1
2
3
4
5
6
7
8
9
10
11
12
pp
t
C
*
anfe
pp
t
D
pp
*
anfo
E
f
pp
F

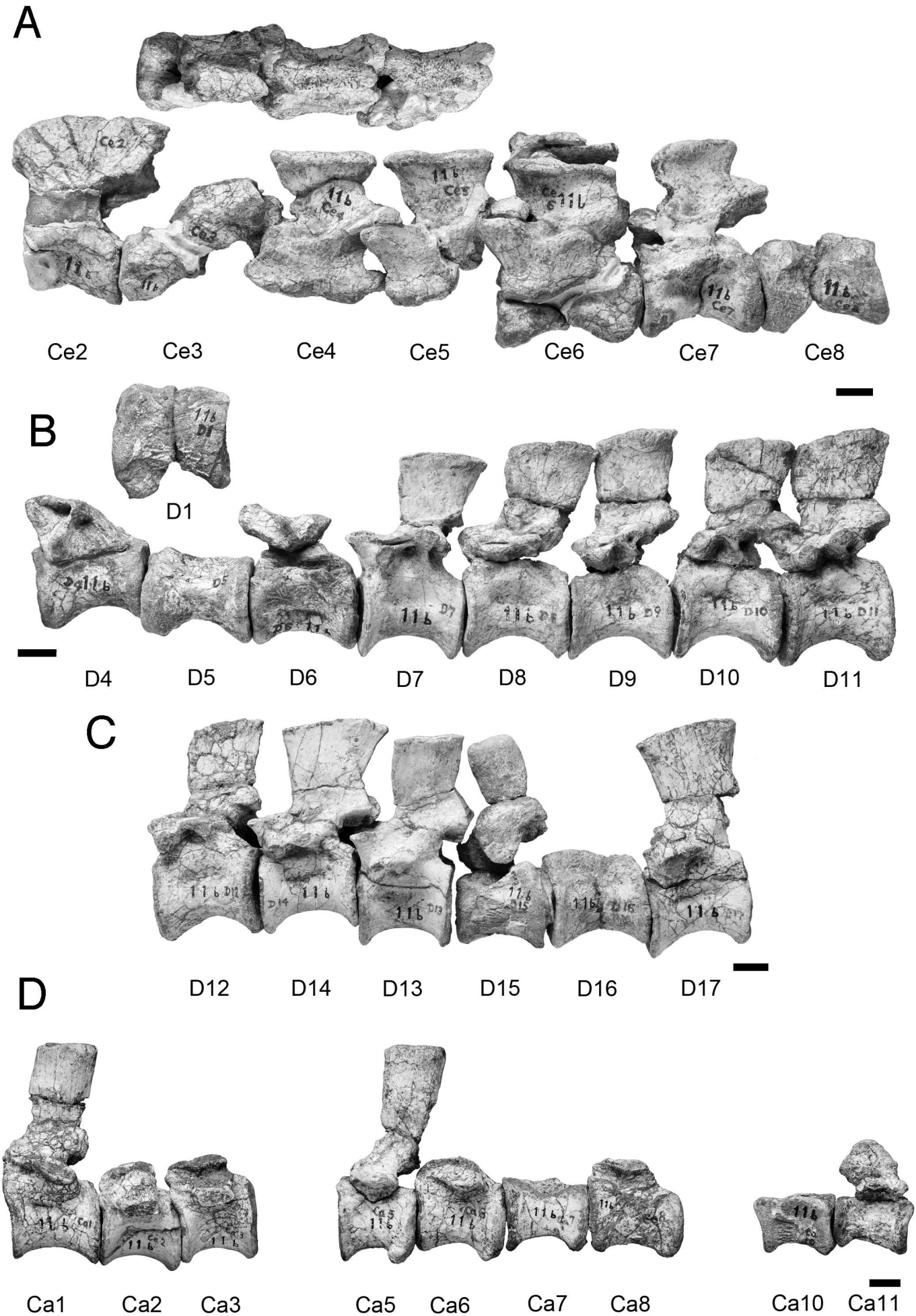
A
Ce2
Ce3
Ce4
Ce5
Ce6
Ce7
Ce8
B
D1
D4
D5
D6
D7
D8
D9
D10
D11
C
D12
D14
D13
D15
D16
D17
D
Ca1
Ca2
Ca3
Ca5
Ca6
Ca7
Ca8
Ca10
Ca11

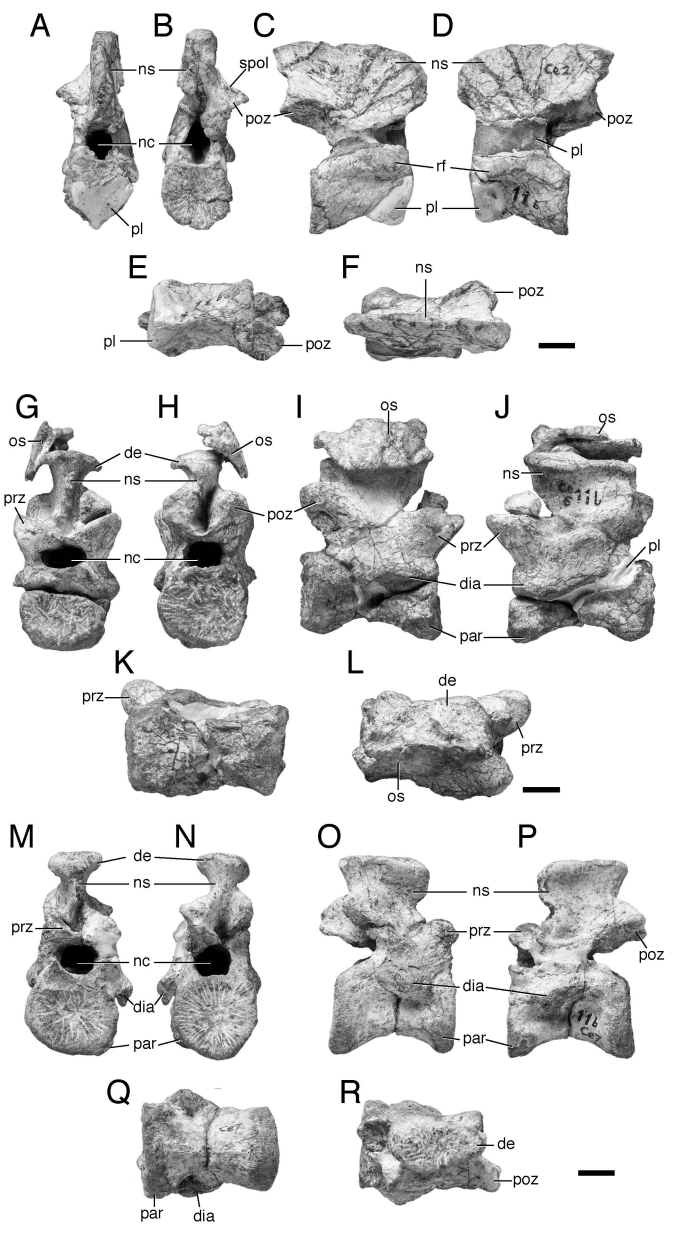
A
B
C
D
ns
spol
poz
nc
pl
ns
poz
rf
pl
E
F
pl
poz
ns
poz
G
H
I
J
os
de
ns
prz
nc
os
poz
os
os
ns
prz
dia
par
pl
K
L
prz
de
prz
os
M
N
O
P
de
ns
prz
nc
dia
par
ns
prz
dia
par
poz
Q
R
par
dia
de
poz

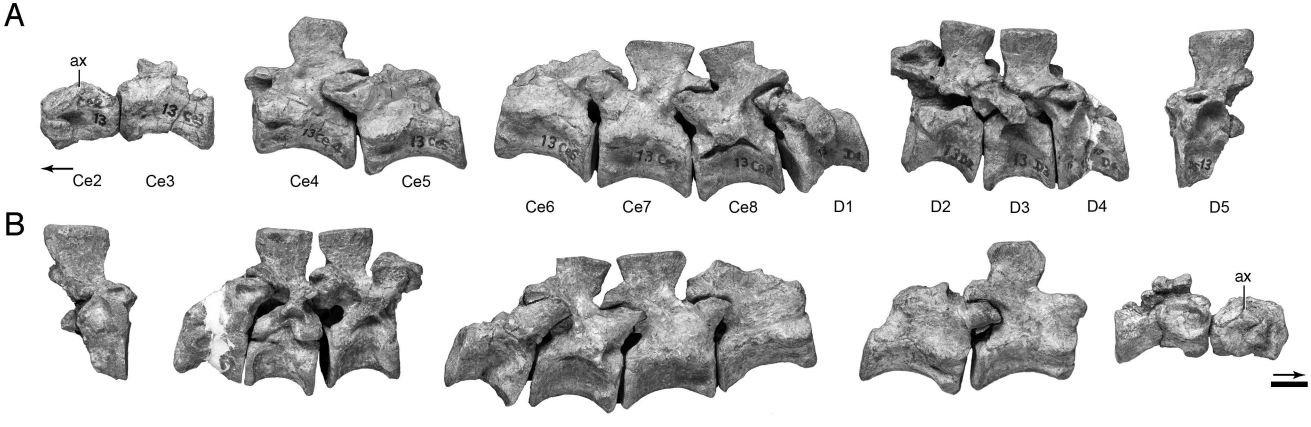
A
ax
Ce2
Ce3
Ce4
Ce5
Ce6
Ce7
Ce8
D1
D2
D3
D4
D5
B
ax

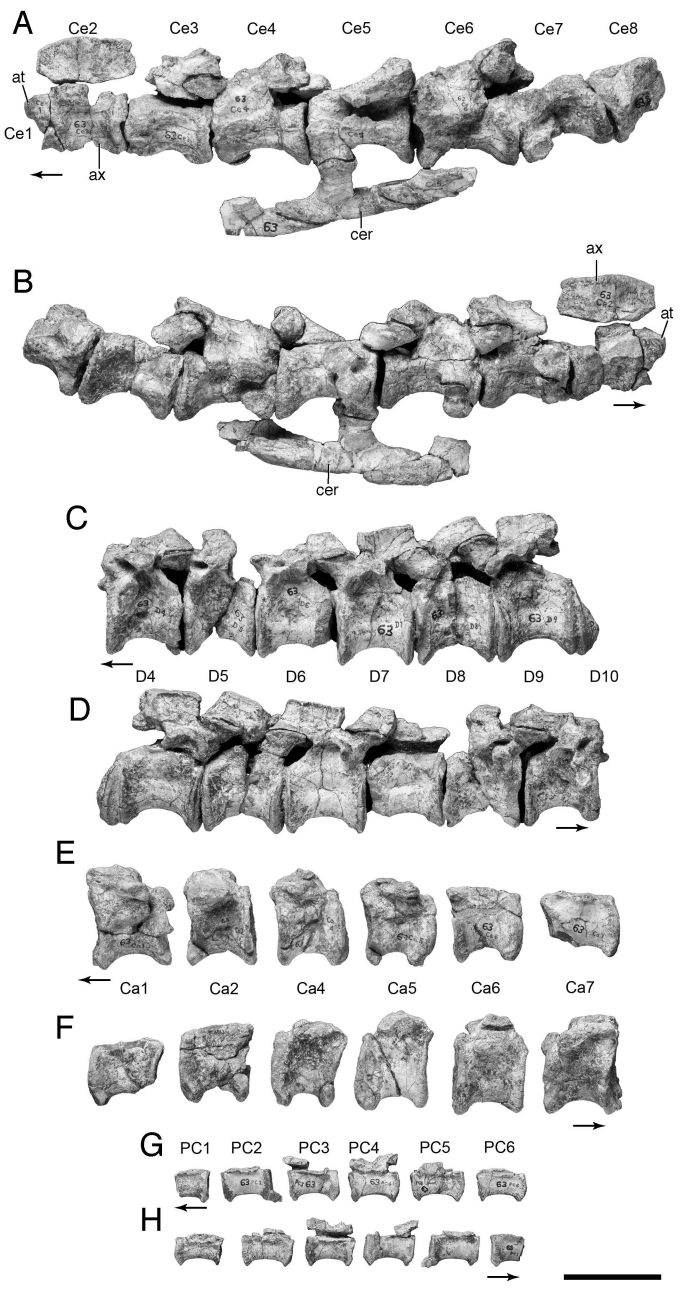
A
Ce2
Ce3
Ce4
Ce5
Ce6
Ce7
Ce8
at
Ce1
ax
cer
B
ax
at
cer
C
D4
D5
D6
D7
D8
D9
D10
D
E
Ca1
Ca2
Ca4
Ca5
Ca6
Ca7
F
G
PC1
PC2
PC3
PC4
PC5
PC6
H

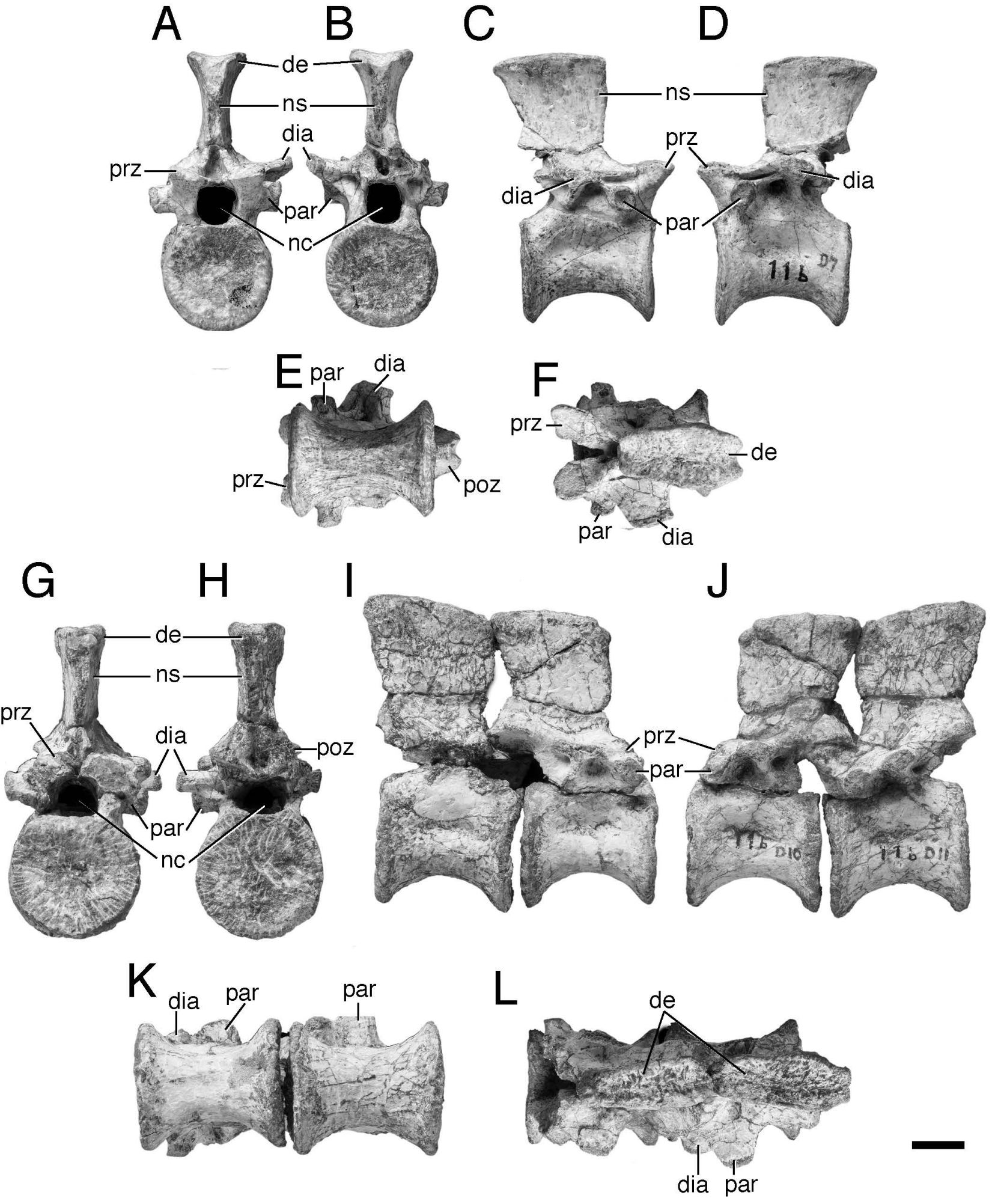
A
B
C
D
de
ns
dia
prz
par
nc
ns
prz
dia
dia
par
11b D7
E
par
dia
prz
poz
F
prz
de
par
dia
G
H
I
J
de
ns
prz
dia
poz
par
nc
prz
par
11b D10
11b D11
K
dia
par
par
L
de
dia
par

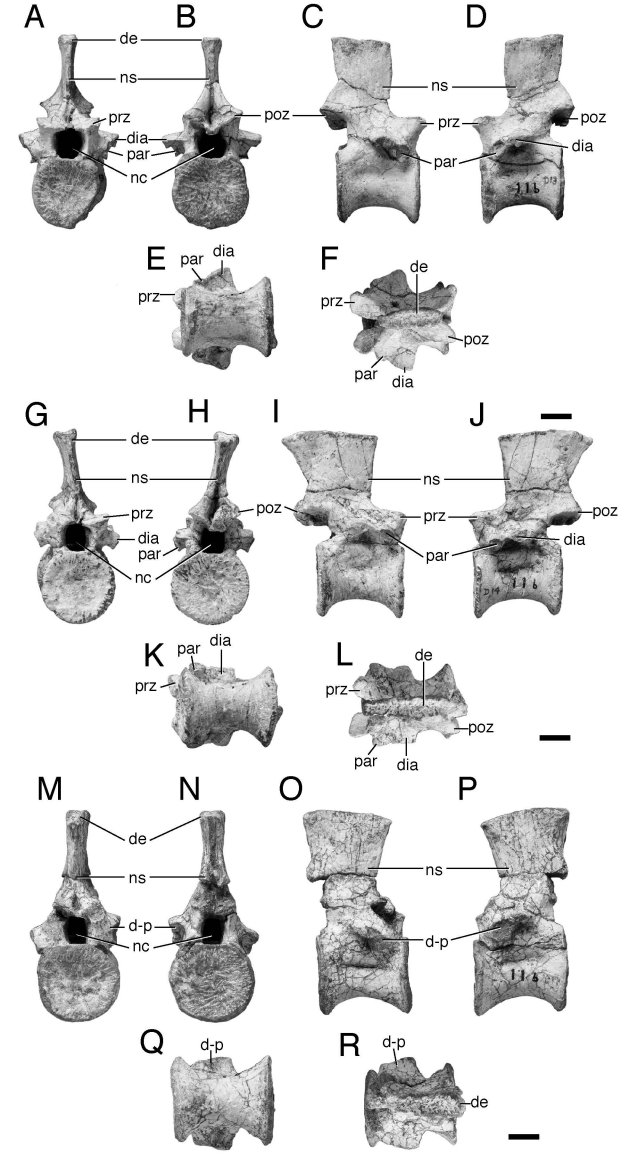
A
B
C
D
de
ns
prz
poz
dia
par
nc
E
F
G
H
I
J
K
L
M
N
O
P
d-p
Q
R

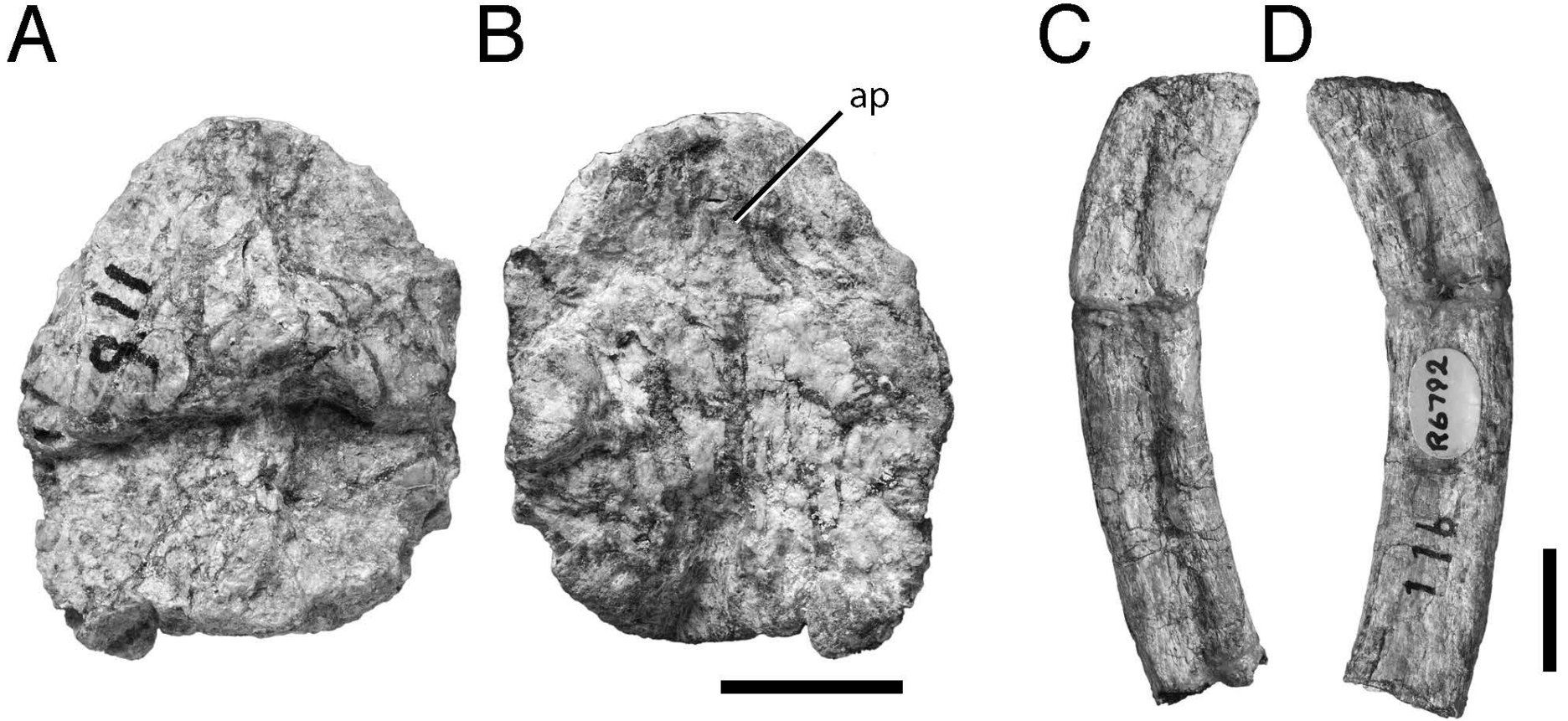
A
B
C
D
ap
R6792

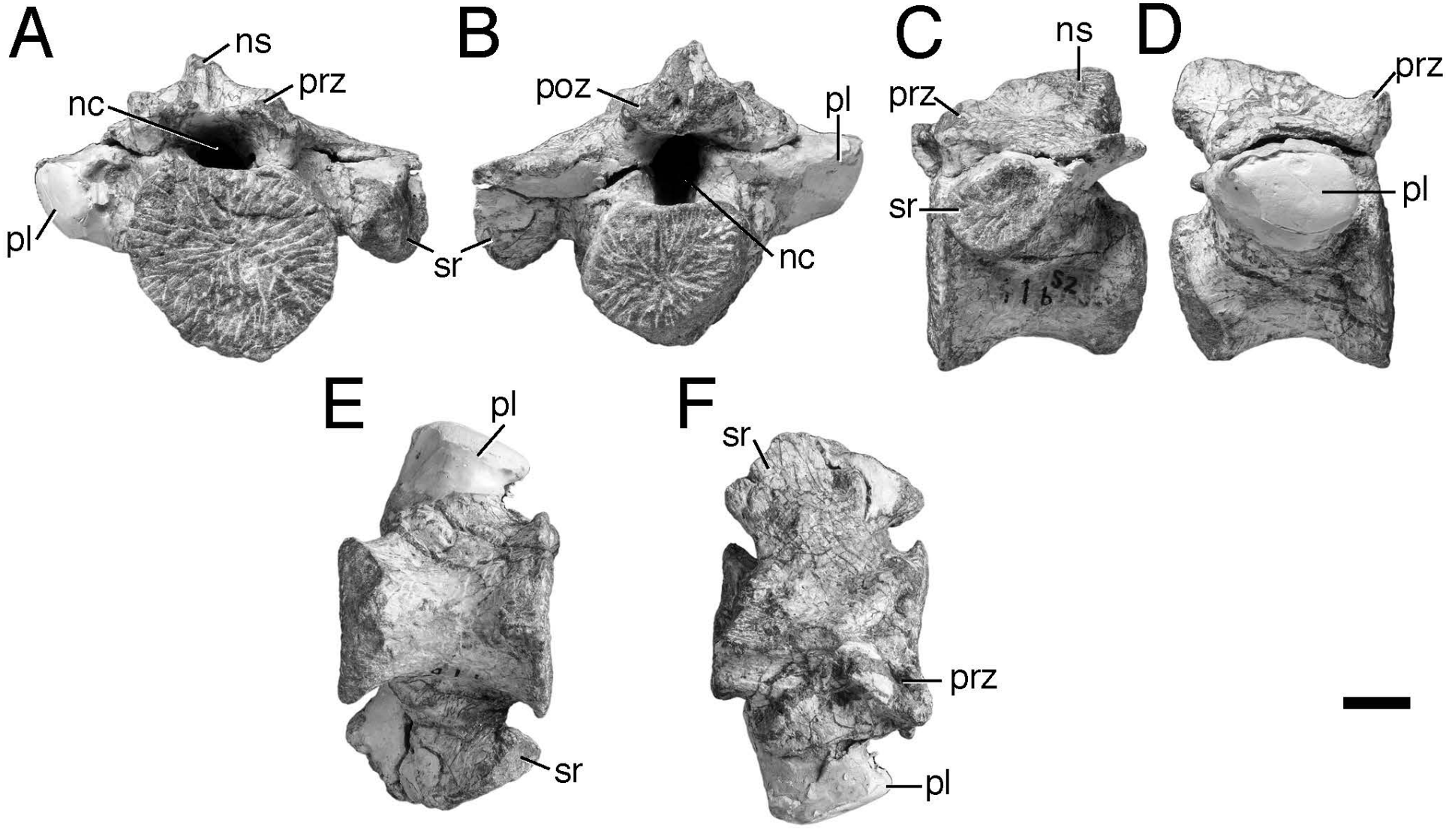
A
ns
prz
nc
pl
sr
B
poz
pl
nc
C
ns
prz
sr
D
prz
pl
E
pl
sr
F
sr
prz
pl

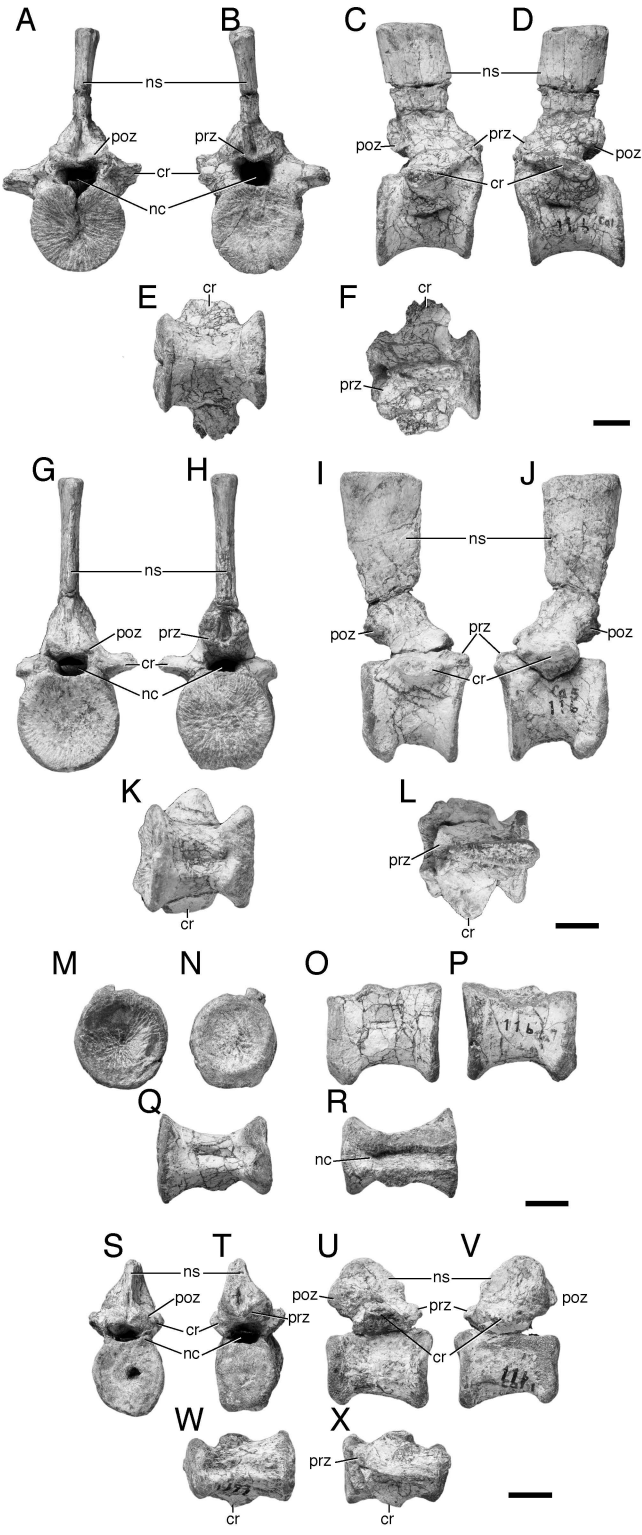
A
B
C
D
ns
poz
prz
cr
nc
E
F
G
H
I
J
K
L
M
N
O
P
Q
R
S
T
U
V
W
X

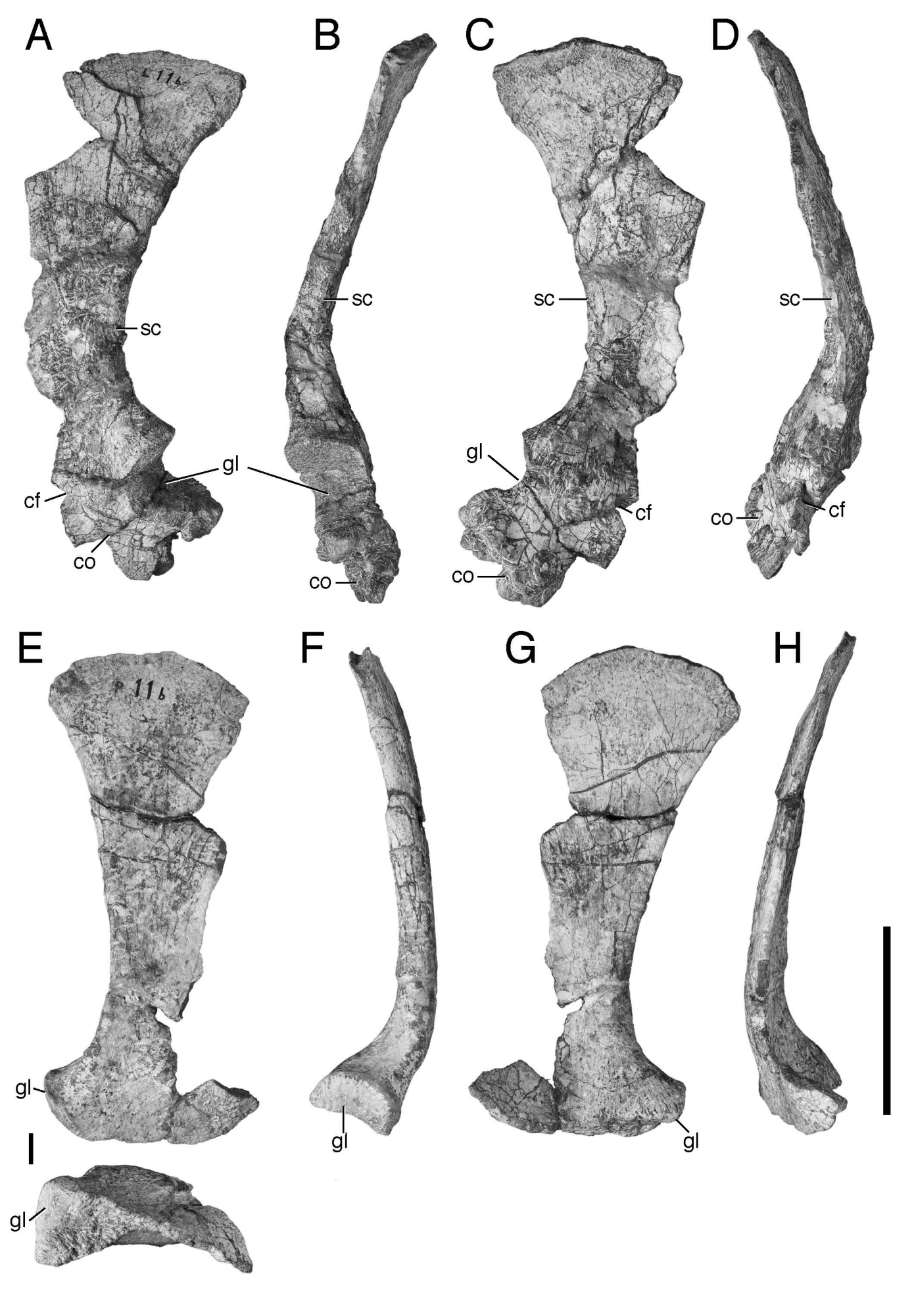
A
B
C
D
E
F
G
H
I
sc
gl
cf
co
L 11b
P 11b

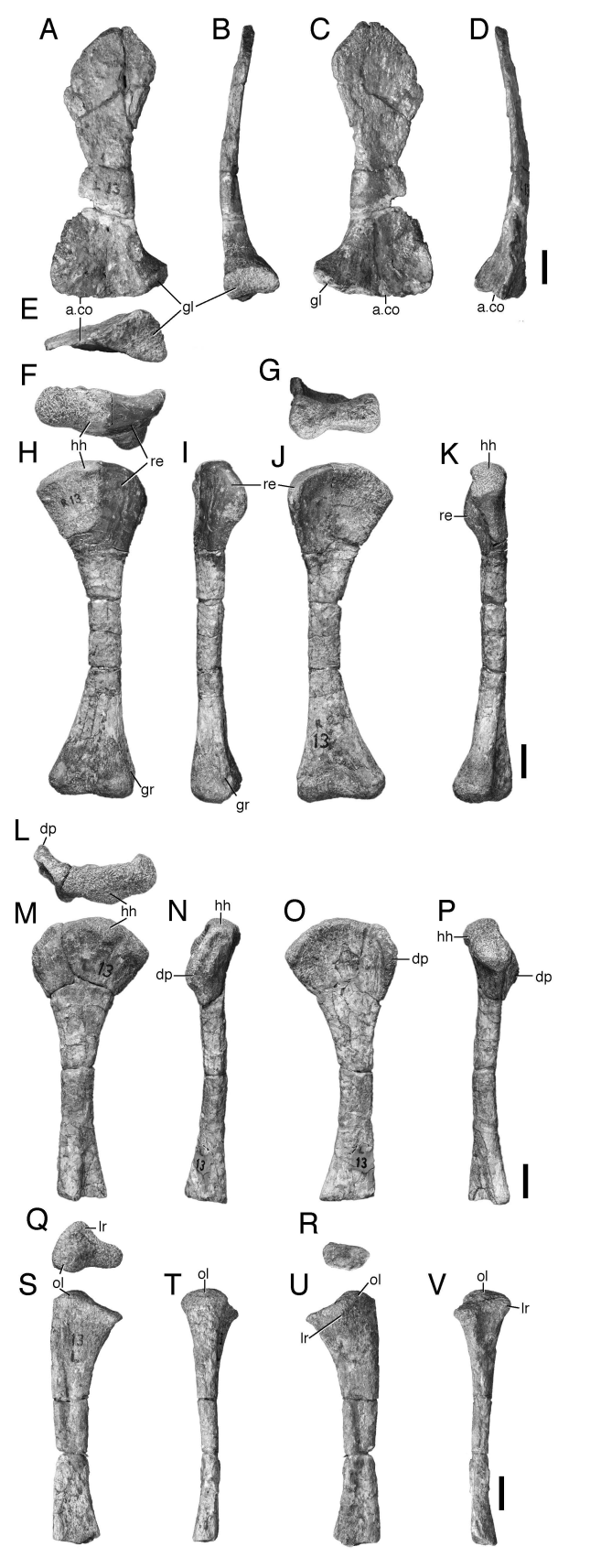
A
B
C
D
a.co
gl
gl
a.co
a.co
E
F
G
hh
re
H
I
re
J
K
hh
re
gr
gr
L
dp
M
hh
N
hh
dp
O
dp
P
hh
dp
Q
lr
ol
R
S
ol
T
ol
U
ol
lr
V
ol
lr

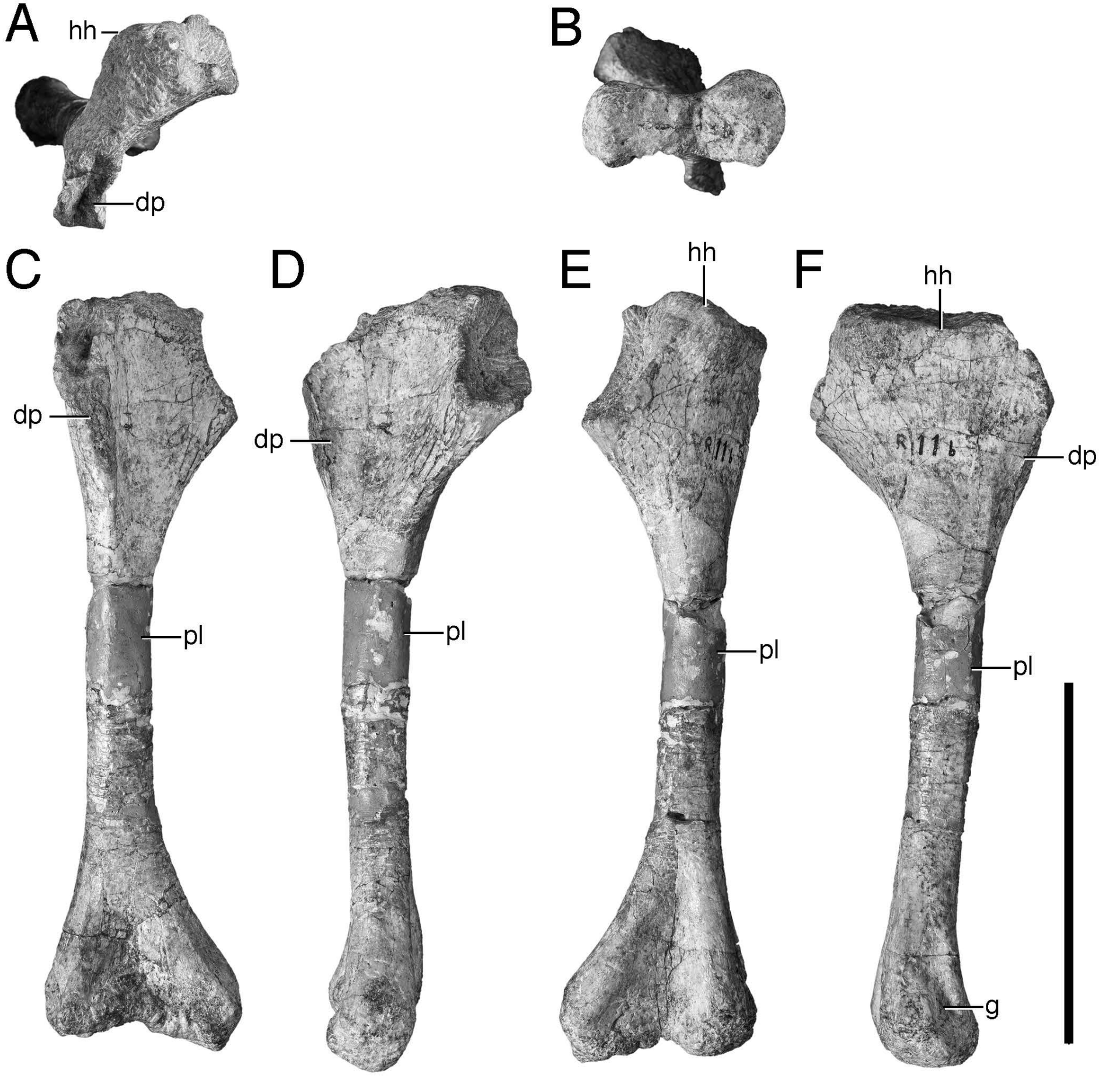
A
hh
dp
B
C
dp
pl
D
dp
pl
E
hh
pl
F
hh
dp
pl
g

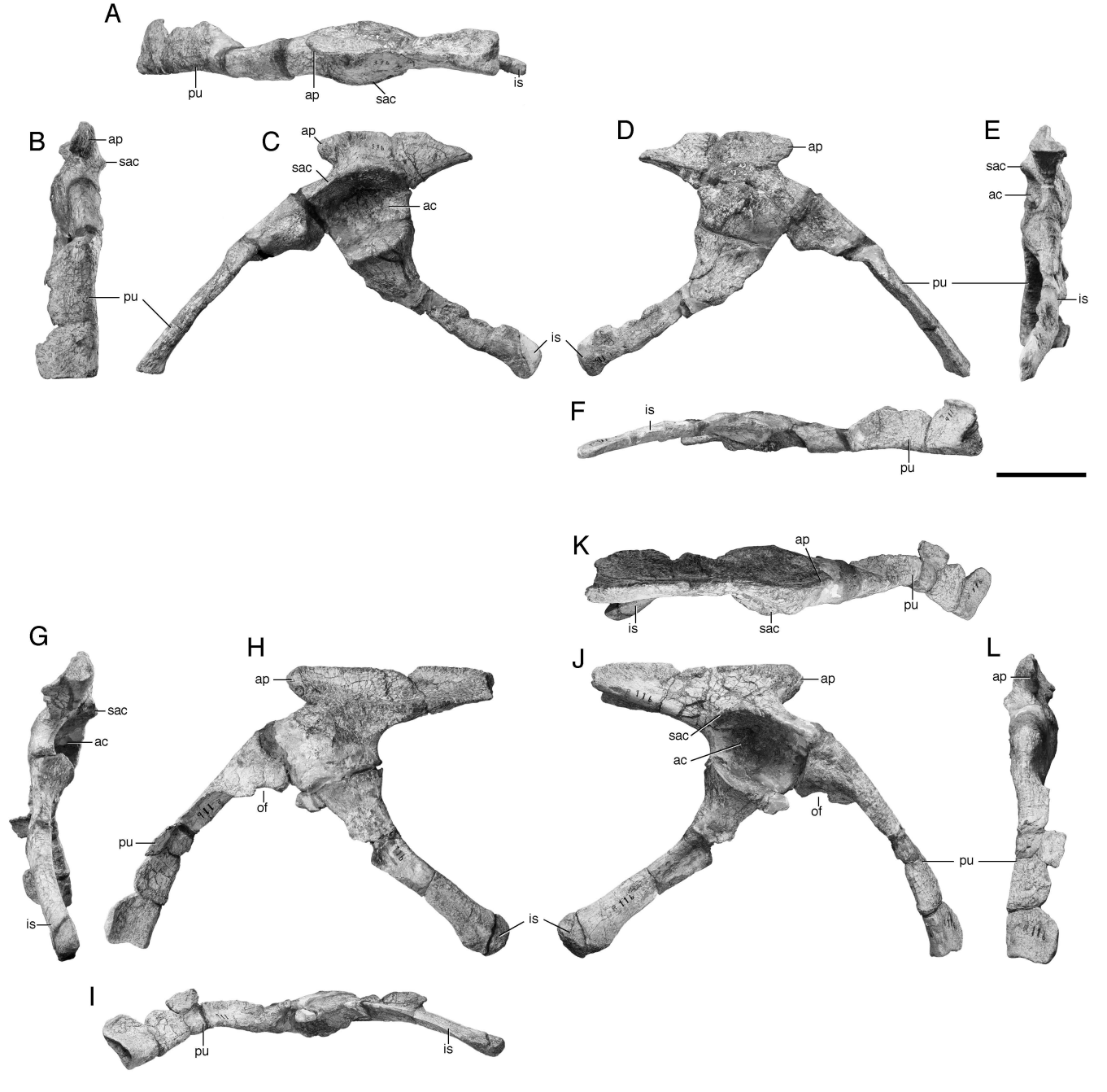
A
pu
ap
sac
is
B
ap
sac
pu
C
ap
sac
ac
is
D
ap
pu
E
sac
ac
is
F
is
pu
K
ap
is
sac
pu
G
sac
ac
is
H
ap
of
pu
is
J
ap
sac
ac
of
pu
is
L
ap
pu
I
pu
is

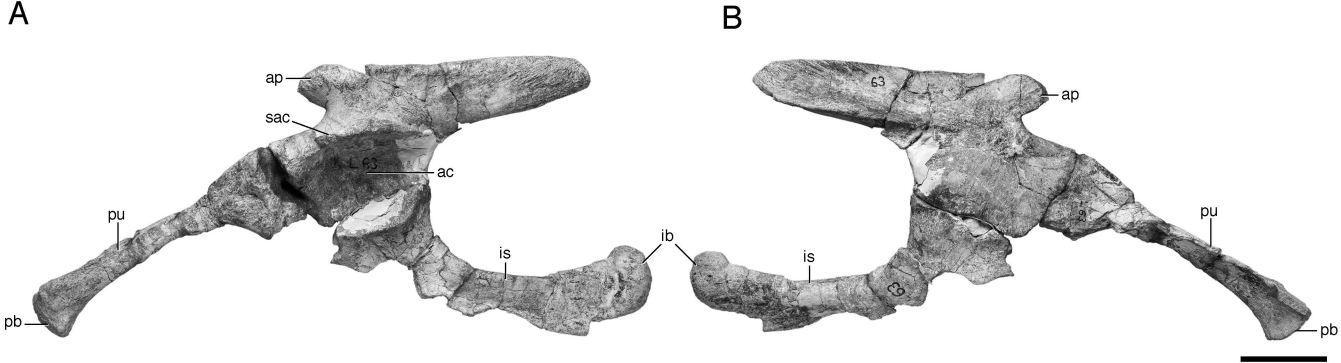
A
ap
sac
ac
pu
is
ib
pb
B
ap
pu
is
pb

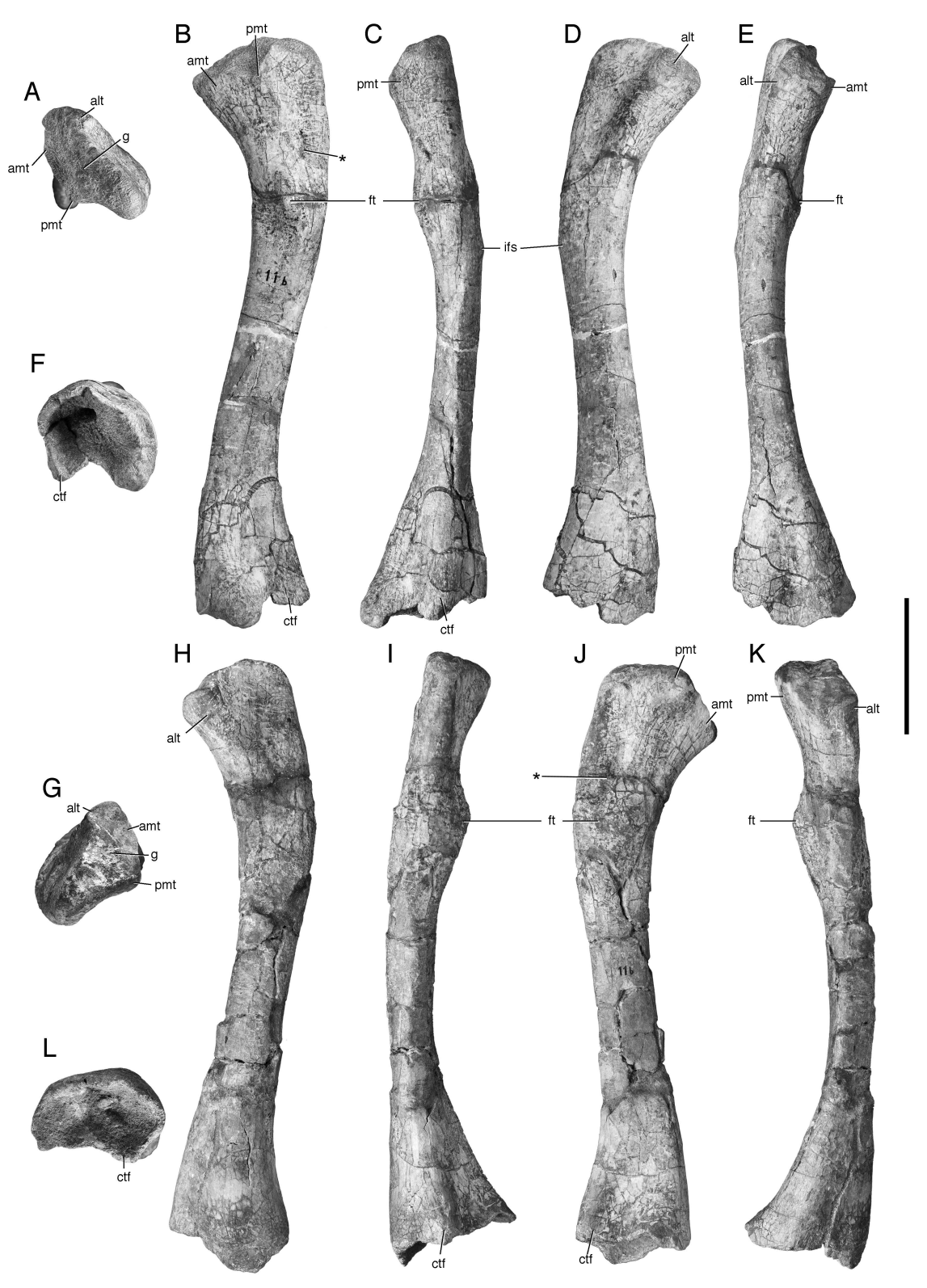
A
alt
g
amt
pmt
B
pmt
amt
*
ft
11b
ctf
C
pmt
ifs
ctf
D
alt
E
alt
amt
ft
F
ctf
G
alt
amt
g
pmt
H
alt
I
ft
ctf
J
pmt
amt
*
ft
11b
ctf
K
pmt
alt
ft
L
ctf

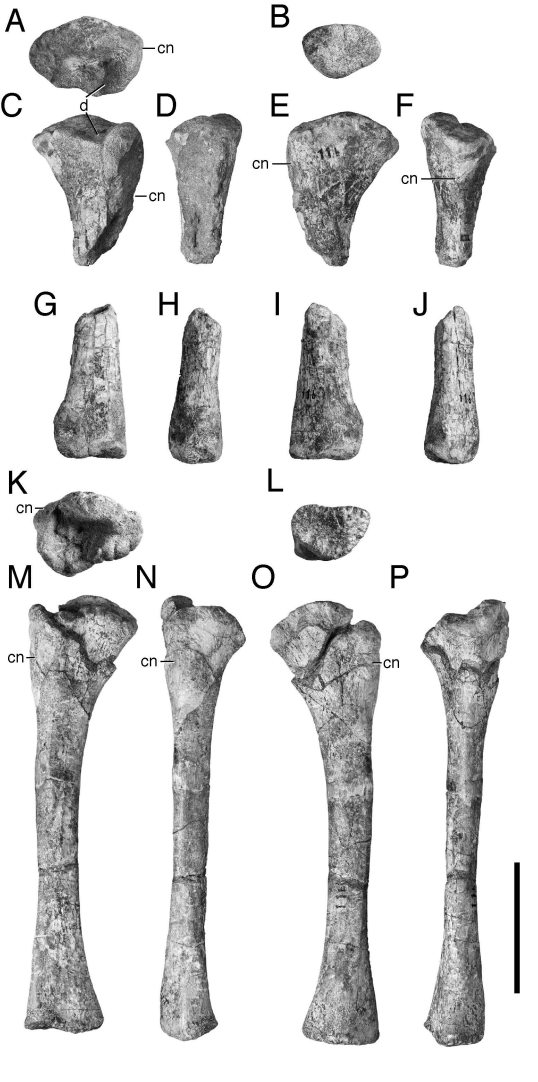
A
cn
B
C
d
cn
D
E
cn
F
cn
G
H
I
J
K
cn
L
M
cn
N
cn
O
cn
P

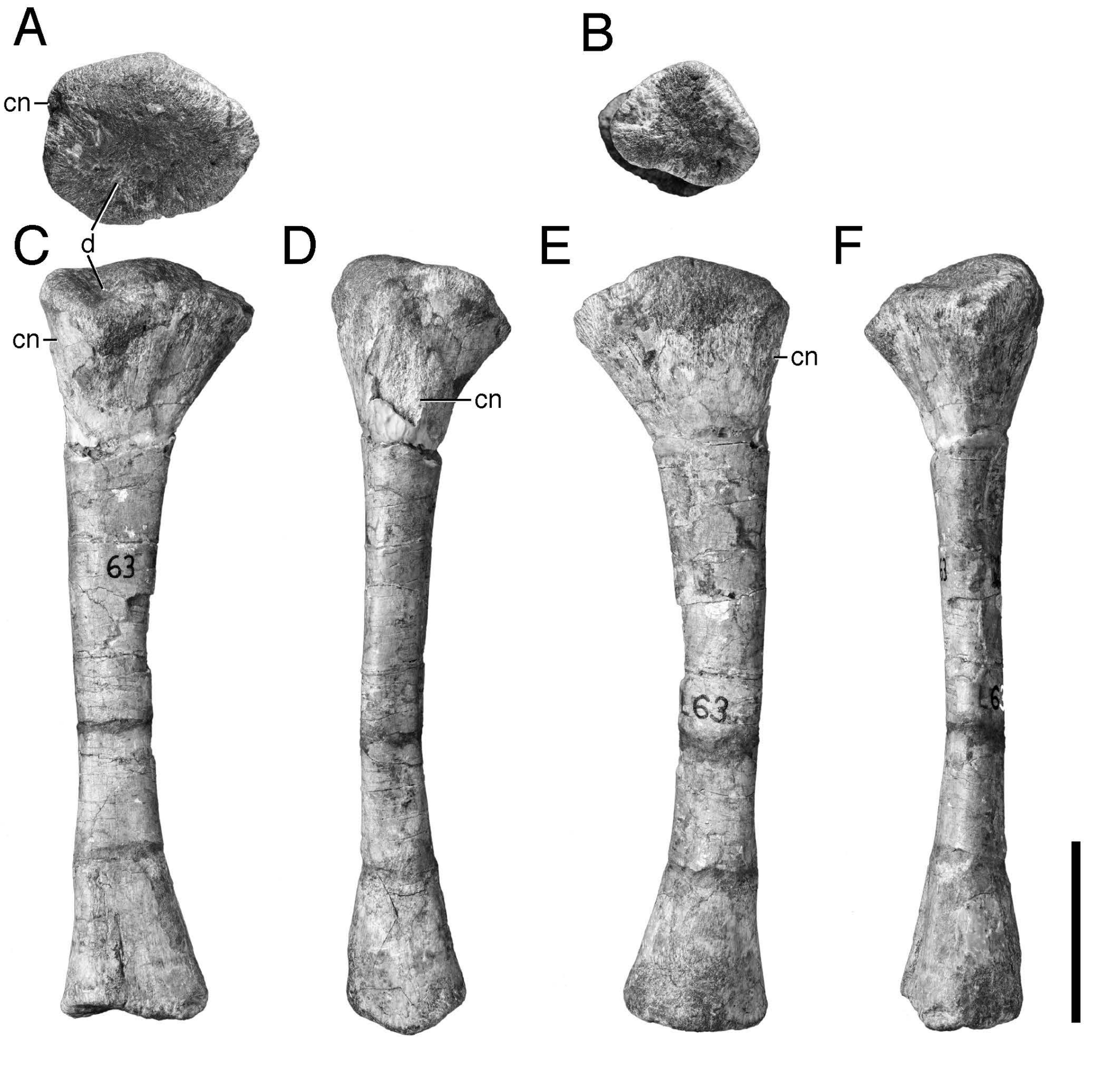
A
cn
d
B
C
cn
63
D
cn
E
cn
63
F

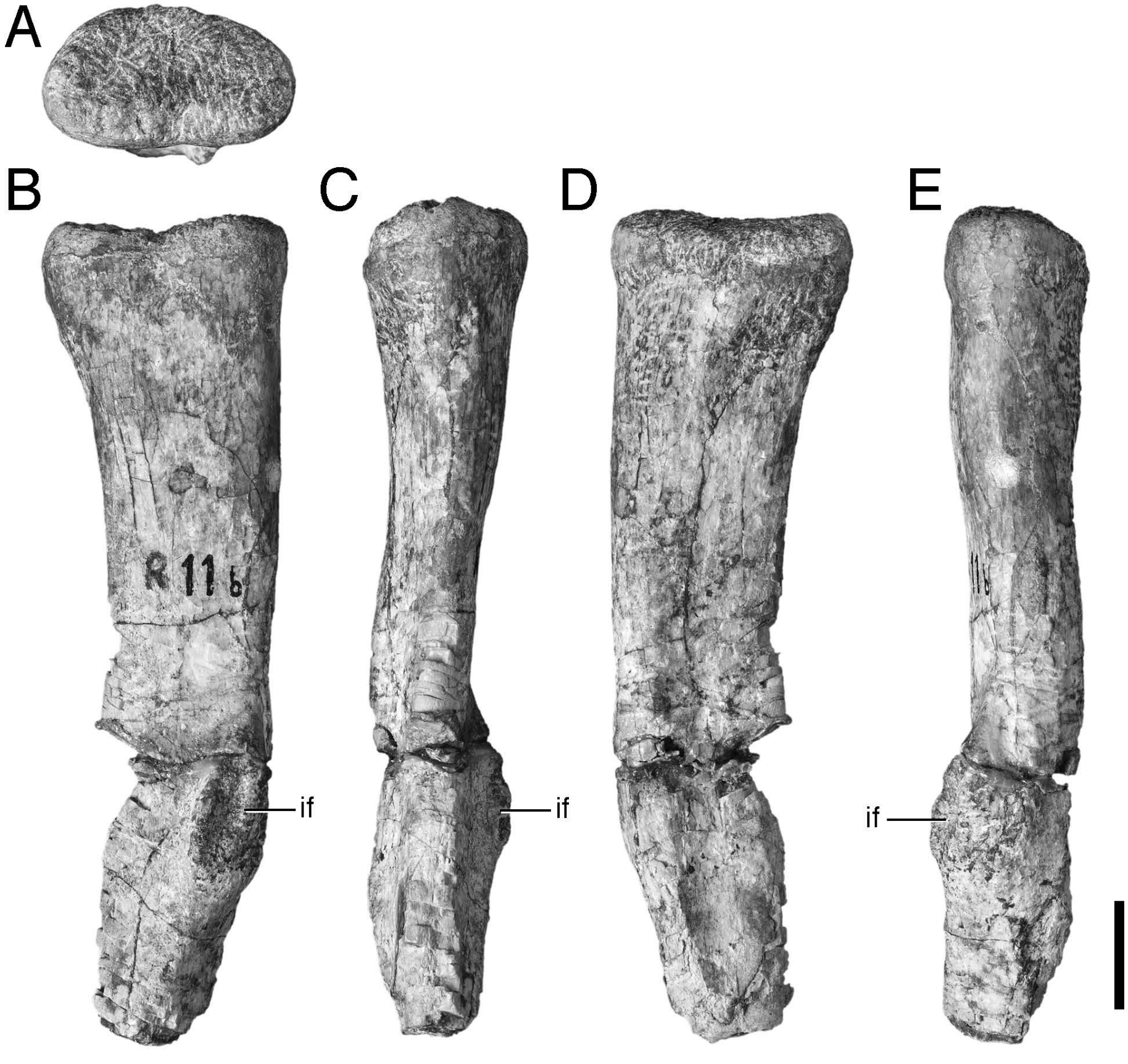
A
B
C
D
E
R 11 b
if
if
if

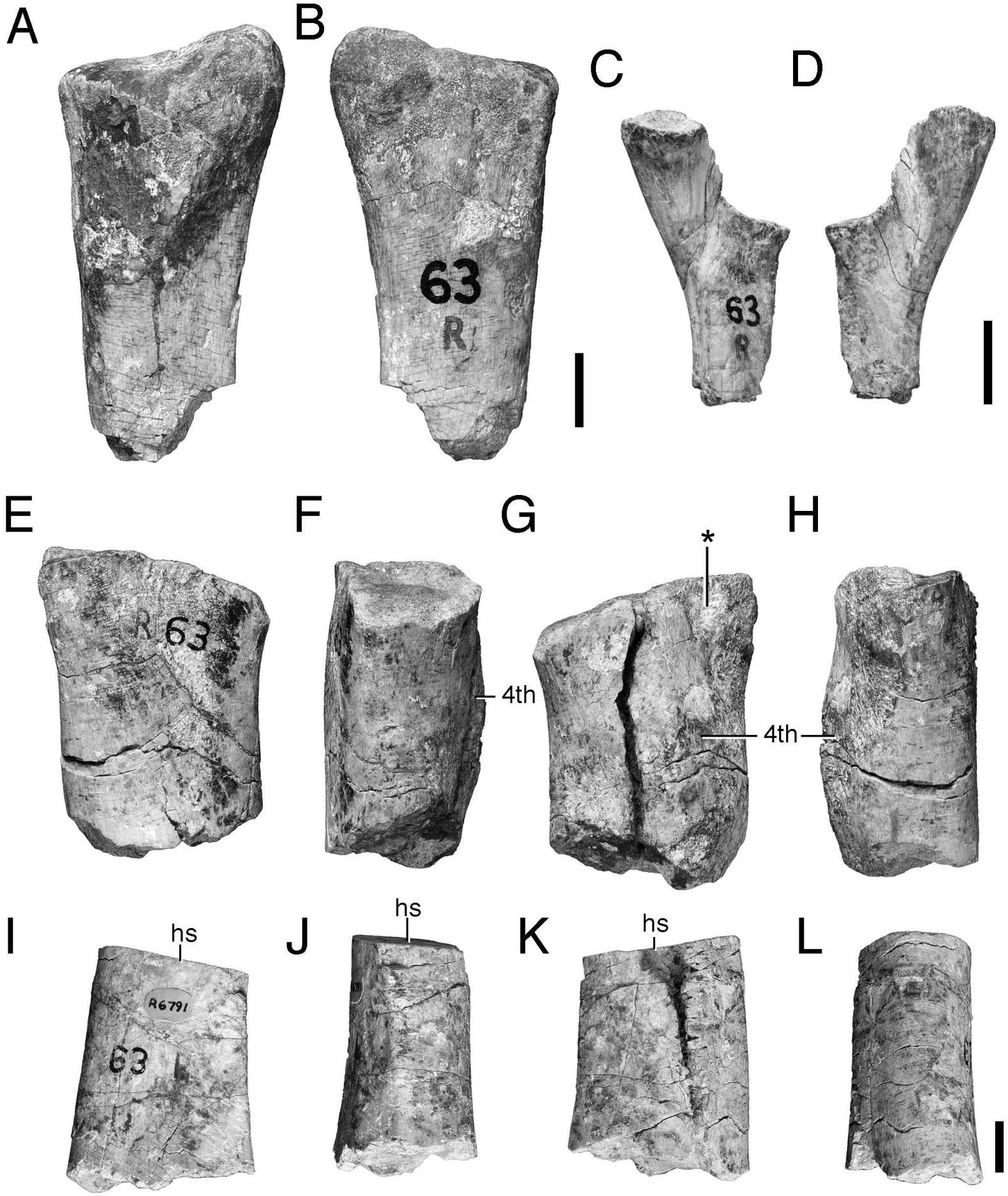
A
B
63
R
C
63
R
D
E
R 63
F
4th
G
*
4th
H
I
hs
R6791
63
J
hs
K
hs
L

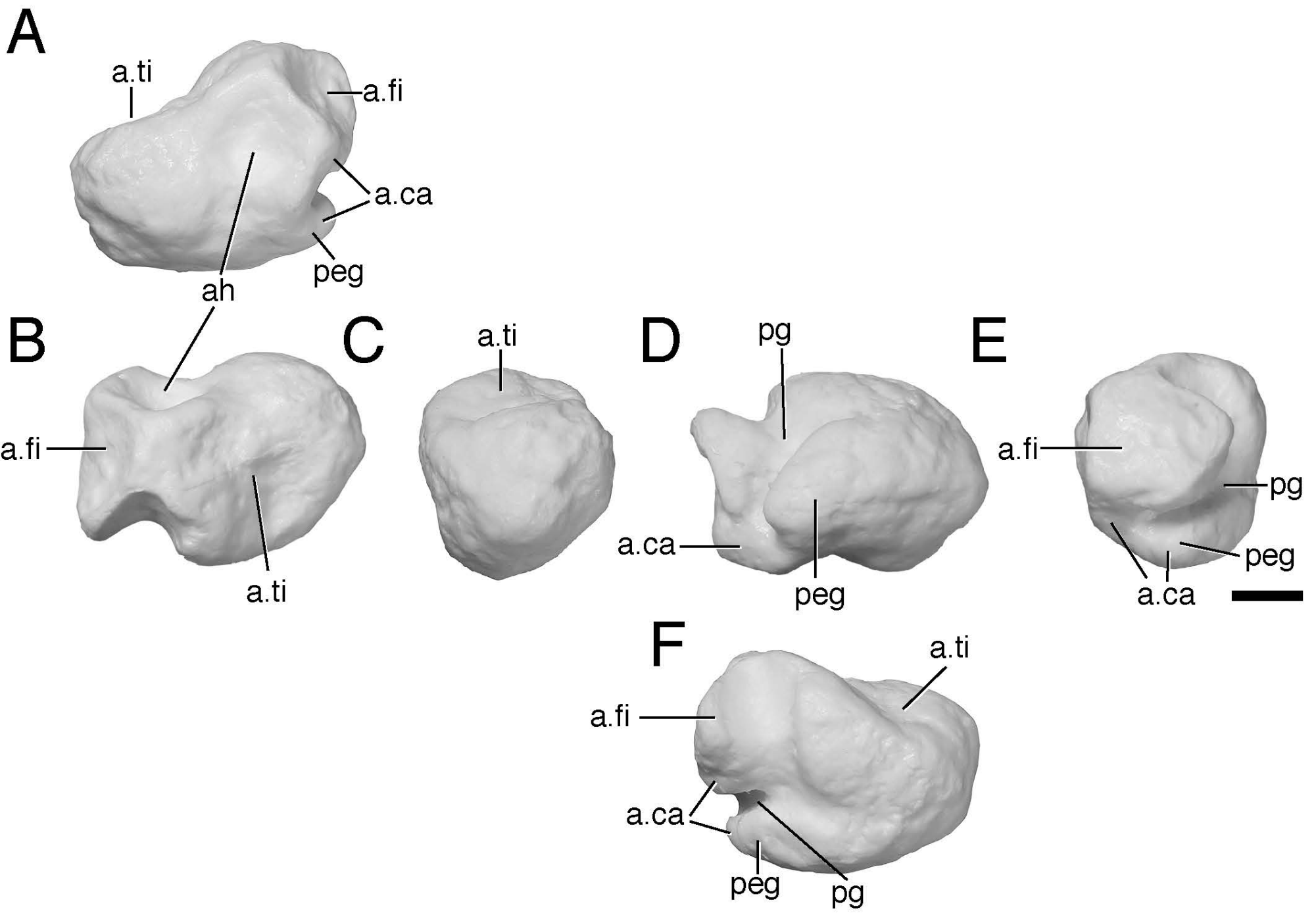
A
a.ti
a.fi
a.ca
peg
ah
B
a.fi
a.ti
C
a.ti
D
pg
a.ca
peg
E
a.fi
pg
peg
a.ca
F
a.ti
a.fi
a.ca
peg
pg

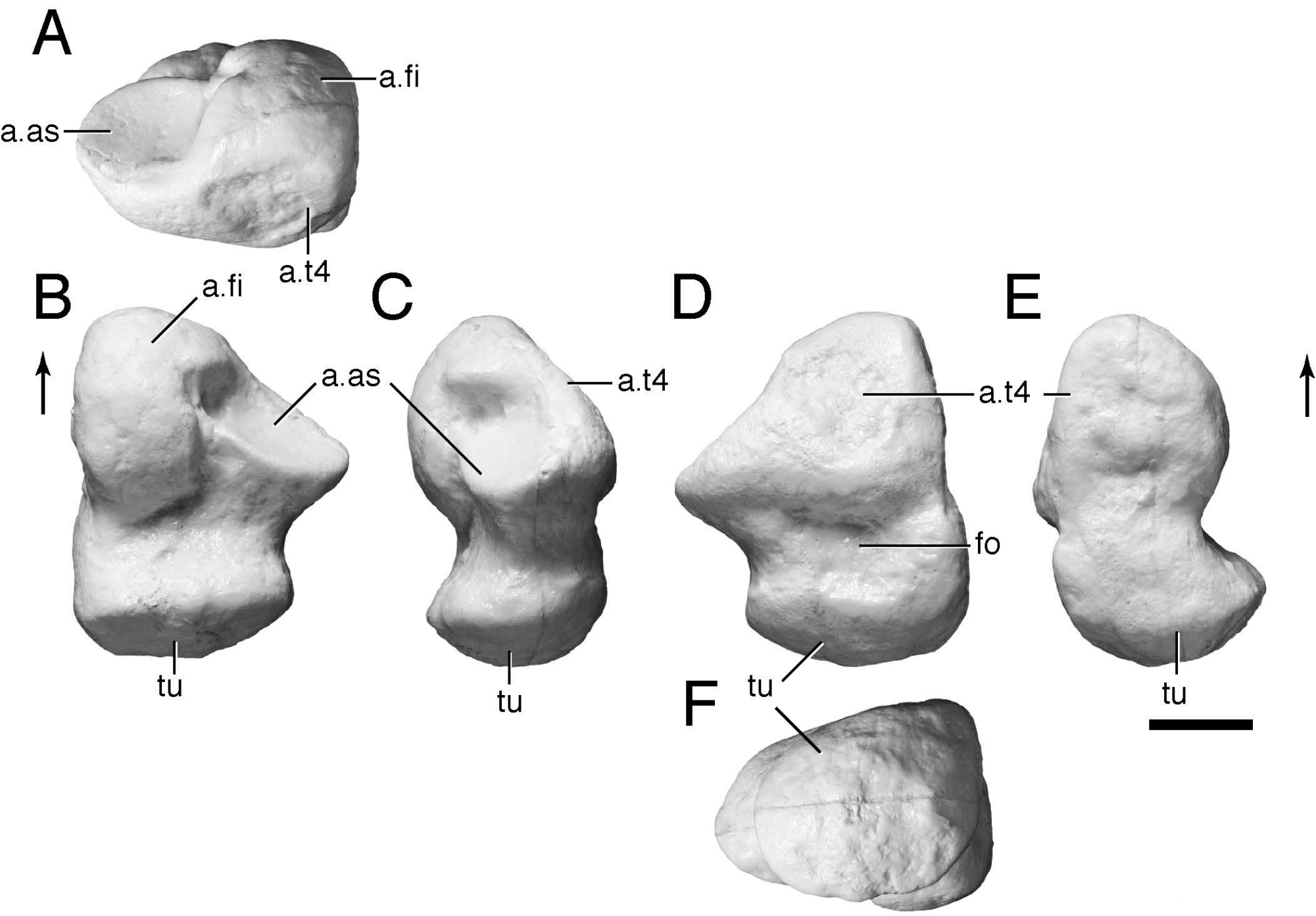
A
a.fi
a.as
a.t4
B
a.fi
a.as
tu
C
a.t4
tu
D
a.t4
fo
tu
E
tu
F

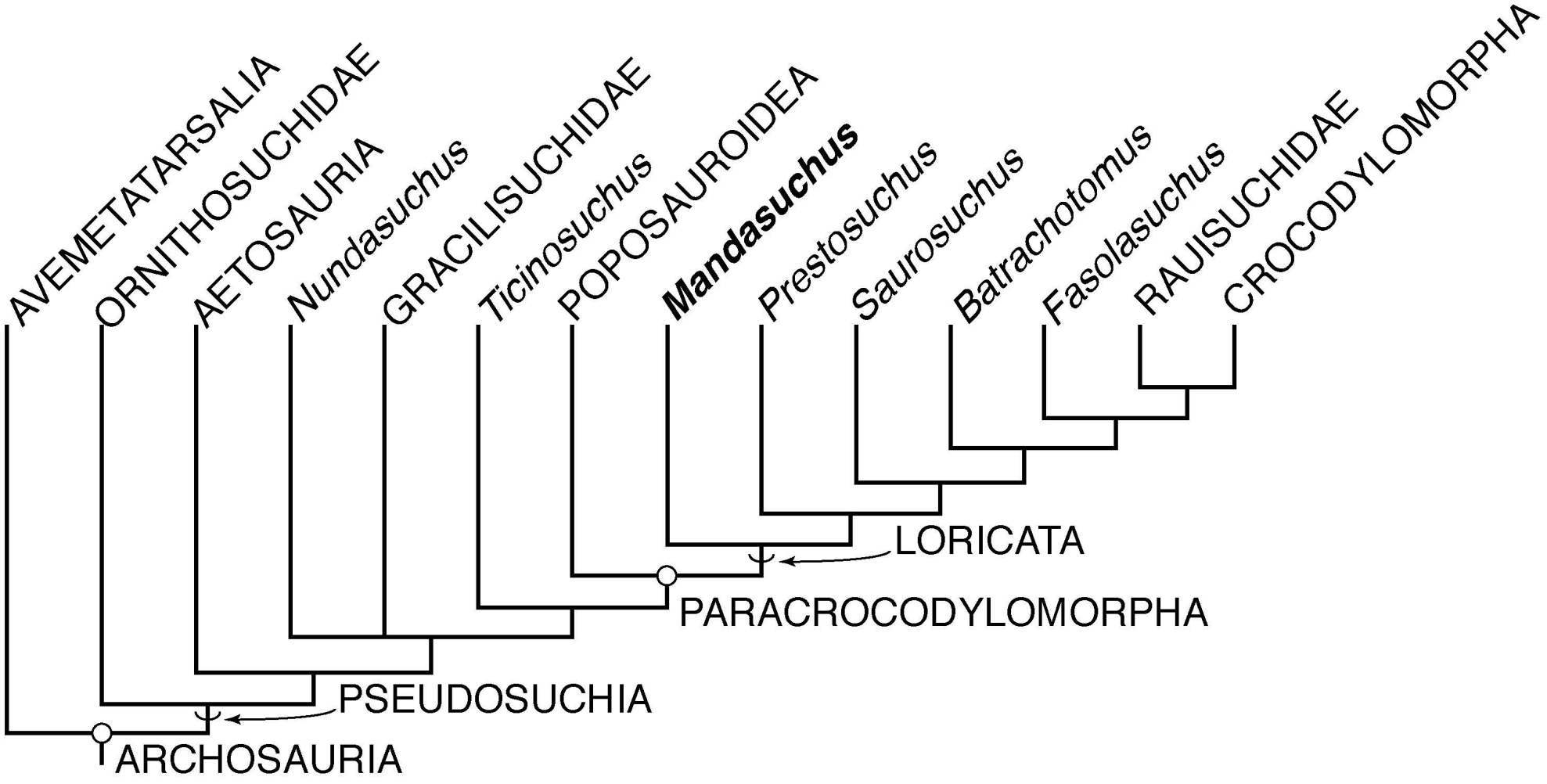
AVEMETATARSALIA
ORNITHOSUCHIDAE
AETOSAURIA
Nundasuchus
GRACILISUCHIDAE
Ticinosuchus
POPOSAUROIDEA
Mandasuchus
Prestosuchus
Saurosuchus
Batrachotomus
Fasolasuchus
RAUISUCHIDAE
CROCODYLOMORPHA
LORICATA
PARACROCODYLOMORPHA
PSEUDOSUCHIA
ARCHOSAURIA